DYNAMIC SIMULATION OF 3D WEAVING PROCESS

by

XIAOYAN YANG

B.S., Tianjin University, China 2008

AN ABSTRACT OF A DISSERTATION

submitted in partial fulfillment of the requirements for the degree

DOCTOR OF PHILOSOPHY

Department of Mechanical and Nuclear Engineering
College of Engineering

KANSAS STATE UNIVERSITY
Manhattan, Kansas

2015

Abstract

Textile fabrics and textile composite materials demonstrate exceptional mechanical properties, including high stiffness, high strength to weight ratio, damage tolerance, chemical resistance, high temperature tolerance and low thermal expansion. Recent advances in weaving techniques have caused various textile fabrics to gain applications in high performance products, such as aircrafts frames, aircrafts engine blades, ballistic panels, helmets, aerospace components, racing car bodies, net-shape joints and blood vessels.

Fabric mechanical properties are determined by fabric internal architectures and fabric micro-geometries are determined by textile manufacturing process. As the need for high performance textile materials increases, textile preforms with improved thickness and more complex structures are designed and manufactured. Therefore, the study of textile fabrics requires a reliable and efficient CAD/CAM tool that models fabric micro-geometry through computer simulation and links the manufacturing process with fabric micro-geometry, mechanical properties and weavability.

Dynamic Weaving Process Simulation is developed to simulate the entire textile process. It employs the digital element approach to simulate weaving actions, reed motion, boundary tension and fiber-to-fiber contact and friction. Dynamic Weaving Process Simulation models a Jacquard loom machine, in which the weaving process primarily consists of four steps: weft insertion, beating up, weaving and taking up. Dynamic Weaving Process Simulation simulates these steps according to the underlying loom kinematics and kinetics. First, a weft yarn moves to the fell position under displacement constraints, followed by a beating-up action performed by reed elements. Warp yarns then change positions according to the yarn interlacing pattern defined by a weaving matrix, and taking-up action is simulated to collect woven fabric for

continuous weaving process simulation. A Jacquard loom machine individually controls each warp yarn for maximum flexibility of warp motion, managed by the weaving matrix in simulation. Constant boundary tension is implemented to simulate the spring at each warp end. In addition, process simulation adopts re-mesh function to store woven fabric and add new weft yarns for continuous weaving simulation.

Dynamic Weaving Process Simulation fully models loom kinetics and kinematics involved in the weaving process. However, the step-by-step simulation of the 3D weaving process requires additional calculation time and computer resource. In order to promote simulation efficiency, enable finer yarn discretization and improve accuracy of fabric micro geometry, parallel computing is implemented in this research and efficiency promotion is presented in this dissertation.

The Dynamic Weaving Process Simulation model links fabric micro-geometry with the manufacturing process, allowing determination of weavability of specific weaving pattern and process design. Effects of various weaving process parameters on fabric micro-geometry, fabric mechanical properties and weavability can be investigated with the simulation method.

DYNAMIC SIMULATION OF 3D WEAVING PROCESS

by

XIAOYAN YANG

B.S., Tianjin University, China, 2008

A DISSERTATION

submitted in partial fulfillment of the requirements for the degree

DOCTOR OF PHOILOSOPHY

Department of Mechanical and Nuclear Engineering
College of Engineering

KANSAS STATE UNIVERSITY
Manhattan, Kansas

2015

Approved by:

Major Professor
Dr. Youqi Wang

Copyright

Abstract

Textile fabrics and textile composite materials demonstrate exceptional mechanical properties, including high stiffness, high strength to weight ratio, damage tolerance, chemical resistance, high temperature tolerance and low thermal expansion. Recent advances in weaving techniques have caused 2D and 3D textile fabrics of various yarn structures begin to gain applications in high performance products, such as military and commercial aircrafts frames, aircrafts engine blades, ballistic panels, helmets, aerospace components, racing car bodies, net-shape joints and blood vessels.

Fabric mechanical properties are determined by fabric internal architectures and fabric micro-geometries are determined by the textile manufacturing process. As the need for high performance textile materials increases, 3D textile preforms with improved thickness and more complex structures are designed and manufactured. Expanding applications of 3D fabrics and increasing complexity of fabric internal structures are challenging textile manufacturing techniques. However, the study of textile fabrics requires a reliable and efficient CAD/CAM tool that models fabric micro-geometry through computer simulation and links the manufacturing process with fabric micro-geometry, mechanical properties and weavability.

Dynamic Weaving Process Simulation is developed to simulate the entire textile process. It employs the digital element approach to simulate weaving actions, reed motion, boundary tension and fiber-to-fiber contact and friction. Dynamic Weaving Process Simulation models a Jacquard loom machine, in which the weaving process primarily consists of four steps: weft insertion, beating up, weaving and taking up. Dynamic Weaving Process Simulation simulates these steps according to the underlying loom kinematics and kinetics. First, a weft yarn moves to the fell position under displacement constraints, followed by a beating-up action performed by

reed elements. Warp yarns then change positions according to the yarn interlacing pattern defined by a weaving matrix, and taking-up action is simulated to collect woven fabric for continuous weaving process simulation. A Jacquard loom machine individually controls each warp yarn for maximum flexibility of warp motion, managed by the weaving matrix in simulation. Constant boundary tension is implemented to simulate the spring at each warp end. In addition, process simulation adopts re-mesh function to store woven fabric and add new weft yarns for continuous weaving simulation.

Dynamic Weaving Process Simulation fully models loom kinetics and kinematics involved in the weaving process. However, the step-by-step simulation of the 3D weaving process requires additional calculation time and computer resource. In order to promote simulation efficiency, enable finer yarn discretization and improve accuracy of fabric micro geometry, parallel computing is implemented in this research and efficiency promotion is presented in this dissertation.

The Dynamic Weaving Process Simulation model links fabric micro-geometry with the manufacturing process, allowing determination of weavability of specific weaving pattern and process design. Effects of various weaving process parameters on fabric micro-geometry, fabric mechanical properties and weavability can be investigated with the simulation method.

Table of Contents

List of Figures

List of Tables

Acknowledgements

Foremost, I would like to express my immense gratitude to my advisor Professor Dr. Youqi Wang for the continuous support of my Ph.D. study and research. I am thankful for her aspiring guidance, invaluably constructive criticism and friendly advice during the research work. Without her persistent help this dissertation would not have been possible.

My sincere thanks also go to my committee members, Dr. Daniel Swenson, Dr. Jack Xin, Dr. Kevin Lease, Dr. Daniel Andresen and Dr. Kim Connell. I would like to express my deepest appreciation for their encouragement, illuminating comments and questions.

It gives me great pleasure in acknowledging the support and help from my group members, Dr. Yuyang Miao, Dr. Lejian Huang Ying Ma, Habib Ahmadi, and Mario Dippolito. I would like to thank them for being good friends, for the stimulating discussions and for the time we have worked together.

This research work is financially supported by US Army Research Laboratory (ARL). Special thanks to Dr. Chian-fong Yen from ARL for their grateful help in finishing the projects.

And last, but not least, I would like to thank my family, for being there for me through the good times and the bad and always being supportive.

Chapter 1 - Introduction

Textile techniques date back to at least 20,000 years ago, when traditional textile products utilized natural materials such as cotton, wool and silk for production of consumer products such as clothing and blankets. In the 1940s, petrochemical synthetic fibers such as nylon, acrylic and Poly Vinyl Chloride fibers were invented and textile materials applications expanded from consumer products to military products. The creation of glass, carbon and Kevlar high-performance fibers in the 1950s through 1970s launched a new era, in which textile materials began to achieve success in high performance products. Various textile fabrics including woven, braided, knitted and stitched fabrics reinforced composites gained applications in military and commercial aircrafts frames, airplane engine blades, ballistic panels, helmets, aerospace components and net-shape joints. As textile materials continue to gain popularity, the current need for high performance textile fabrics also significantly increases. Therefore, textile fabrics with increased thickness and more complex structures are designed and manufactured in order to satisfy the growing demand.

Mechanical properties of textile products rely on fabric properties and fabric internal architectures because fabrics are the major load-bearing components. Fabrics are produced through textile processes, so fabric micro-geometries and mechanical properties are determined by manufacturing process dynamics. Expanding applications of 3D fabrics and increasing complexity of fabric internal structures are challenging textile manufacturing techniques. Weavability becomes a crucial research topic in order to improve manufacturing safety, productivity and efficiency. Fabric design and textile manufacturing require a reliable, efficient CAD/CAM tool that simulates fabric manufacturing process, models fabric micro-geometry and links manufacturing process to fabric micro-geometry, mechanical properties and weavability.

Several models have been established to simulate fabric geometries at various structural levels, including continuous level models, yarn level models and fiber level models. The continuous method models the textile on the fabric level; internal structural details of individual yarns or fibers are not considered. Yarn level models are established based on yarn axial path and yarn cross-section shape. Assumptions on yarn geometry are established based on experimental observations. However, in reality yarns are composed of thousands of fibers, and fabric geometries, including yarn paths and cross-sectional shapes, are determined by fiber distributions. Fiber level modeling is therefore required in order to provide accurate simulation of fabric micro-geometries independent of experimental data.

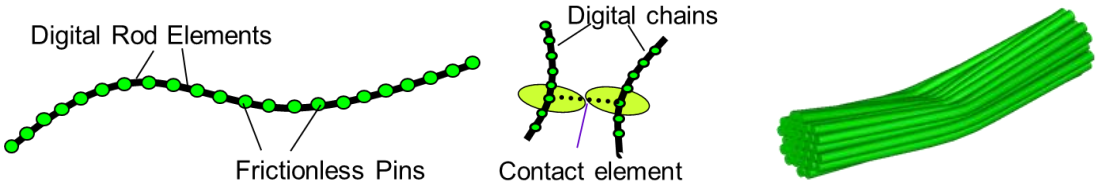

Figure 1-1. Digital element model

In order to determine fabric micro-geometries at fiber level, Wang and her coworkers developed a digital element approach to simulate textile processes [1][2][3][4], as illustrated in Figure 1-1. In this approach, yarn was modeled as an assembly of digital fibers and each digital fiber was divided into short elements connected by pins. Nodal contacts between fibers were searched during simulation. If contact occurred, a contact element was inserted and contact forces were calculated.

With this approach, Wang and her coworkers developed quasi-static simulation, static relaxation and dynamics relaxation methods in order to model fabric micro-geometry. The quasi-

static method simulated step-by-step 3D braiding processes and 2D weaving processes based on a quasi-static assumption. This quasi-static model can be used to derive basic geometry of 2D woven and 3D rectangular braided fabrics. However, computer resources required for the simulation presented a major obstacle preventing wide application of this approach. In addition, the method was not applicable for complex weaving or braiding processes simulation. Therefore, a static relaxation approach and a dynamic relaxation approach were developed to replace the quasi-static step-by-step simulation. The static relaxation method was more efficient than the quasi-static simulation because it implemented implicit algorithm and solved the fabric global matrix. The dynamic relaxation approach established cell topology based on weaving pattern, applied yarn tension and adopted periodic boundary condition. Yarns inside the unit cell deformed to minimum potential energy state. Because only one unit cell was involved in the numerical model, computation time was no longer a concern. Unit cells of various woven fabrics with complex yarn patterns were generated with the dynamic relaxation method. A software package, Digital element approach Fabric Mechanics Analyzer (DFMA), was developed based on this digital element approach.

In the static relaxation and dynamic relaxation approaches, fabric relaxed to minimum potential energy state and only fabric topology was considered in determining unit cell micro-geometry; effects of weaving and braiding process dynamics were neglected. In reality, however, fabric micro-geometries do not reach minimum potential energy states due to fiber-to-fiber friction. Fabrics are produced by textile weaving machines and fabric internal structures and mechanical properties are determined by weaving process dynamics. Weaving process kinematics determines fabric topology and weaving process kinetics, such as yarn tension, weaving velocity, beating-up velocity, and fiber-to-fiber friction, determines detailed fabric

internal structure. Therefore, a dynamic weaving process simulator that can incorporate weaving process dynamics is essential to study manufacturing induced fabric deformation, fiber damage, fabric stress distribution and weavability. Furthermore, fabric internal structures demonstrate growing complexity, thereby requiring increasingly complicated manufacturing processes and intensifying the need for optimized manufacturing processes and machines in order to reduce friction and impact force. Therefore, A CAD/CAM numerical model capable of textile process simulation, fabric geometrical modeling and analysis is required.

This research aimed to develop a dynamic weaving process simulator according to the textile process physics. The model simulated weaving process dynamics, and linked the fabric pattern, micro-geometry, process weavability and fabric mechanical properties to the weaving process. Kinetics and kinematics of all weaving actions were fully modeled. The dynamic weaving process simulator was successfully employed to generate various fabrics.

Thus dissertation presents the following research:

1) Dynamic weaving process simulator

The dynamic weaving process simulator, developed according to textile process dynamics, is capable of fabric geometric modelling and weaving process analysis. Key components of a weaving machine and weaving actions were studied and modelled and a weaving matrix was implemented to control the weaving process. The simulation model was established based on fabric pattern and weaving process dynamics. Digital element approach was employed to simulate weaving actions and boundary conditions. Four primary weaving actions were simulated according to underlying loom kinematics and kinetics: weft insertion, beating up, weaving and taking up. Tension-induced, contact-induced and friction-induced nodal forces were calculated during process simulation. Parallel computing was employed to promote efficiency.

2) Dynamic weaving process analysis

Parametric analysis was implemented using the dynamic weaving process simulator. Relationships between weaving process dynamics and yarn stress, fabric micro-geometry and weavability were studied. Effects of weaving process kinetics and kinematics parameters, including yarn tension, weaving velocity, reed spacing, beating-up velocity, and fiber-to-fiber friction on fabric yarn stress and fabric mechanical properties were also studied.

Reed load estimation was implemented in dynamic weaving process simulator in order to provide instructions regarding machine and manufacturing process design. Textile fabrics complexity has been rising significantly, generating challenges for textile manufacturing. Reed damage during weaving impact presents a major manufacturing problem. Therefore, reed load estimation was implemented and the relationship between weaving process parameters and reed load were investigated using dynamic weaving process simulator. Weaving process parameters such as taking-up frequency and velocity and reed impact velocity significantly affect reed load but yarn tension and fiber-to-fiber friction only moderately affect reed load. Optimal fabric design and machine design can be implemented with manufacturing process simulation.

In the dynamic relaxation approach, unit cell micro-geometry was determined by minimizing potential energy. Only fabric topology was used to determine micro-geometry in the relaxation approach. However, fabrics are produced by textile weaving machines and fabric micro-structures are determined not only by topology, but also by weaving process kinetics, such as yarn tension, weaving velocity, beating-up velocity, and fiber-to-fiber friction. Process dynamics determines fabric micro-geometry, and affects fabric mechanical properties. Effects of weaving process on fabric micro-geometry were studied and presented in this dissertation. Comparison of process simulation and dynamic relaxation was implemented and discussed.

Chapter 2 - Literature Review

2.1 Development of Textile Fabrics and Textile Composites

Archaeological evidence suggests that the skill of hand-weaving and hand-spinning to make coarse textile clothing from natural fibers was developed at least 20,000 years ago [5]. Hand woven fabrics made from natural materials such as cotton, wool and silk were utilized to produce consumer products such as clothing and blankets that provided warmth and basic protection for human bodies.

In the 1800s, the Industrial Revolution initiated a transition from hand-spinning methods to weaving machines powered by steam or water. Textile output significantly increased because of mechanized cotton spinning. However, little innovations were made on textile materials and textile products.

In the 1940s, emergence of the petroleum industry prompted the invention of petrochemical synthetic fibers such as nylon, acrylic and Poly Vinyl Chloride fibers. Applications of synthetic fiber textiles expanded from consumer products to military products including soldier protection and parachutes. During World War II, ballistic vest "flak jacket" made from ballistic nylon and steel plates sewn into the cloth was introduced. The "flak jacket" offered protection from munitions fragments, but was heavy, bulky and ineffective against most pistol and rifle threats [6].

In the 1950s and 1960s, the creation of high-performance glass fibers and carbon fibers launched a new era of textile materials. Weaving technique advances allowed manufacturing of fabrics with complicated internal structures, making textile fabrics gain applications in composite materials. Fiber reinforced composites consist of reinforcing fabrics and matrix material. Reinforcing fabrics are the principal load-bearing components of textile composites, and matrix

functions primarily consist of load transmission, damage tolerance, corrosion resistance and thermal and environmental stability [10]. Several processes can be utilized to manufacture the reinforcing fabric, including weaving, knitting, and braiding. Molding methods of fiber-reinforced composites include hand lay-up of prepreg materials, automated tape lay-up of prepreg materials, resin-transfer molding, vacuum-assisted resin transfer molding, resin film infusion, wet lay-up, filament winding, pultrusion, and compression molding of sheet molding or bulk molding compound [10][11]. Properties such as high stiffness, high strength to weight ratio, damage tolerance, chemical resistance, high temperature tolerance and low thermal expansion have made high-performance fabric reinforced composites very ideal for aircrafts components. Carbon fiber textile materials gained application for military aircraft in the 1970s, when aircrafts engine blades and frames implemented carbon fabric reinforced composites to produce lighter stronger structures. Reduced airframe weight promotes fuel economy, so carbon fiber reinforced materials have also recently been used for commercial transport aircrafts. The Boeing 787 Dreamliner contains approximately 35 short tons (32,000 kg) of carbon fiber reinforced polymer (CFRP), making it 20% more fuel efficient than the Boeing 767 [7].

In the 1970s, DuPont invented Kevlar fiber, which made the first generation of real bullet-proof soft armor possible [6]. A series of researches on Kevlar concluded that the light-weight Kevlar fabrics present excellent ballistic resistant properties, that are 5 times stronger than steel [8]. The Kevlar ballistic vest also offered flexibility and comfort, allowing full-time wear, and it could be customized with various types of fibers and manufacturing methods. As textile technique advanced, Kevlar fabrics also gained application in impact resistance armors such as helmets and ballistic panels. Stress wave travels in multiple directions in textile fabrics, improving damage tolerance and withstanding multi-directional mechanical stresses. However,

special applications of textile fabrics require particular design and complicated manufacturing processes. Micro-level modeling is therefore required to simulate the manufacturing process and analyze fabric properties.

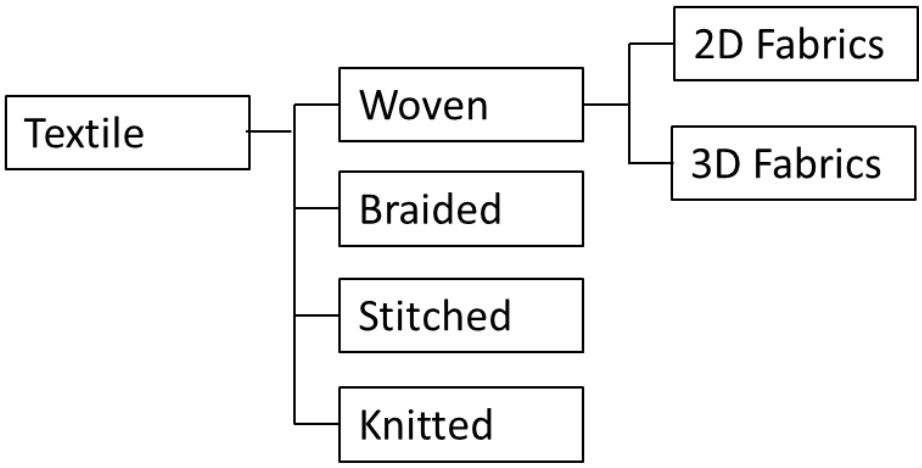

(a) Textile catogory

(b) 2D woven fabric

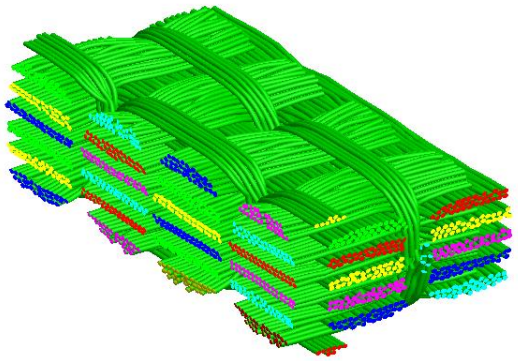

(c) 3D woven fabric unit cell

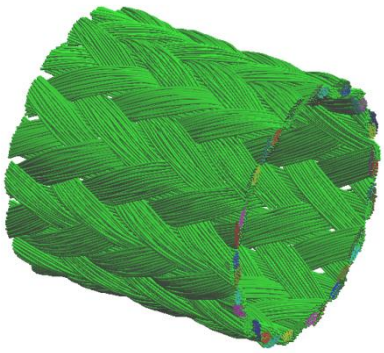

(d) Tubular braided fabric

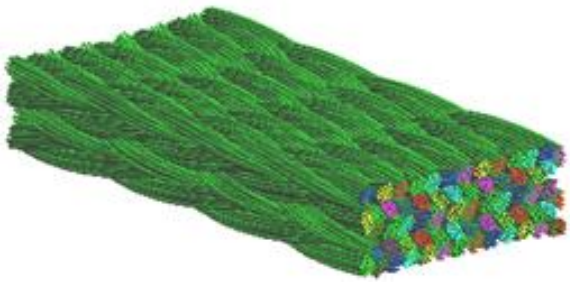

(e) Rectangular braided

Figure 2-1. Textile category

Textile fabrics can be categorized by textile processes employed for production，including woven, braided, stitched, and knitted [12][13]. Woven fabrics can be further classed as 2D and 3D preforms according to the degree of reinforcement in the thickness direction, as demonstrated in Figure 2-1 (a). Typically, 2D woven fabric has one layer of weft interlaced by one layer of warp yarns, as shown in Figure 2-1(b). Textile composites are commonly reinforced by laminated 2D woven fabrics in order to achieve target thickness and structure, but delamination adversely affects material mechanical properties and reliability. In the 1990s, weaving technique advancements led to the invention of 3D woven fabrics. 3D woven fabrics are comprised of multiple layers of weft yarns interlaced with warp yarns located in various warp sections, as shown in Figure 2-1 (c). 3D woven textile fabrics are superior to traditional laminated 2D woven fabrics as reinforcement of textile composite structures for several reasons: 1) Integrated structures of 3D fabrics offer improved damage tolerance, eliminate delamination that occurs in 2D laminated structures, and withstand multi-directional mechanical stresses; 2) 3D fabrics can be used in complex composite design, thereby achieving increased thickness in composite structure; 3) 3D reinforcing textile determine the pattern of stress wave propagation

inside composites and the impact energy dissipation improves impact strength; 4) 3D fabrics have the advances of near-net shape manufacturing. The advantageous mechanical properties lead to the used of 3D fabric s as reinforcement of composite structure. 3D fabric reinforced composite materials are lightweight, high strength, corrosion and thermal resistant so that they are able to withstand tough loading conditions. These beneficial properties have increased their popularity for manufacturing of high-performance products such as military and commercial aircrafts frames, air plane engine blades, ballistic panels, helmets and aerospace components.

Braided fabrics are produced by plaiting, but they do not present two distinguished sets of perpendicular yarns typically identified as warp yarns and weft yarns in woven fabrics. Tubular braided fabric and rectangular braided fabrics are shown in Figure 2-1 (d) and (e). Tubular braided fabrics can be used as reinforcement of circular cylindrical structural components. A hybrid of various fibers is often used to achieve desired elasticity. A micro-braiding machine has recently begun development in order to fabricate bio-structures such as blood vessels.

Textile fabrics are the primary load-bearing components in textile products; therefore, product mechanical properties principally rely on fabric properties, which are determined by fabric structures at the micro level. Fabric micro-geometry is determined by textile manufacturing process dynamics. However, reinforcing fabrics usually demonstrate complex structural design, thereby requiring complicated manufacturing methods in order to survive designated loading conditions. The challenge for 3D fabrics design and manufacturing is to develop a reliable and efficient CAD/CAM tool that models fabric micro-geometry through computer simulation and links the manufacturing process with fabric micro-geometry, mechanical properties and weavability. The objective of the research is to develop a CAD/CAM tool to satisfy the need. The dynamic weaving process simulator implements the digital element

approach, while strictly following manufacturing process physics, and simulating all weaving actions and process dynamics. The relationship between design and manufacturing process parameters and fabric micro-geometries, and the relationship between manufacturing process and machine behavior were investigated using the process simulator.

2.2 Fabric Structural Analysis

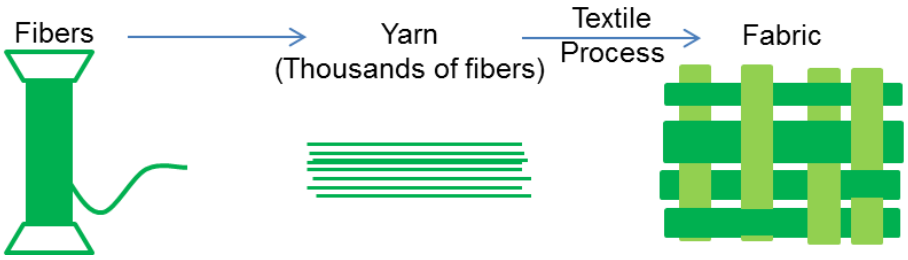

Figure 2-2. Textile structure

Mechanical properties of textile fabric are determined by fabric internal structures; therefore, the study of textile fabric and composites requires a structural modeling and analysis tool. Textile fabric has internal structure on three scales [12], as demonstrated in Figure 2-2. At the molecular scale, fibers exhibit structural details that profoundly affect strength and stiffness. On a coarser scale, typically 1 mm, lots of 10^3 - 10^4 fibers are bundled together to form yarns or tows. The cross sections of the yarns or tows in the final fabric at relaxed state are defined by fiber distribution within the yarn. In the final scale, yarns are woven into textile fabric, forming part of an engineering structure. The placement or lacing pattern of yarns defines textile fabric structure.

Models to simulate fabric geometries can be categorized as continuous level models, yarn level models and fiber level models according to simulation scales for textile fabric internal structures.

2.2.1 *Continuous level analysis*

The continuous method regards textile fabric as a homogenized material. Collier et al [15] used the four-node shell element with orthotropic properties to model the fabric. The fabric, which was considered as a solid continuum, was simulated using finite shell elements. However, the continuous method did not model fabric internal structure such as yarn paths and yarn cross-sectional shapes.

2.2.2 *Yarn level analysis*

Yarn level models are established based on yarn axial path and yarn cross-section shape. According to assumptions made regarding cross-section shape, yarn level models were categorized into constant cross-section models and variable cross-section models.

2.2.2.1 *Constant cross-section model*

Yarn cross-section shapes are commonly assumed to be circular, elliptic, semi-circular and lenticular in constant cross-section models.

In the 1930s, Peirce published a geometrical model [16] to display the basic pattern of plain woven fabric. This model built a unit cell of 2D plain woven fabric. As shown in Figure 2-3(a), the yarn cross section was assumed to be constant circular and the yarn path was composed of straight lines and arcs where two yarns contacted. Radius of the arcs equaled yarn diameter. Yarns were assumed to be incompressible and completely flexible; and bending rigidity was ignored. However, this model was limited for use in open structures with loose

density. Peirce improved this model and proposed an elliptic cross-section accounting for yarn flattening due to inter-yarn pressure during weaving of tightly woven fabrics, as shown in Figure 2-3(b). Because such geometry was complex and laborious in operation, an approximation was taken by replacing circular yarn diameter with minor diameter of ellipse. However, this model still cannot be applied to very tightly woven fabric.

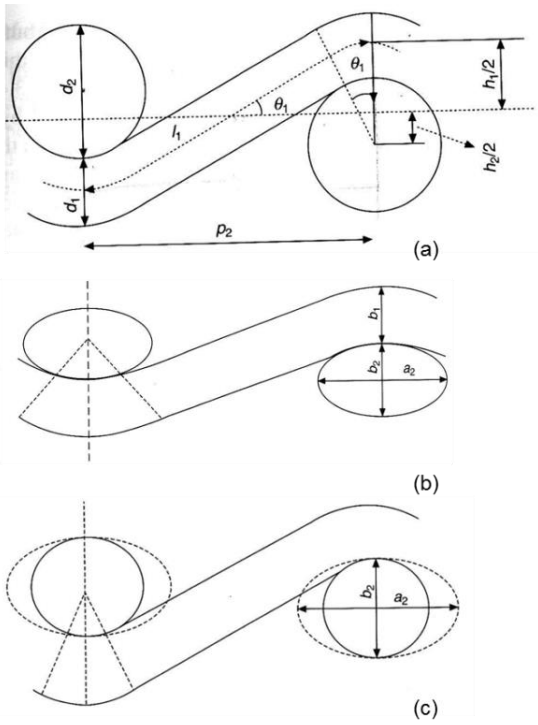

Figure 2-3. (a)Peirce's circular cross-section model (b) Peirce's elliptic cross-section model (c) Peirce's approximation of yarn flattening elliptic geometry [16]

In the 1950s, Kemp developed a race-track section model in order to modify the yarn cross-section shape and represent yarn flattening more acurrately, as shown in Figure 2-4 [17]. The yarn cross-section shape was assumed to be a rectangle enclosed by two semi-circular, and

this shape, as compared to Peirce's elliptical section, simplified yarn path caculation. However, the cross-section shape could not represent realistic yarn flatterning in most cases.

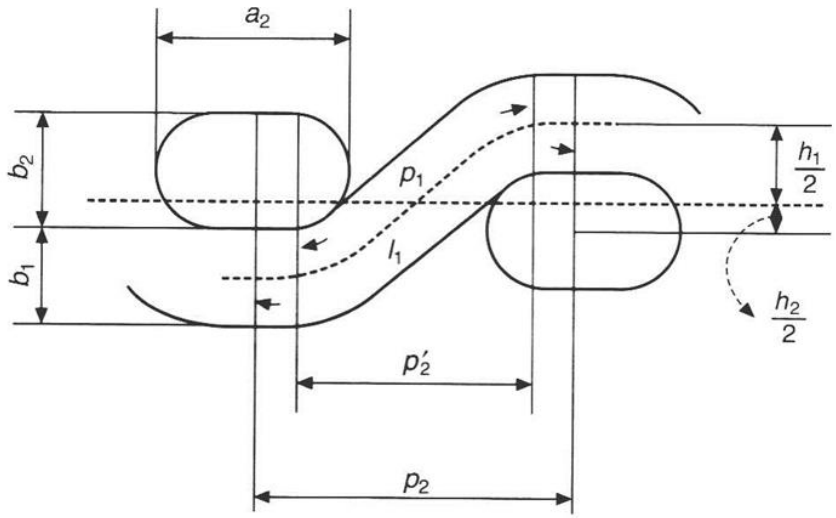

Figure 2-4. Kemp's racetrack section model [17]

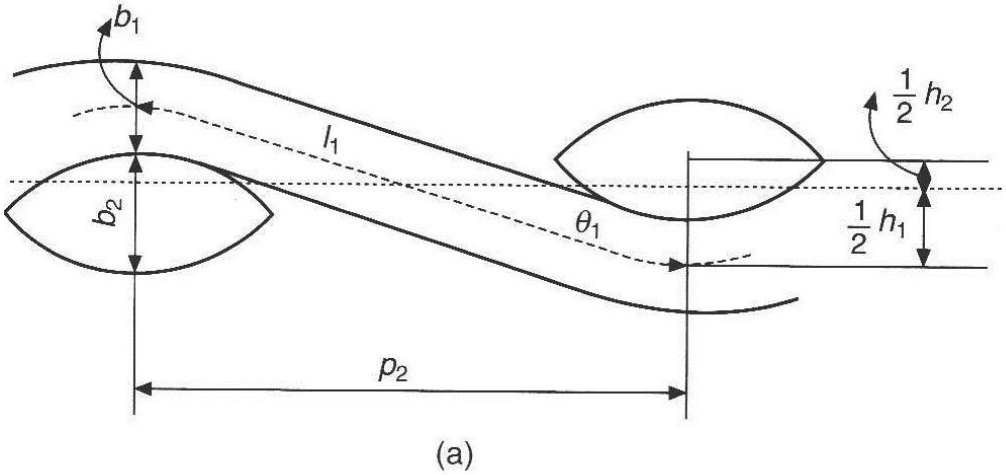

Figure 2-5. Hearle's lenticular geometry [18]-[20]

In the 1970s, Hearle and Shanahan [18]-[20] proposed a mechanical model that considered bending energy. They found that the semi-circular shape used in Kemp's model increased bending energy, so they improved the model using a lenticular (Figure 2-5) cross section, with a lower curvature and no rapid increase of bending energy. Hearle and Shanahan's model is considered the most general model mathimatically. The yarn cross-section asumed the intersection shape of two equal-radius circles offset by a certain distance. Peirce's circular section model is a special caese of this model in which the offset distance equals zero.

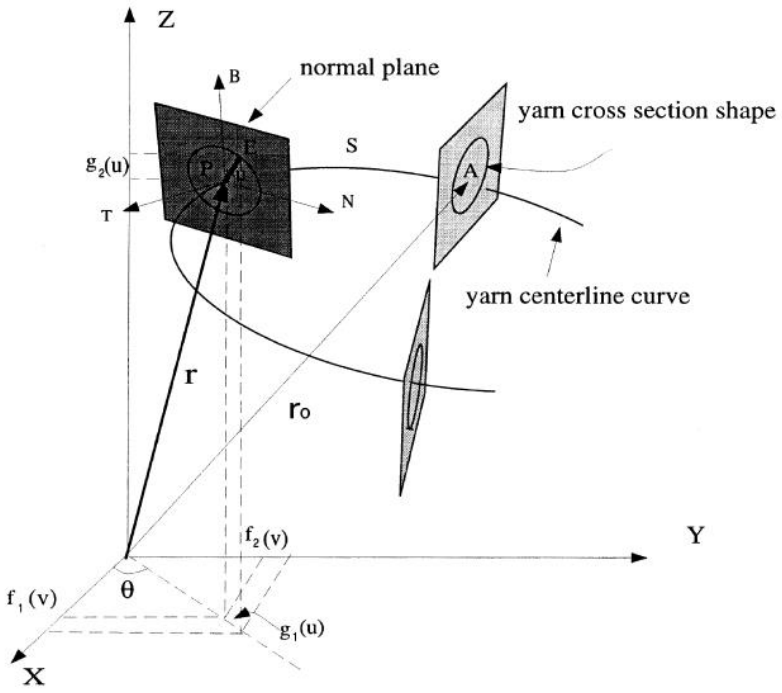

Figure 2-6. Adanur and Liao's model through cross-section shape and center line curve [21]

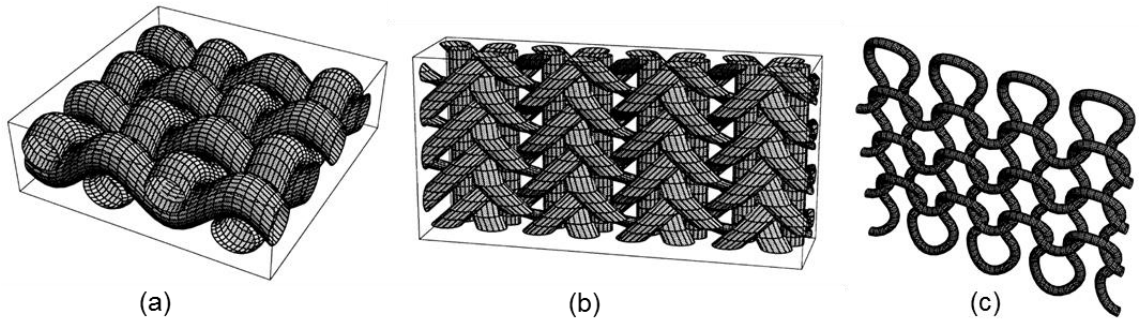

Figure 2-7. 3D model of (a) 2D woven, (b) 3D braided, (c) weft knitted fabrics [21]

The models introduced so far are all targeting 2D plain woven structures. In the 1990s, Adanur and Liao [21][22] proposed a computer aided geometric design(CAGD) technique to present a 3D model of fabric reinforcement, capable of producing a 3D representation of any 2D or 3D fabrics. The model was generated by sweeping the yarn cross-section shape through the yarn center line curve. A perpendicular plane could be recognized at any point on the yarn center line, and the yarn cross-section could be drawn, thereby allowing the bounding yarn surface to be derived, as shown in Figure 2-6. This method was used to generate 3D models for various fabrics with woven, braided, and knitted structures (Figure 2-7). However, this model also assumed constant elliptical cross-section shape.

2.2.2.2 *Variable cross-section model*

All described models utilized constant yarn cross-section shapes. In reality, however, yarn cross-sections vary along the yarn path due to contact. In the 1990s, Kuhn and Charalambides [23][24] proposed a model with variable yarn cross-section for plain 2D fabric. Assumptions made in this model included: 1) Periodical undulation of the tows follows a sinusoidal form in the longitudinal direction, 2) Fibers are parallel within each tow, 3) Fiber density is uniform, 4) The cross-sectional area remains constant, 5) Tows in-plane width remains

constant, and 6) Weft and warp tows are in full contact throughout the interlace region. The unit cell was divided into interlacing regions (e.g. *cghd* and *ejkf* in Figure 2-8) and bridge regions connecting interlacing regions. The cross-section shape was assumed to have a sinusoidal top and bottom based on micrographs observations, as shown in Figure 2-8. In the interlacing region, the profile constrained by contact had lower amplitude than the opposing unconstrained profile, and the bridge region was established by linear interpolation, as shown in Figure 2-8. This model also targeted 2D plain weave fabrics.

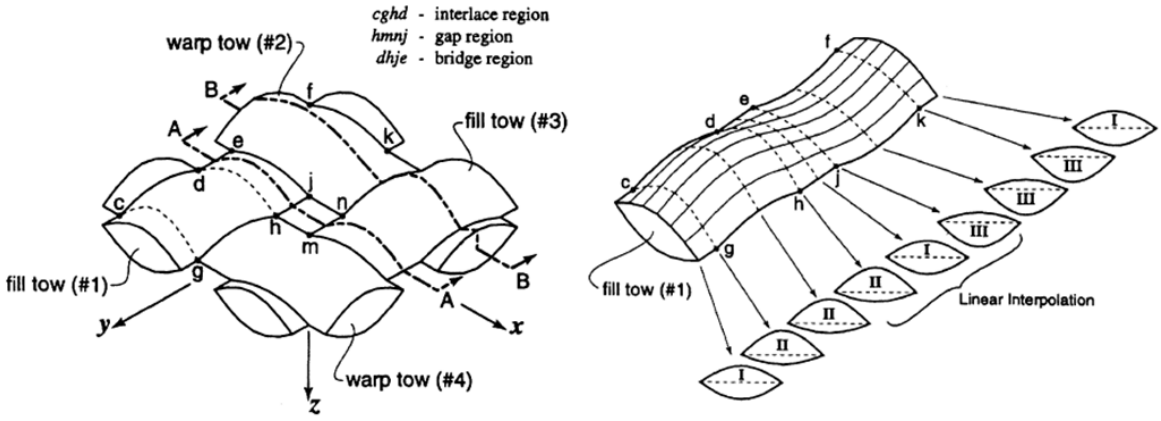

Figure 2-8. Kuhn and Charalambides's model [23]

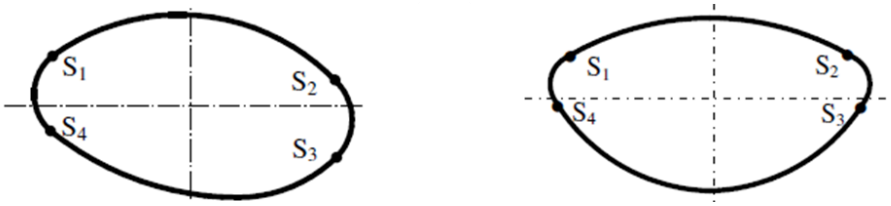

(a) Generic model (b) Plain weave model

Figure 2-9. Hivet and Boisse's model for cross-sections [25]

In the 2000s, Hivet and Boisse [25][26] proposed another variable cross-section model that defined three zones for yarn cross-sections, as shown in Figure 2-9: a contact zone (S_3S_4), a contact free zone (S_1S_2), and a lateral zone between the two (S_2S_3). In general, these three zones could be approached by four conic curves. The yarn "trajectory", or yarn center line path, was constrained by necessary 3D consistency. For plain weaves, an identical conic was used in contact zone for the cross-section and yarn path. In the contact-free zone, the yarn path was a straight line, and, for more complex twills, the assumption was made that the transverse cross-section flattens and the longitudinal yarns remained straight (Figure 2-10). Control sections at control points on yarn path were defined first, and the yarn model was generated through a smooth interpolation, while accounting for variations in section shapes.

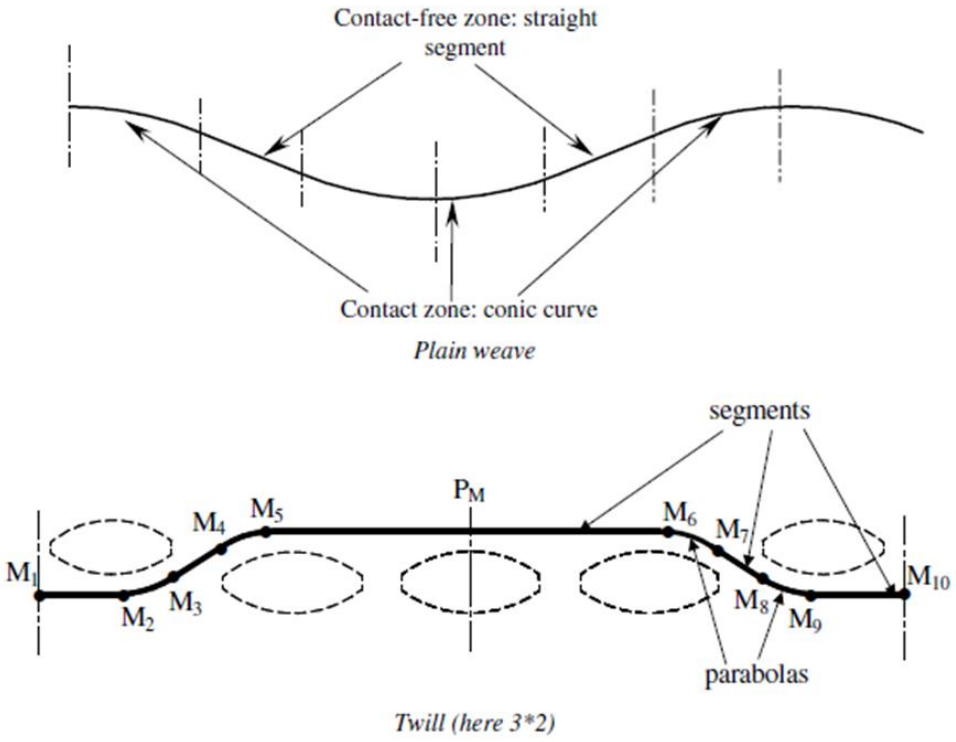

Figure 2-10. Hivet and Boisse's model for yarn path [25]

2.2.2.3 *FEM model*

Early published models were simple models that displayed yarn path and cross-section, and provided estimation of volume fraction and fabric strength, but they did not produce detailed fabric micro geometries or yarn deformations. As textile composites gain popularity, more attempts are being made for structural analysis, leading to the development of several FEM textile models.

In the 2000s, Lin and Zeng developed a textile software TexGen [27][28][29] for 3D modeling of textiles. Early versions of this software specified yarn path by a series of vectors representing center lines of yarns. To avoid retention of redundant information, yarn path was revised to be defined by master nodes along its length, and an interpolation function to give the exact path between these nodes (Figure 2-11). Five options were provided to describe yarn cross sections: ellipse, power ellipse, lenticular hybrid and polygon. Lenticular hybrid and polygon provided maximum flexibility. An interpolation function was embedded in TexGen to describe changes in cross-section shapes along the length of the yarn. Figure 2-11 presents a yarn model with variable yarn cross-sections built by TexGen. Intersection of yarns was addressed in this model by adjusting the yarn width and rotating yarn sections at crossovers. However, small intersections remained. Yarn properties, such as yarn linear density, fiber density, fiber diameter, fibers per yarn, Young's modulus, and Poisson's ratio could be assigned to each yarn. Compared to previous models, TexGen is a generic model capable of modeling textiles with various structures (Figure 2-11).

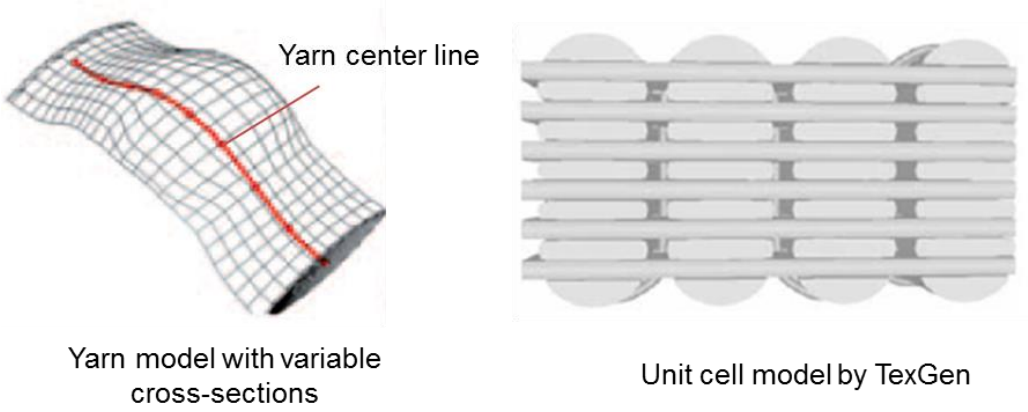

Figure 2-11. TexGen model [27][28]

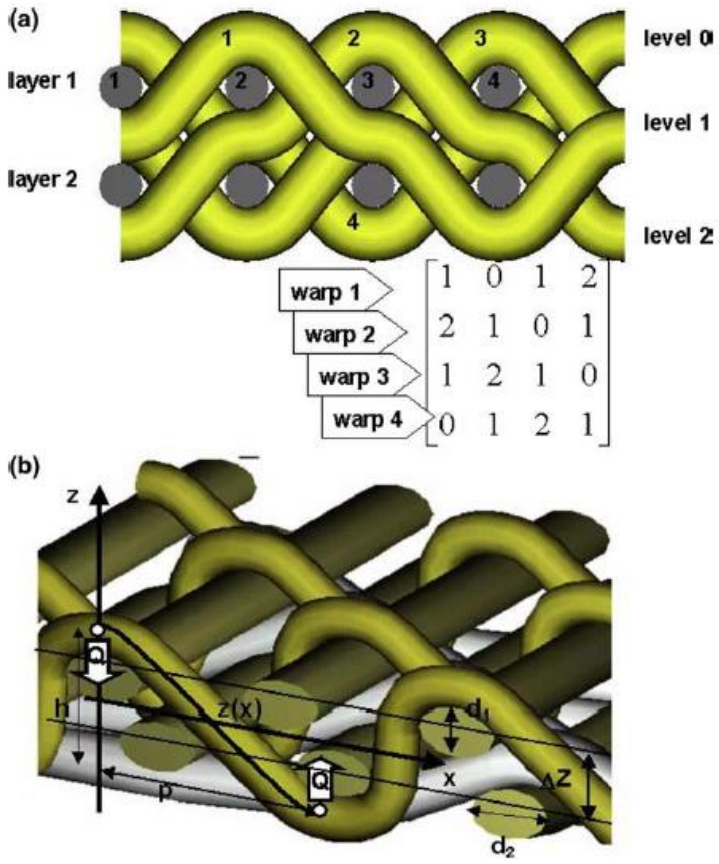

Figure 2-12. WiseTex model (a) coding of the weave; (b) description of the yarn path [34]

In the 2000s, Lomov and Verpoest [30]-[33] developed a software package WiseTex that was capable of modeling the internal geometry of fabrics including 2D and 3D woven, two and three axial braided, knitted, multi-axial multi-ply stitched fabric. Models were established based on yarn properties, yarn interlacing pattern, and yarn spacing within fabric repeat. The yarn interlacing pattern was coded by a weave structure matrix that recorded the warp layer ID, as shown in Figure 2-12 (a). Yarn shape was described using a parameterized function ***z(x; h/p)***, where ***z*** and ***x*** are coordinates of the yarn middle line, ***h*** is the crimp height and ***p*** is the distance between interval ends (spacing of the yarns). The shape ***z(x; h/p)*** for a given relative crimp height ***h/p*** was computed using the principle of minimum of bending energy of the yarn on the interval.

2.2.3 *Fiber level analysis*

Yarns are composed of hundreds or thousands of fibers. Fabric micro geometries, including yarn paths and cross-sectional shapes, are determined by fiber distributions. Therefore, assumptions of constant or variable yarn cross sections are not applicable for accurate simulation of fabric micro-geometries.

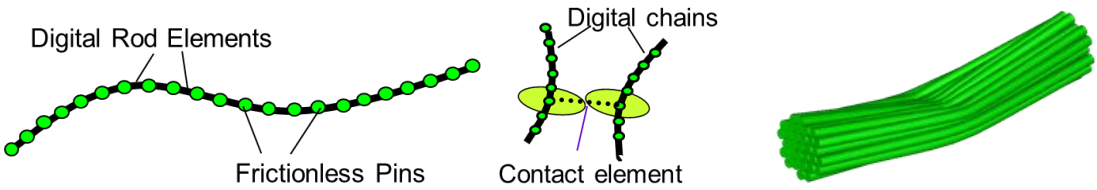

Figure 2-13. Digital element model

Wang and her coworkers developed the first fiber level model. The digital element approach was employed to simulate the internal structure of textile fabrics [1]-[4]. This approach

has three key concepts: digital fiber, yarn assembly and contact between digital fibers, as shown in Figure 2-13. A digital fiber is a physical representation of a fiber, composed of small rod elements connected by frictionless pins. Digital fibers can be organized together to form a bundle that represents a yarn. If the distance between two digital nodes of two neighboring digital fibers is smaller than the fiber diameter, a contact element is established and recorded.

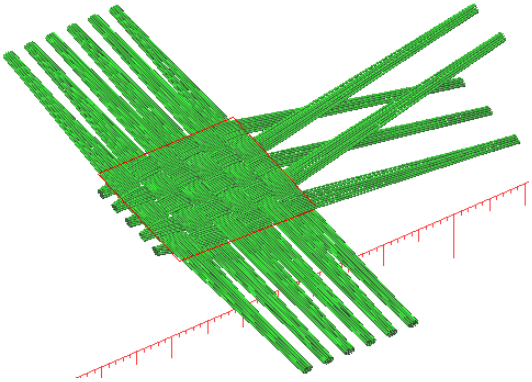

(a) 2-D weaving

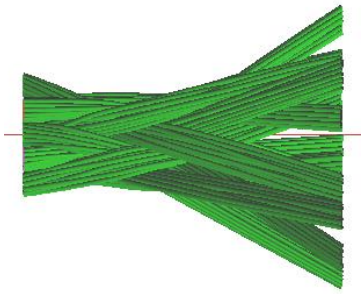

(b) 3-D braiding

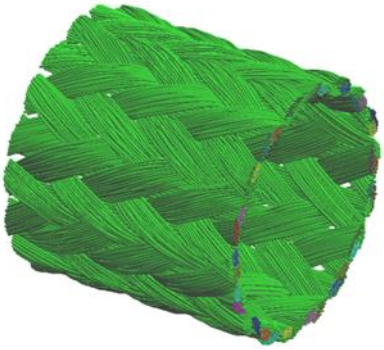

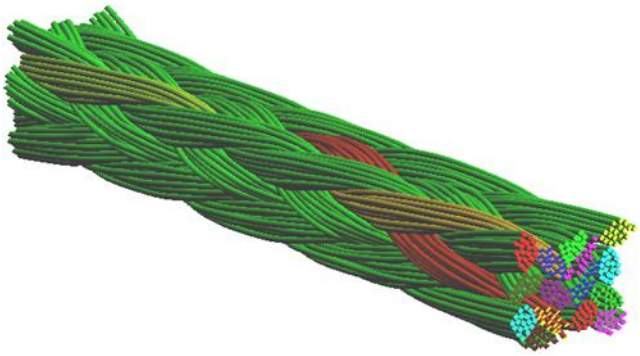

(c) 3D braiding

Figure 2-14. Wang's quasi static simulation model [3]

Wang and her coworkers utilized the digital element approach and simulated step-by-step 3D braiding processes and 2D weaving processes based on a quasi-static assumption [3], as shown in Figure 2-14. Tensions were applied to weft and warp yarns during the simulation. However, the primary obstacle preventing wide application of this approach is the extensive time and computer resource required for simulation. Therefore, it is difficult use the method to simulate complex weaving or braiding processes.

Static relaxation approach and dynamic relaxation approach were developed to replace the quasi-static step-by-step simulation. In the dynamic relaxation approach [2][3], a unit cell topology was established based on the weaving pattern, as seen in Figure 2-15 (a). Yarn properties, including yarn diameter, Young's modulus, and density were assigned to each yarn and multiple digital fibers were bounded to represent a physical yarn. Yarn tension was applied and periodic boundary condition was adopted. Yarns inside the unit cell deformed to the minimum potential energy state. Because only one unit cell was simulated in the numerical model, computation was no longer a concern. This method has been used to generate unit cells of various multi-layer 3D woven fabrics with complex yarn patterns, at fiber level and yarn level, as shown in Figure 2-15 (b) (c). A software package, Digital Fabric Mechanics Analyzer (DFMA), was developed based on this digital element approach.

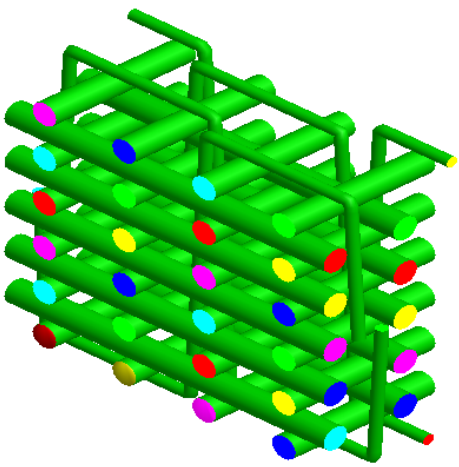

(a) Unit cell topology

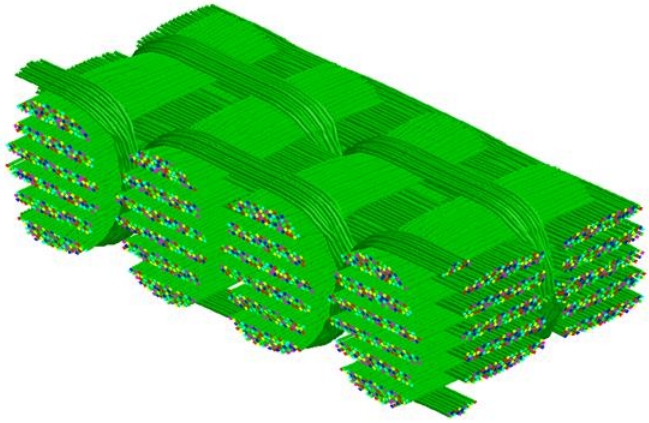

(b) Fiber-level model

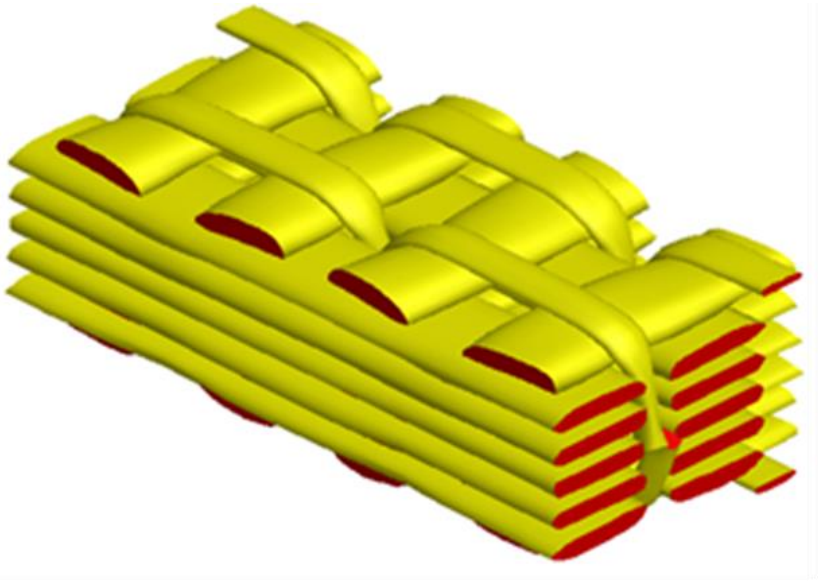

(c) Yarn-level model

Figure 2-15. Dynamic relaxation model[14]

In 2010s, Durville [36][37][38] developed an enriched kinematic beam model to simulate fibers based on the concept of digital element approach. The initial fabric model, as demonstrated in Figure 2-16(a), was an arbitrary configuration in which all tows lay on the same plane, and were assumed to be straight with elliptical cross-sections. At crossings, tows were

interpenetrating. Contacts were determined in three steps, as shown in Figure 2-17. First, regions in which contacts are likely to occur were determined. Then intermediate geometry was defined for each region as illustrated by the red line in Figure 2-17. Pairs of cross-sections likely to contact were defined by a plane orthogonal to the intermediate geometry. Finally, particles candidate to contact were located on the edge of the cross sections. Derived 2D plain weave and twill weave fabrics models are shown in Figure 2-16 (b) and (c). Durville's model was used to determine 2D woven fabric structures.

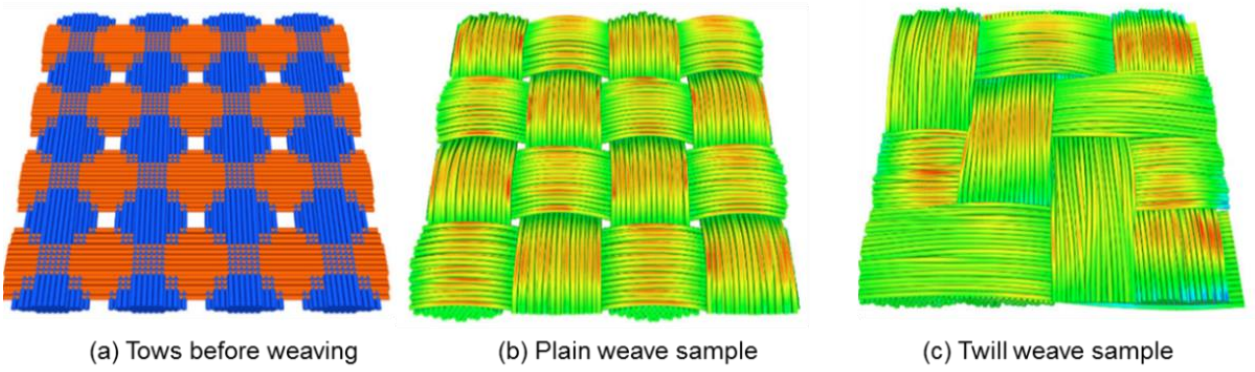

Figure 2-16. Durville's model [36][37][38]

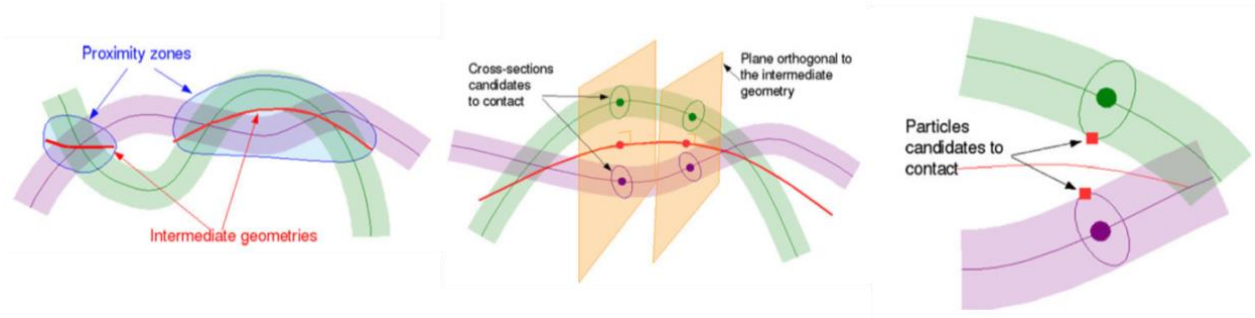

Figure 2-17. Determination of contact elements [37]

2.3 Conclusions

Proper fabric design requires investigation of loading conditions under which the textile composite is to be used. Results from the investigation subsequently define desired mechanical properties of textile fabrics. Mechanical properties of fabrics are determined by the micro-structure, including placement or lacing pattern of yarns and fiber distribution. The best suited textile manufacturing technique to fabricate the textile is selected and employed to manufacture the fabric [12].

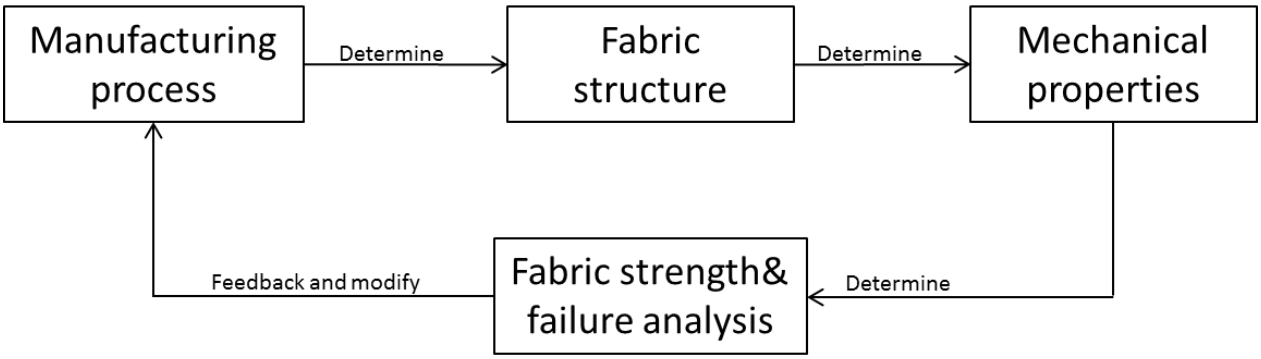

Figure 2-18. Fabric design process

As shown in Figure 2-18, mechanical properties textile preforms for fiber-reinforced composites are determined by fabric internal structure. Because textile fabrics are produced by a variety of weaving processes, the process kinematics and kinetics to manufacture 3D fabrics determine micro-structures and mechanical properties of fabrics. Fabric strength and failure analysis provide feedback to modify manufacturing process. In the current weaving industry, fabric geometric modeling is established based on laboratory observations; fabric design and manufacture parameters, such as yarn dimensions, reed dent, weaving velocity and tension settings, are established based on manufacturer experiences. There lacks a tool that can link

fabric design and manufacturing with fabric micro-geometry and predict fabric micro-geometry with provided weaving process parameters. The effects of manufacturing process kinetics and kinematics on fabric micro-geometries and mechanical properties remain unclear. In the dynamic relaxation approach, the micro-geometry of a unit cell is determined by minimizing potential energy. Only fabric topology is used to determine the micro geometry with relaxation approach. In reality, fabrics are produced by textile weaving machines, so fabric micro-structures are determined by topology and weaving process kinetics, such as yarn tension, weaving velocity, reed spacing, beating-up velocity, and fiber-to-fiber friction. Process dynamics not only determines fabric micro-geometry, but also affects the fiber/yarn strength and fabric mechanical properties. The need for a model that can incorporate the weaving process dynamics becomes evident.

As textile fabrics gains popularity and the knowledge of textile composites properties and applications grows, the need for 3D textile fabrics with greater thickness and more complex pattern rises significantly, creating challenges for textile manufacturing. Textile products are designed to withstand very tough loading conditions that the textile manufacturing machines may be damaged during weaving processes. The influences of textile fabrics on weaving machines during manufacturing process becomes an important research topic in order to improve manufacturing safety, productivity and efficiency.

The relationship between design and manufacturing process parameters and fabric micro-geometries, and the relationship between manufacturing process and machine behavior are crucial in order to effectively produce textile fabrics with desired mechanical properties. However, numerical textile models published to date, including TexGen, WiseTex and DFMA's dynamic relaxation, are established based on laboratory data, including measurements of existing fabric unit cells and observation of fabric topologies and micro-geometries under micro-scope, which cannot fully account for weaving process kinetics and kinematics, and cannot instruct the

design and manufacturing process of fabric. The popularity of textile composites, the complexity of the production process and structures of fabrics leads to the need for a reliable and efficient approach that can virtually simulate the textile weaving and braiding process, in order to 1) connect weaving machine actions with fabric pattern and micro geometries, 2) study the effects of weaving process parameters, 3) instruct the fabric design and manufacture, 4) study fabric damage during weaving process, 5) study machine load during weaving process.

The objective of the research was to dynamic weaving process simulator to satisfy this need. The aim of this simulator was to simulate the actual textile weaving process in order to derive 3D fabric micro-geometry and study weavability of certain weaving processes. Work needed in order to develop this simulator includes: 1) Establish a digital model to represent yarns and fibers in textile fabrics; 2) Identify the major components of a Jacquard machine which are necessary and sufficient to perform all the weaving functions; 3) Identify the parameters of the fabric and the textile machine for modeling of machine structure and actions; 4) Create a mathematical algorithm to simulate all principal weaving actions and calculate fiber deformation and machine load with necessary input data.

The dynamic weaving process simulator implemented the digital element approach, strictly followed the physics of manufacturing process, and simulated all weaving actions and process dynamics. This dissertation presents the dynamic weaving process simulator and the simulation method is explained in detail. Various fabrics generated by the simulator are also presented. The effects of weaving process dynamics, such as yarn tension, weaving velocity, reed spacing, beating-up velocity, and friction coefficient on fabric micro-geometry and machine load are discussed.

Chapter 3 - 3D Dynamic Weaving Process Simulator

Development of the dynamic weaving process simulator requires in-depth knowledge of weaving machine structure and the weaving process. In order to implement accurate modeling and simulation, key components of a weaving machine must be identified and process dynamics must be studied.

3.1 Weaving Machine Structure

Figure 3-1 illustrates the basic structure of a 2D weaving machine. A weaving machine interlaces two distinct sets of yarns, referred to as the warp and the weft. As illustrated in Figure 3-1, warps are the long green yarns runs lengthwise, and weft yarns runs across the width of the fabric [41] . Major components of a weaving machine include: harnesses, heddles, shuttle, reed and take-up roll.

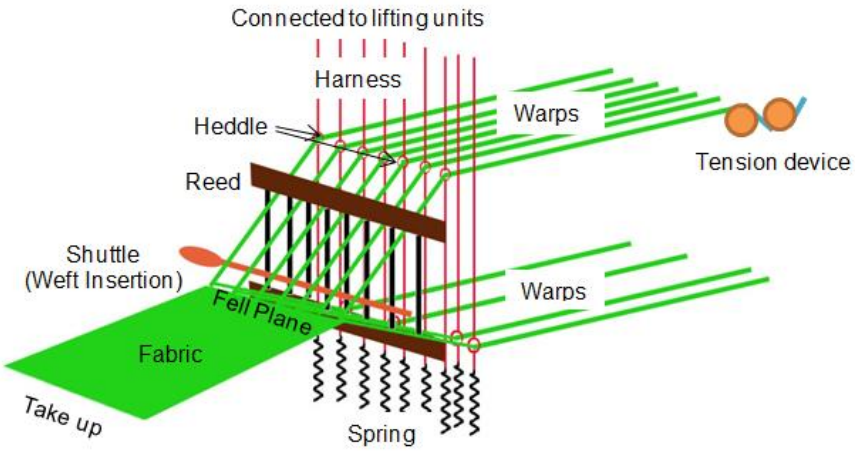

Figure 3-1. Weaving machine

3.1.1 *Harnesses and heddle*

Harnesses are cords arranged vertically, as illustrated in Figure 3-1, the upper ends of harness cords are connected to lifting units and lower ends are connected to springs. Heddles are carrier devices for warp yarns. One heddle is attached to one harness cord and each heddle contains an eye, and each warp yarn passes through the eye of one heddle. Harnesses cords move vertically during weaving and change up/down positions of attached heddles. Heddle positions control the weaving motions of warp yarns and determines fabric interlacing pattern. In Jacquard Loom, each harness cord has an individual lifting unit, allowing independent control of each warp yarn; therefore Jacquard Loom enables maximum flexibility of weaving actions. Portions of warp yarns in front of heddles participate in the weaving action and the portions of warp yarns behind the heddles are stored length released continuously during weaving and used in subsequent weaving actions. During weaving heddles change positions following harness and generate various fabric patterns. Warp yarn tensions are controlled by tension devices connected to the ends of warp yarns, as illustrated in Figure 3-1.

3.1.2 *Shuttle*

Shuttle is the carrier device for weft yarns and it inserts weft yarns into fabric during weaving. As illustrated in Figure 3-1, the fell position is defined at the edge of fabric where new fabric is formed. Heddles lift or lower connected warp yarns to form a space between fell and heddle for shuttle motion. Shuttle is located near the fell in which the weft yarn is stored, and it moves across the fabric and lays one weft yarn. In modern weaving technology, advances in the weaving industry have changed the method of weft insertion from shuttle to shuttle-less weaving. In the illustration of weaving machine structure, the term “shuttle” represents any kind of weft insertion device, such as a rapier, projectile, or fluid jet [39][40].

3.1.3 *Reed and take- up roll*

The reed is a comb-like frame structure. Warp yarns proceed through intervals of the reed according to pre-designed warp sections and fabric structure. During manufacturing, the reed pushes weft yarns into the fabric. A take-up roll is located on the left end of the fabric in order to roll up woven fabric during continuous weaving.

3.2 Weaving Actions

A weaving cycle primarily consists of four actions: weft insertion, beating-up, weaving and taking-up. Multiple weaving cycles are required in order to produce whole fabric.

In the first step, the shuttle moves across the loom near fell, laying down a weft yarn between the space formed by lifted and lowered warp yarns. A beating-up action follows the weft insertion step. The reed begins at its original position and moves towards fell, beating the inserted weft yarn against the portion of fabric that has already been formed. This beating-up action stops at fell and then the reed returns to its original position. In the weaving action, each harness cord is alternatively lifted or lowered to change the position of the attached heddle. Warp yarns follow the motion of the heddles, moving upward or downward while generating various fabric patterns. The warps are separated by the comb-like reed. Yarns of one or multiple warp sections pass through one reed interval according to fabric pattern design. Reed interval width determines the distance between warp sections. The newly constructed fabric is collected by the take-up roll. Take-up action determines the distance between neighboring weft columns.

In 2D weaving machine only one layer of weft yarn and one layer of warp yarn are interlaced to produce 2D woven fabric. 3D weaving machine have similar structure with 2D machine. Major components of a 3D weaving machine also include harnesses, heddles, shuttle,

reed and take-up device. The only difference is that multiple layers of weft and warp yarns are used in 3D weaving and each warp yarn is controlled by individual harness and heddle.

3.3 Weaving Matrix

The Weaving Process Simulator implements a weaving matrix to control warp yarn positions at each step. The weaving matrix can be input directly by user and also can be generated by the simulator with user-defined unit cell topology. The weaving matrix instructs warp weaving motions throughout the entire weaving process and target 3D woven patterns can be produced through dynamic weaving process simulation.

3.3.1 *Weaving matrix determines unit cell topology*

Weaving pattern is determined by heddle positions in each weaving action, and heddle positions are defined by a weaving matrix. In Jacquard Loom, the upper end position of each harness cord (position of each heddle) is controlled independently, enabling design of a 3D fabric with a complex weaving pattern.

In the 3D weaving process introduced in Section 3.3, multiple weaving actions are required to produce one unit cell. A weaving matrix is implemented to control positions of each warp yarn at each weaving step, so that the weaving matrix instructs the entire weaving process and determines the yarn interlacing pattern. One weaving matrix defines heddle positions of all warp yarns belonging to one warp section. One unit cell generally contains multiple warp sections, so the weaving pattern must be defined by multiple weaving matrices. In dynamic weaving process simulator, a weaving matrix to produce one unit cell is separately defined for each warp section and a weaving matrix for the entire fabric is generated automatically.

Weaving matrix size indicates the number of yarns in one unit cell. The column number of a weaving matrix generally equals the number of warp yarns in one unit cell, and the row number equals the step number to weave one unit cell. This is also the number of weft yarns of one unit cell because one weft yarn is inserted in one step. Elements in a weaving matrix represent the up and down positions of heddles. Each element typically specifies one warp yarn's position at one weaving step.

Table 1. A Simple weaving matrix

	Warp 1	Warp 2	Warp 3
Step 1	up	down	down
Step 2	up	up	down
Step 3	down	down	up
Step 4	down	up	up

Table 1 is a weaving matrix example and the weaving process controlled by the matrix is shown in Figure 3-2 (a). The weaving matrix has three columns and four rows, indicating three warp yarns and four weft yarns in one unit cell. The first row of the weaving matrix defines warp positions for weaving step 1: warp 1 is at up position, warp 2 and 3 are at down position. As demonstrated in Figure 3-2 (a) step 1 of warp 1(purple) is at up position, warp 2(red) and 3(green) are at down position, and one weft yarn is inserted into the structure. The second row of the weaving matrix defines the warp pattern for step 2: warp 1 and 2 are at up position, and warp 3 is at down position. The step 2 in Figure 3-2 (a) shows such warp pattern and the second weft is then inserted. Similarly, in step 3, warps 1 and 2 move to down positions and warp 3 moves upward. In step 4, warp 2 moves up. These four steps complete one weaving cycle and generate a unit cell as shown in Figure 3-2 (b). A total of four wefts are inserted during one weaving cycle.

The process continues as warps return to positions as defined in step 1, then a new weaving cycle begins. The weaving matrix that defines the weaving cycle is shown in Table 1. The weaving matrix controls the position of each warp yarn in every weaving step.

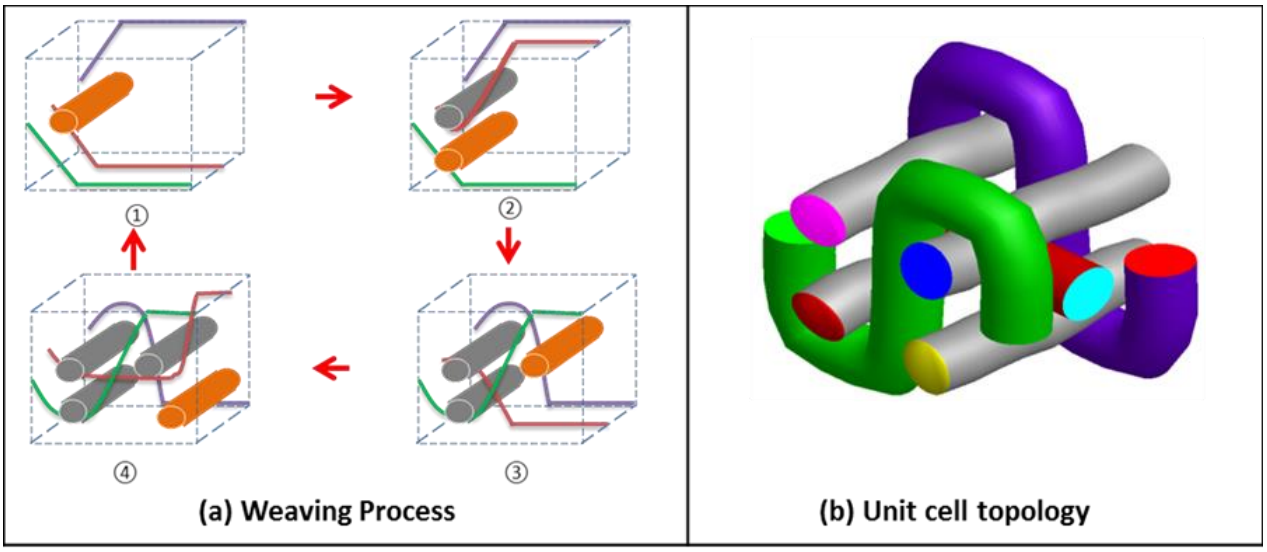

Figure 3-2. Weaving process and unit cell topology

3.3.2 *Define weaving matrix for target fabric pattern*

The weaving matrix is an instructive matrix that controls heddle positions during the weaving process and determines unit cell topology. Therefore, a weaving matrix should be defined according to the warp pattern of target fabric unit cell topology in order to implement weaving process simulation. Warp yarns with axial lines on one plane are defined as warp yarns in one warp section. Weaving matrix should be defined according to warp interlacing pattern of each section in order to produce target fabric unit cell topology.

Dynamic Weaving Process Simulation provides two options for weaving matrix input: 1) direct input: input heddle up/down positions for each yarn at each step; 2) warp pattern input:

input unit cell topology based on warp interlacing pattern and weaving matrix is generated automatically.

3.3.2.1 *Direct input weaving matrix*

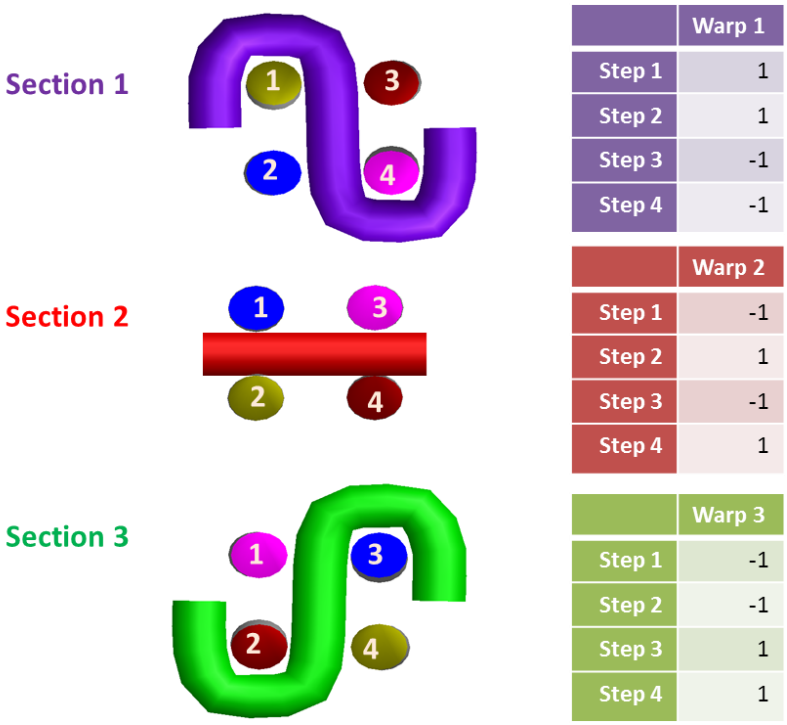

	Warp 1
Step 1	1
Step 2	1
Step 3	-1
Step 4	-1

	Warp 2
Step 1	-1
Step 2	1
Step 3	-1
Step 4	1

	Warp 3
Step 1	-1
Step 2	-1
Step 3	1
Step 4	1

Figure 3-3. Define weaving matrix

Unit cell topology shown in Figure 3-3 is an example of a weaving matrix definition. The unit cell includes three warp sections, with one warp yarn in each section. In order to define weaving matrix for this unit cell pattern, each weft yarn receives an ID. The ID of weft yarns also represents the insertion sequence number. After ID numbers are assigned to all weft yarns, elements of weaving matrix for the unit cell can be defined. Weaving matrices for each warp section are demonstrated in Figure 3-3. The number of columns equals the number of weft yarns in a unit cell, and the number of rows equals the number of warp yarns in a warp section. “-1” is

used to represent warp down position and "1" is used to represent up position while defining weaving matrix for convenience. As demonstrated in section 1 of Figure 3-3, warp 1 is above weft 1 and weft 2, but below weft 3 and weft 4. Therefore, warp 1 should be at the up position in weaving steps 1 and 2 and at the down position in the remaining steps until the machine cycle is completed. As shown in the weaving matrix for warp section 1 in Figure 3-3, warp positions are defined as "1" for step 1 and 2, and "-1" for step 3 and 4. Weaving matrices of each section can be defined with this method and a weaving matrix for the entire unit cell can be generated.

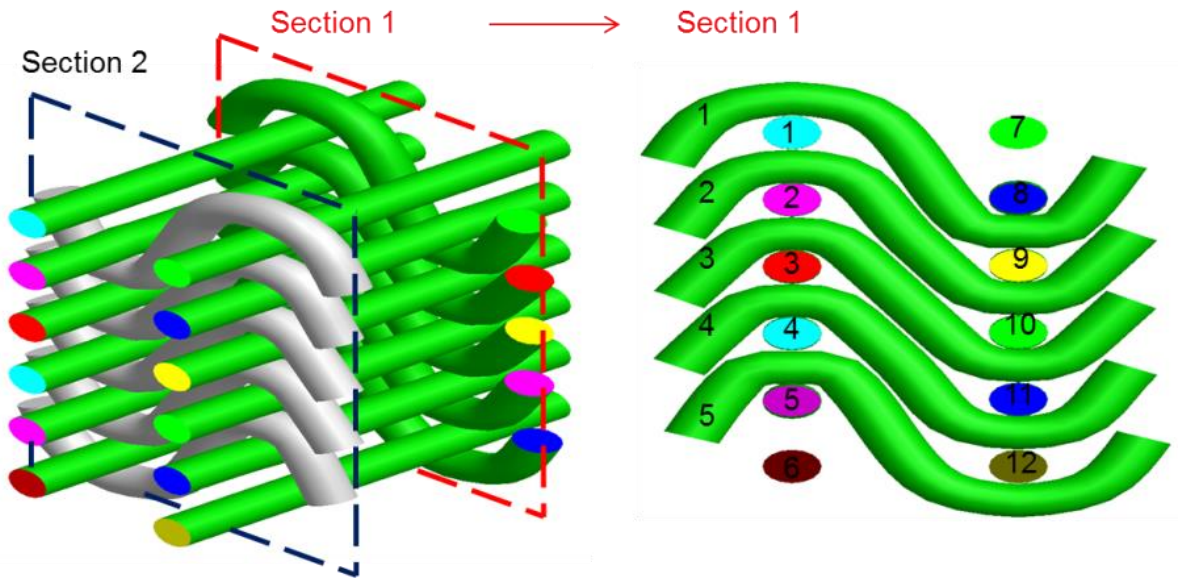

Figure 3-4. Target unit cell topology

As an expansion of the direct input method, a more complex unit cell is shown in Figure 3-4 as an example; the unit cell includes two warp sections, with five warp yarns in each section. For clarity and convenience, weaving matrix is defined section by section.

Table 2. Weaving matrix for target unit cell topology

	warp 1	warp 2	warp 3	warp 4	warp 5
step 1	1	-1	-1	-1	-1
step 2	1	1	-1	-1	-1
step 3	1	1	1	-1	-1
step 4	1	1	1	1	-1
step 5	1	1	1	1	1
step 6	1	1	1	1	1
step 7	-1	-1	-1	-1	-1
step 8	-1	-1	-1	-1	-1
step 9	1	-1	-1	-1	-1
step 10	1	1	-1	-1	-1
step 11	1	1	1	-1	-1
step 12	1	1	1	1	-1

For the warp section 1 shown in Figure 3-4, 12 weft yarns are arranged in two columns and six layers. Each weft yarn has an ID, starting from 1. The ID of weft yarns also represents the insertion sequence number. For example, weft yarn 1 will be inserted in step 1 and weft yarn *i* will be inserted in step *i*. In addition, each warp yarn also receives an ID number, starting from 1. After ID numbers are assigned to each yarn, the weaving matrix for the unit cell can be defined. Table 2 shows a 12×5 weaving matrix for the first warp section. The number of columns equals the number of weft yarns in a unit cell, and the number of rows equals the number of warp yarns in this warp section. In Figure 3-4, warp 1 is below weft 1 and weft 2, but above all other weft yarns. Therefore, the heddle of warp 1 should be located at the lower position in weaving steps 1 and 2 and at the upper position in the remaining steps until the machine cycle is completed (Table 2). Heddle positions of warp 1 in the machine cycle are listed in the first column of the weaving matrix. In steps 1 and 2, heddle positions are defined as "-1",

meaning “lower position”. From steps 3 to 12, heddle positions are defined as “1”, meaning “upper position.” Similarly, warp 2 is below weft 1, 2, 3 and 7. Therefore, “-1” is used to define the heddle position of warp 2 in steps 1, 2, 3, and 7. In the other weaving steps, the heddle should be in the upper position, represented by “1” in the warp 2 column. Using the same principles, heddle positions of warps 3, 4, and 5 can be defined, as listed in the third, fourth, and fifth columns of the weaving matrix, respectively.

3.3.2.2 *Unit cell topology input*

In the examples demonstrated in section 3.3.2.1, weaving matrix is input according to unit cell topology to generated target interlacing pattern. Dynamic weaving process simulation also allows users to input unit cell topology with warp pattern matrix; weaving matrix can be automatically generated with the warp interlacing pattern. Fabric design typically begins with interlacing pattern sketching and weaving matrix for manufacturing is calculated manually based on fabric unit cell topology design. The demonstrated steps in section 3.3.2.1 to calculate only one section of weaving matrix for the six layer fabric example require a great amount of work. In addition, a miss typing of “1” and “-1”may result in an invalid matrix and produce inaccurate simulation results. For very complex fabric topologies involving more layers and columns of weft yarns and sections of warps, the weaving matrix definition process becomes even more burdensome. In Dynamic Weaving Process Simulation, warp position matrix allows users to input fabric unit cell topology for complex patterns and weaving matrix is automatically generated.

Figure 3-5 demonstrates warp interlacing patterns of two warp sections from unit cell topology shown in Figure 3-4. Circles in the illustration represent weft yarns and solid lines represent warp yarns. The unit cell has six layers and two columns of weft yarns with two warp

sections, and interlacing pattern is shown in Figure 3-5. As introduced in the direct weaving matrix input section, two 12 × 5 matrices are required in order to define weaving matrix for this unit cell pattern. The direct weaving matrix input method is very time consuming and error prone.

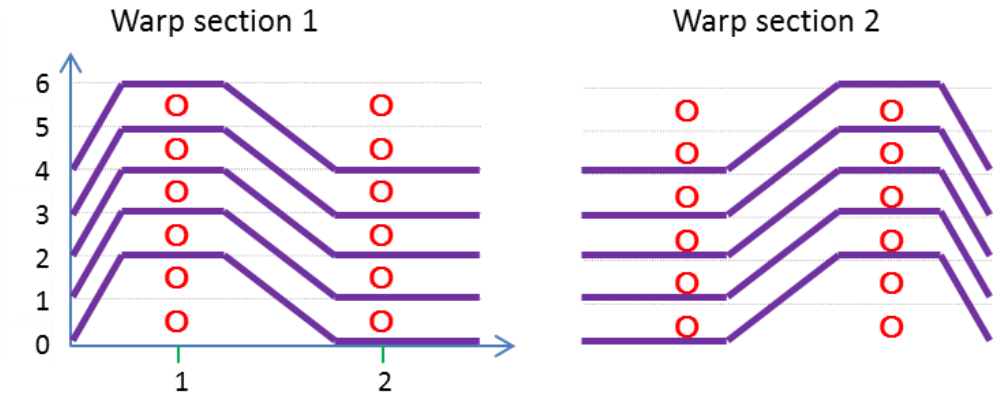

Figure 3-5. Warp interlacing pattern

Warp position matrices demonstrated in Figure 3-6 provide a simpler input option to define weaving matrix. A weaving matrix for the unit cell pattern specified by warp position matrix can be automatically generated. Warp position matrix is defined for each section. As shown in Figure 3-6, each warp yarn in one section receives an ID, from top to bottom. The size of warp position matrix for one section is determined by weft column number per unit cell and total warp number of the section. For the example in Figure 3-6, one 2×5 matrix is input for each section, that is much smaller than the weaving matrix from direct input. Each element in a warp position matrix indicates the interlacing position of the corresponding warp yarn at corresponding weft column. Interlacing position data can be found at the vertical axis, and is determined by weft layer numbers. For example, warp 1 is a weaver yarn that interlaces at the 6^{th} layer of weft yarns for the first weft column and at the 4^{th} weft layer for the second weft column.

In the first row of warp position matrix, interlacing position 6 and 4 are respectively defined for corresponding columns. Similarly in the warp pattern illustrated in Figure 3-6, warp 1 is at interlacing position 4 at the first weft column and position 6 at the second weft column; therefore 4 and 6 are input respectively in the first row of warp position matrix.

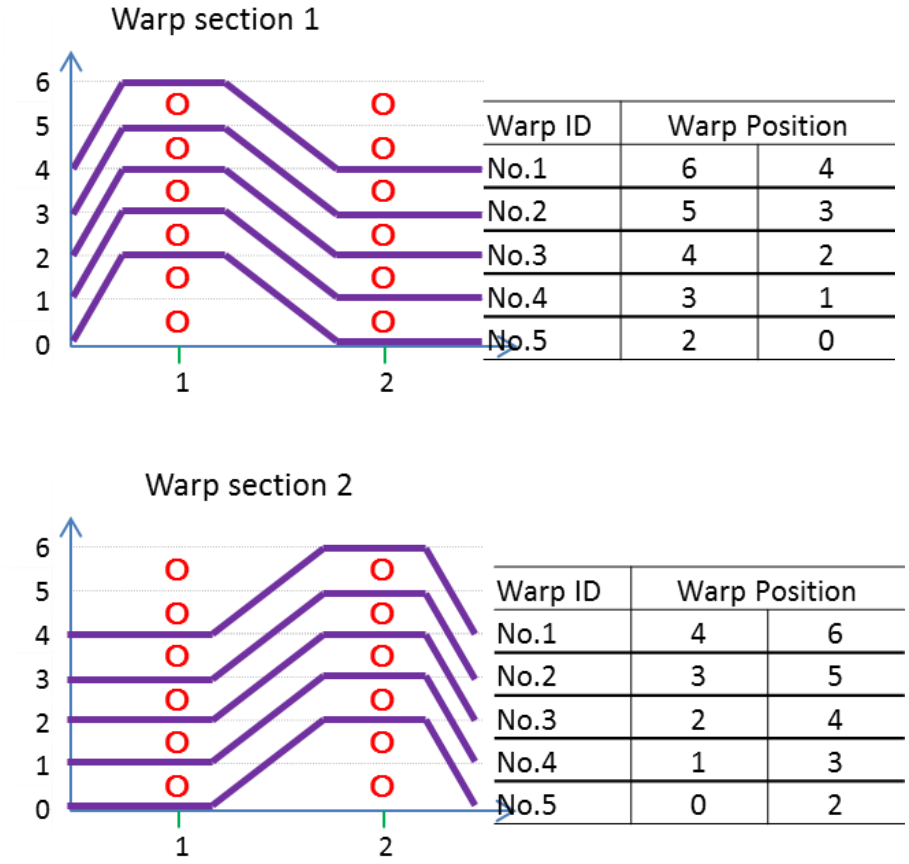

Warp ID	Warp Position	
No.1	6	4
No.2	5	3
No.3	4	2
No.4	3	1
No.5	2	0

Warp ID	Warp Position	
No.1	4	6
No.2	3	5
No.3	2	4
No.4	1	3
No.5	0	2

Figure 3-6. Warp position matrix

Warp position matrices for all warp sections must be defined by user and weaving matrix can be generated automatically in Dynamic Weaving Process Simulation. An algorithm to derive weaving matrix from warp position matrix was designed, which translates one row of a warp position matrix into a column of weaving matrix. From the interlacing position in a warp position

matrix, weft yarns above and below the corresponding warp yarn can be derived. For example, as shown in warp section 1 of Figure 3-6, the first row indicates that there are six weft yarns below warp 1 in the first column and four weft yarns below warp 1 in the second column. Because weft yarn ID is considered weaving step ID while defining weaving matrix, so heddle up position is defined for the first to sixth layers of weft yarns in the first weft column and first to second layers of weft yarns in the second weft column.

Two options are available for weaving matrix definition and weaving process control. The direct matrix input method allows users to define warp yarn up/down positions at each weaving step and is applicable to relatively simple unit cell patterns and circumstances when unit cell pattern is not available. Warp position matrix provide an option for complex unit cell patterns. It allows users to define unit cell topology through input interlacing positions of warp yarns. Weaving matrix is generated automatically in order to generate target unit cell topology.

3.4 Dynamic Weaving Process Simulation

3.4.1 *Establishment of simulation model*

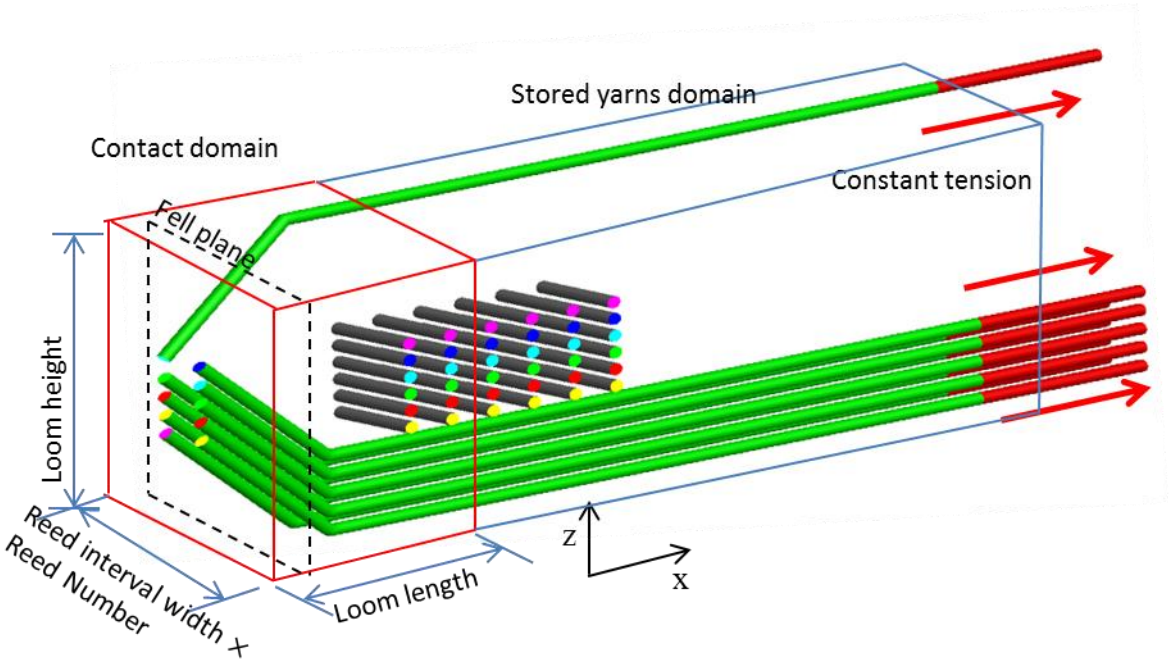

Figure 3-7. Simulation model

The digital element approach [1]-[4] is employed for textile process simulation. The simulation model is established based on machine structure and weaving process introduced in Chapter 3.2. Target unit cell topology is shown in Figure 3-4. The initial ready-to-weave pattern is simulated as shown in Figure 3-7. In the simulation model, warp yarns are parallel to the x-axis and weft yarns are parallel to the y-axis. Parameters required to build and simulate the model include:

1) Yarn properties: cross-section area, Young's modulus, density
2) Weft pattern: weft column, weft layer
3) Warp pattern: warp section, warp layer per section, weaving matrix
4) Machine data: reed number, reed interval width, loom length, loom height
5) Dynamic weaving process parameters: weaving matrix, beating-up velocity, weaving velocity, taking-up velocity, yarn tension, friction

In the simulation model, full scale fabric simulation can be implemented because periodical boundary is adopted in weft direction. User can model one unit cell in y-direction, or the fabric width direction and fabric micro-geometry can be assembled with periodical boundary condition. The number of warp yarns in the simulation model equals the number of warp yarns in one unit cell. Warp yarns belonging to one warp section are placed in a plane perpendicular to the y-axis. One or multiple warp sections can present in one reed interval, and warp sections are evenly distributed within the reed interval width. As shown in Figure 3-7, two warp sections were arranged in two reed intervals, located in the center of the reed intervals. The left warp yarn ends were simply assumed to be a fixed boundary. A tension spring element was attached to the right end of each warp yarn, thereby applying a constant tensional force to the yarn and simulating the function of tension devices.

Weft yarns are stored inside the shuttle and inserted at fell in a weaving machine. In the simulation model, the user defined the number of weft layers and weft columns per unit cell and the number of unit cells to produce. For this example, six layers of weft yarns in two columns, and three unit cells were fabricated in simulation. As shown in Figure 3-7, all weft yarns waiting to be woven were initially stored in the back of the model. A total of six columns of weft yarns were presented. The interval of two neighboring weft columns was determined based on the taking up speed of a weaving machine. During weaving, one weft yarn was moved to the position of the fell at each weft insertion step.

The simulation model was divided into three domains: contact search domain, stored yarns domain and tensile spring domain. The size of contact search domain was defined according to heddle positions of a weaving machine. The front plane of contact search domain was at fell, defined as the x=0 plane, as shown in Figure 3-7, and the back plane was at heddle

position, defined as x=loom length plane. The height of the domain in fabric thickness direction was defined by loom height according to the distance between heddle up and down positions. Therefore, the contact search domain was defined by loom length and loom height, which also determined the slope of the portion of warp yarns within the domain. In numerical simulation, warp yarns were lifted or lowered to form a space for weft to enter, and interlaced inserted weft yarns to form textile fabrics in the contact search domain,.

The stored yarns domain was defined by stored warp yarn length. It contained the part of model from heddle position to the start of constant tension springs, as shown in Figure 3-7. Warp and weft yarns in this domain were stored yarns waiting to be woven.

During weave simulation, nodal contacting relationships were only identified within the contact search domain at each simulation step; fiber-to-fiber compression forces and friction forces were calculated. Tensions for all elements inside and outside the contact search domain were calculated. Nodal acceleration, velocity and displacements were calculated based on an explicit procedure. In the stored yarns domain, warp yarn nodal movements in the z-direction were constrained based on the weaving matrix and weaving velocity, which instructed warp yarns motions.

3.4.2 *Yarn structure and internal force calculation*

In the initial simulation model, only single-chain yarns were used. In reality, though, one yarn consists of thousands of fibers. Therefore, the digital element method was implemented in order to utilize a bundle of digital chains to represent an individual yarn. However, simulation of each fiber as a digital chain is not feasible due to computing resources, so one digital chain in simulation represents a bundle of real fibers. Seven to thirty-seven digital fibers per yarn

typically are adequate to predict fabric micro-geometry. The simulation model was then further discretized into fiber level model, using the yarn discretization method by Huang [1][2].

The weaving process described in Section 3.2 determines fabric topology. The number of reed sections per unit cell and reed interval widths control the distance between warp sections and unit cell width. The take-up flags per column and take-up distance determine distance between weft columns and unit cell length. Weaving matrix controls warp position in each weaving step and determines interlacing pattern. However, fabric properties are not only determined by fabric topology, but also detailed fabric micro-geometry, which is determined by weaving process kinetics. Weaving process kinetic parameters include weaving velocity, beating-up velocity, yarn tension and inter-yarn friction. These parameters affect fiber deformation during manufacturing and determine fabric micro-geometry, thickness, and volume of fraction.

Two types of forces are considered in the Dynamic Relaxation model: tension induced force and fiber-to-fiber compression induced force. Fiber-to-fiber friction is neglected in this model. However, frictions significantly impact fabric micro-geometries and they affect fabric mechanical properties. To improve simulation accuracy, the Dynamic Weaving Process Simulation considers tension induced force, fiber-to-fiber compression force and fiber-to-fiber friction force. In beating-up action, reed impacts inserted weft towards woven fabric. Reed is simulated as cylindrical bars with user defined diameter and reed impact load is calculated by contact force between reed and fabric. In weaving and taking-up action, spring elements attached to the end of warp yarns apply constant tensile force to yarn end nodes. Fiber-to-fiber friction and contact are calculated during the entire weaving process simulation.

Tension-induced force and fiber-to-fiber compression force have been introduced in previous literatures [10]-[13] and are briefly introduced here for an integral view of Digital Element Approach.

3.4.2.1 *Tension-induced force*

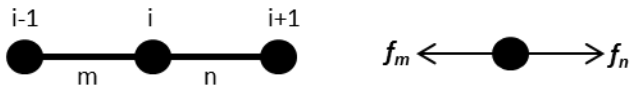

Figure 3-8. Tension induced force

Tension induced nodal forces are calculated using element length. As shown in Figure 3-8, *m* and *n* are two elements connected by node *i*. To calculate nodal force on node i:

$$f_m = EA\frac{l_m - l_o}{l_o}$$
$$f_n = EA\frac{l_n - l_o}{l_o} \quad (1)$$

Where E is the fiber longitudinal modulus; A is the fiber cross section area; l_m and l_n are deformed element lengths of *m* and *n*; and l_o is the original element length. The nodal force on node *i* is:

$$f_{ti} = \overrightarrow{f_m} + \overrightarrow{f_n} \quad (2)$$

3.4.2.2 *Compression force calculation*

Nodal contacting forces must be calculated when contacts are determined. The direction of contact force is calculated based on coordinates of neighboring nodes of the pair of contacting nodes, as introduced in the literature [10].

Contact stiffness is calculated as:

$$k_n = \frac{E_T A_c}{l_c} \tag{3}$$

Where E_T is the digital fiber transverse modulus; l_c is the contact distance between two nodes; l_e is element length, and A_c is the contact area. The contact area is given by:

$$A_c = 2al_e$$
$$a = \sqrt{R^2 - (R - \frac{\delta}{2})^2} \approx \sqrt{R\delta} \tag{4}$$

Compressive force between two digital fibers is calculated as

$$f_{ci} = \int_0^{\delta} k_n \, d\delta = \frac{4E_T l_e \sqrt{R} \delta^{\frac{3}{2}}}{3l_c} \tag{5}$$

3.4.2.3 ***Fiber-to-fiber friction***

Fiber-to-fiber friction during the manufacturing process has important effect on fabric micro-geometries and fabric damage. Friction is not considered in Dynamic Relaxation model. In order to improve simulation accuracy, nodal friction forces are calculated when contacts are detected in Dynamic Weaving Process Simulation. When the distance between two nodes from two fibers is smaller than fiber diameter during contact search, a contact element and a friction element are established and recorded.

The method to determine nodal compression force direction must be introduced in order to determine nodal friction. The direction of the contact force is calculated based on coordinates of neighboring nodes of the pair of contacting nodes. As illustrated in Figure 3-9, ***n*** and ***n'*** is a pair of contacting nodes, and ***n-1***, ***n+1***, ***n'-1***, ***n'+1*** are neighboring nodes of ***n*** and ***n'***. Vector cross product is calculated to derive vector $\vec{N}$, which is perpendicular to $\overrightarrow{nn'}$ and $\overrightarrow{(n-1)(n+1)}$:

$$\vec{N} = \overrightarrow{nn'} \times \overrightarrow{(n-1)(n+1)} \tag{6}$$

Vector cross product is calculated to derive vector $\overrightarrow{d_n}$, which is the direction vector of contact force, perpendicular to $\vec{N}$ and $\overrightarrow{(n-1)(n+1)}$:

$$\overrightarrow{d_n} = \vec{N} \times \overrightarrow{(n-1)(n+1)} \tag{7}$$

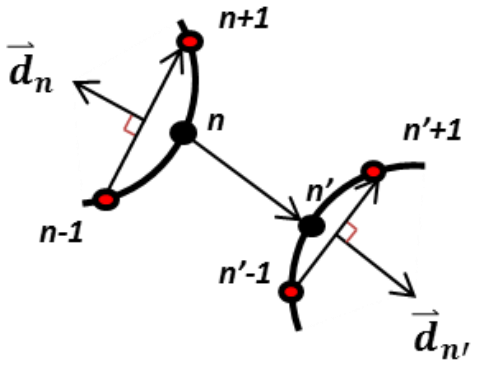

Figure 3-9. Nodal compression force

A similar procedure is taken to derive contact direction on node ***n'***, as illustrated in Figure 3-9. All direction vectors derived are transformed into unit vectors for future use.

Nodal friction is calculated based on nodal compression force. An original contact directional vector from target node 1 pointing at contacting node 2, $\vec{d}_{org}$ and an identifier

$F_{ID} = 1$ are recorded when a friction element containing node 1 and node 2 is established during contact search, as illustrated in Figure 3-10 (a).

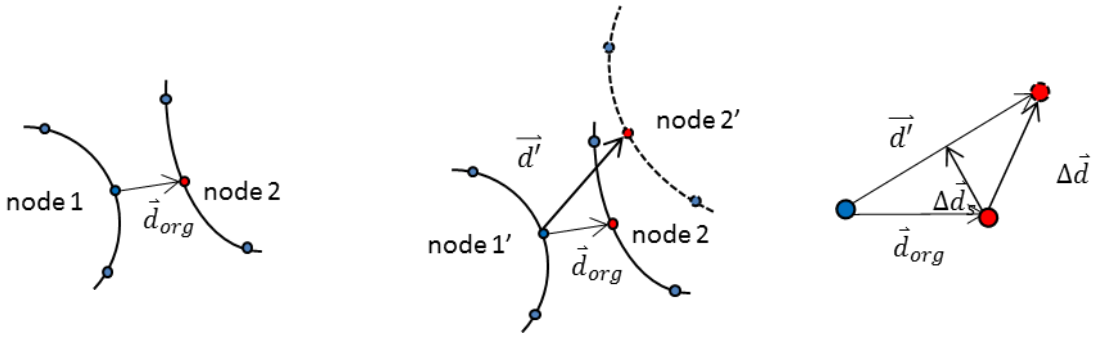

(a) (b) (c)

Figure 3-10. Friction calculation

As illustrated in Figure 3-10 (b), node 2 then moves to a new position node 2' due to fiber deformation, and another directional vector $\overrightarrow{d'}$ is calculated using deformed nodal coordinates of node 1' and node 2'. As shown in Figure 3-10 (c), friction element deformation is calculated as:

$$\Delta\vec{d} = \overrightarrow{d'} - \vec{d}_{org} \tag{8}$$

Friction force is calculated as:

$$f = k_n \mu |\Delta\vec{d}_s| \tag{9}$$

Where k_n is contact element stiffness, μ is the friction coefficient, and $\Delta\vec{d}_s$ is the vector component of $\Delta\vec{d}$ perpendicular to $\overrightarrow{d'}$. If $f > \mu f_{ci}$, sliding will occur and then let $f_s = \mu f_{ci}$, where f_{ci} denotes contact force. The direction of friction on node 2' is perpendicular to compression force direction as illustrated in Figure 3-11. Similarly the direction of friction on node 1' can be determined using compression force direction$\vec{d}_n$.

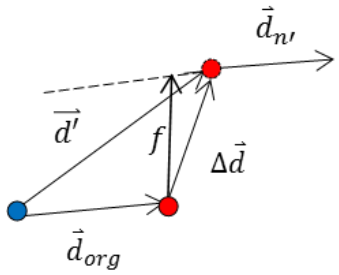

Figure 3-11. Friction direction

Nodal friction and compression forces are calculated at each time step and the original contact directional vector $\vec{d}_{org}$ is not edited during subsequent simulation time steps once contact is detected and a friction element is established through verification of the value of F_{ID}, which is set to be 1 when $\vec{d}_{org}$ is assigned an initial value. If the value of F_{ID} equals 1, no change can be made to $\vec{d}_{org}$. When the distance between contacting nodes becomes larger than fiber diameter, the friction element is deleted and F_{ID} is re-set to 0. Therefore, if a new friction element containing the two nodes must be re-established, $\vec{d}_{org}$ must be renewed.

3.4.3 *Weaving process simulation*

3.4.3.1.1 Weft yarn tension and deformation

As introduce in Chapter 3, during weaving process simulation, one weft yarn is inserted at each step, from its original position to the fell position and reed push the inserted weft yarn towards the woven fabric. Figure 3-12 (a) illustrates weft yarn deformation during the weaving process. Weft yarns are drawn from thread spools as slightly curved yarns without pre-applied yarn tension and are inserted by shuttle at a certain distance from fell. Considering the curvature, inserted weft yarn length is slightly longer than fabric nominal width, so weft length coefficient

is adopted to apply to weft yarn original element length in tension calculation. Weft length critically affects weft yarn tension.

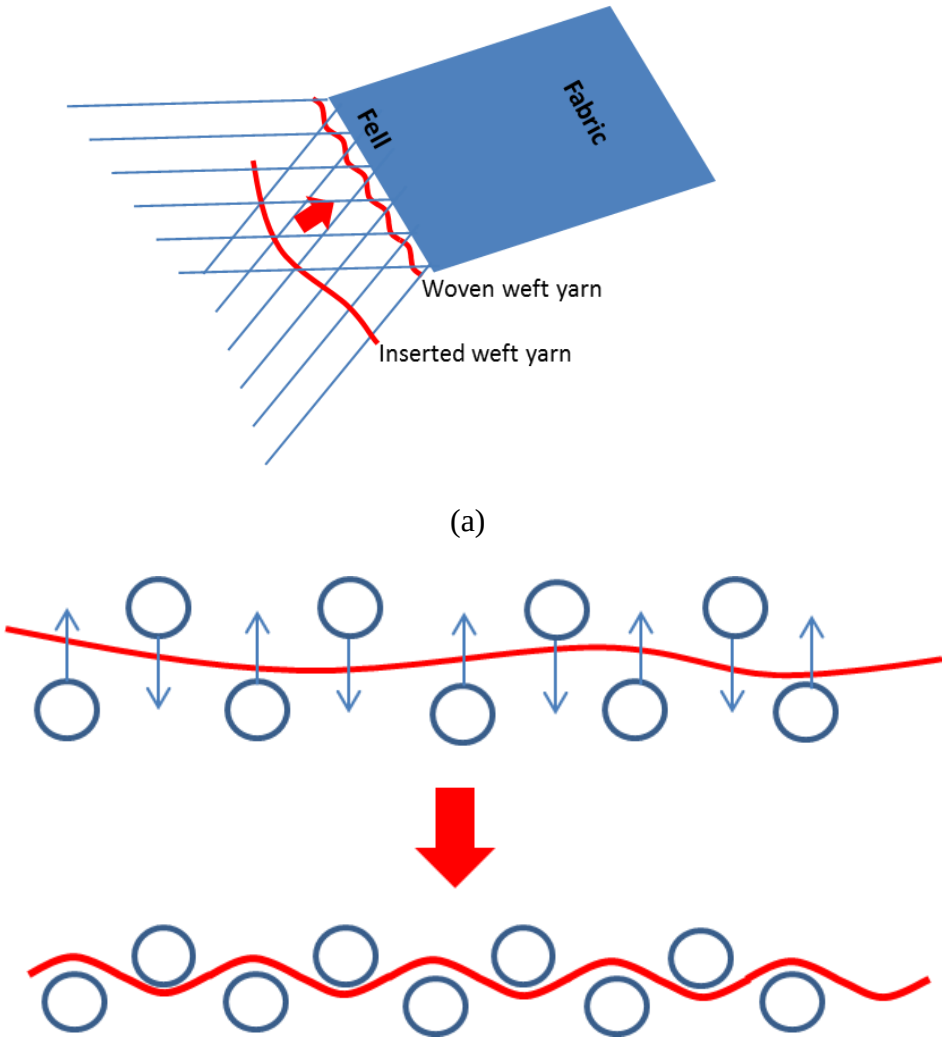

(a)

(b)

Figure 3-12. Weft deformation

Weft yarn is inserted without pre-tension, and yarn tension and deformation are developed during beating-up and weaving actions. The primary reasons for weft yarn tension and deformation development include fiber-to-fiber friction, warp yarn tension and reed impact.

Reed pushes inserted weft towards fabric and warp yarns interlace weft yarns to form woven fabric. Contacts occur during this process and nodal compression and friction prevent weft yarn motion and deformation.

3.4.3.1.2 Weft yarn defamation and tension development during weaving action

Figure 3-12 (b) illustrates weft yarn deformation and tension development during warp weaving action. Warp yarns are stretched by end tension and interlace with inserted weft yarn to form a fabric. The interlacing pattern is determined by weaving matrix introduced in Chapter 3. In Figure 3-12 (b), warp yarns, illustrated as circles in Figure 3-12 (b), force inserted weft yarn, illustrated as a solid line, to transform to sine curve in weaving action. The weaving action generates compression force and friction. Fiber-to-fiber fiction in weft direction significantly prevents inserted weft yarn from curving.

3.4.3.1.3 Weft yarn defamation and tension development during beating-up action

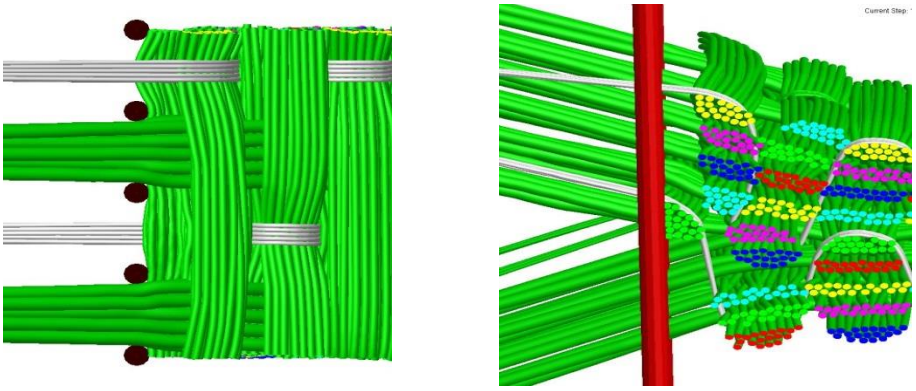

(a) Top view (b) Side view

Figure 3-13. Reed impact induced weft yarn tension and deformation

Beating-up actions following weft insertion push inserted weft yarn towards woven fabric as demonstrated in Figure 3-13. Weft yarn is inserted without pre-tension and only slightly curved. As the reed approaches inserted weft yarn, pushes it against woven fabric, nodal contacts are detected, nodal compression and friction forces are calculated and weft yarn tension and deformation are generated, as demonstrated in Figure 3-13 (a).

Interlacing warp yarns must be designed to prevent weft yarns from falling out, while simultaneously preventing weft yarns from moving in-ward and causing weft yarn tension and deformation, as demonstrated in Figure 3-13 (b). Warp yarns with larger yarn tension typically generate greater preventing force; therefore constant tension applied to warp yarns play an important role in determining fabric micro-geometry and weft yarn tension.

3.4.3.1.4 Periodical boundary in weft direction

During the fabric manufacturing process, boundary effect exists near fabric edges. Fabric micro-geometry near edges presents none-periodical properties. Fabric micro-geometry in fabric middle area is considered free from boundary effects, thereby allowing periodical boundary condition to be implemented.

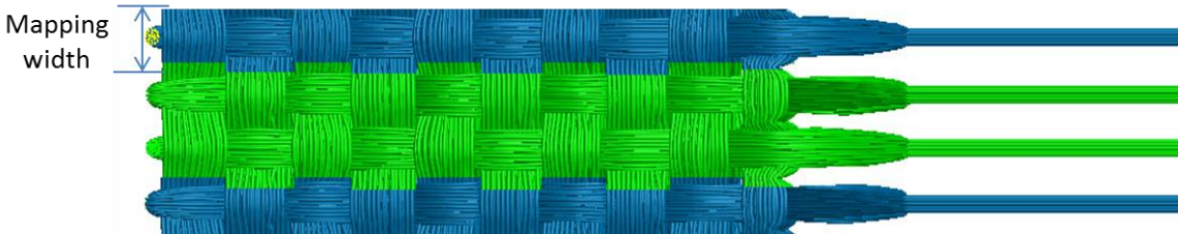

Figure 3-14. Periodical boundary in weft direction

Similar to the periodic boundary condition used in the dynamic relaxation approach [2], Dynamic Weaving Process Simulation applies a periodic boundary condition in the weft direction, as shown in Figure 3-14. The simulation domain includes a primary region and two image regions. In each simulation step, nodal forces, nodal accelerations, nodal velocities, nodal displacements and nodal positions are calculated for the primary region. Nodal positions in the primary zone are then mapped to the two image regions based on the periodic principle. Nodal positions in image zones are used to calculate contact forces in the boundary vicinity of the primary region.

3.4.3.2 ***Beating up and reed load***

After each weft insertion, the reed impacts the inserted weft yarn and pushes it towards the woven fabric, finally stopping at fell. This is the beating-up action in the manufacturing process. In simulation, reeds are modeled as cylindrical bars parallel to the z axis, as shown in Figure 3-15. These cylindrical bars move towards the fell immediately after weft insertion. The user defines initial reed position, travel distance s_r and beat-up time T of reed. Reed motion is simulated as constant acceleration motion beginning at 0m/s. Reed acceleration is calculated as:

$$a = \frac{2 \times s_r}{T^2} \tag{10}$$

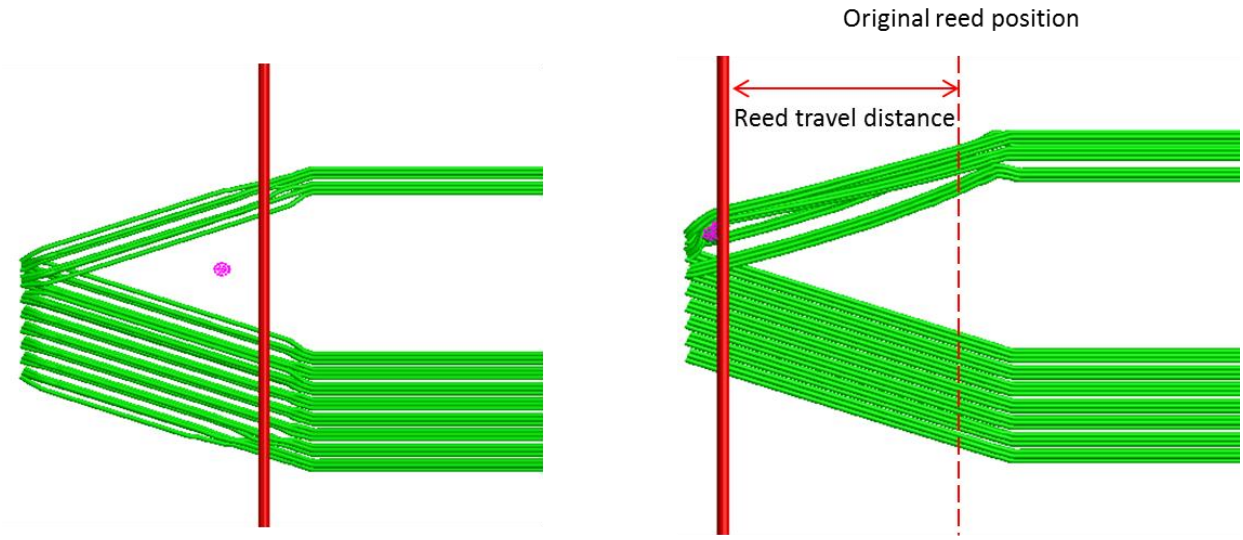

(a) Weft insertion (b) Beating-up

Figure 3-15. Weaving process (a) weft insertion, (b) beating-up

The reed continues accelerating and contacts between reed bars and yarns are identified. In addition, reed-to-fiber compression and friction forces are calculated. Reed bars are subjected to contact and friction induced forces from fabric during impact and reed load is calculated using compression and the friction forces calculation method introduced in Chapter 3. Because the original reed position is close to weft insertion position, reed velocity is small while approaching the inserted weft yarn. No significant impact force is detected at this stage. As the reed moves towards fell and approaches the woven fabric, it impacts an increasing amount of digital fibers and changes yarn cross-section shapes, as shown in Figure 3-15 (b). Reed-to-fiber contact and friction increase and load on reed varies during the process.

3.4.3.3 ***Warp yarn tension and weaving***

3.4.3.3.1 Heddle position approximation

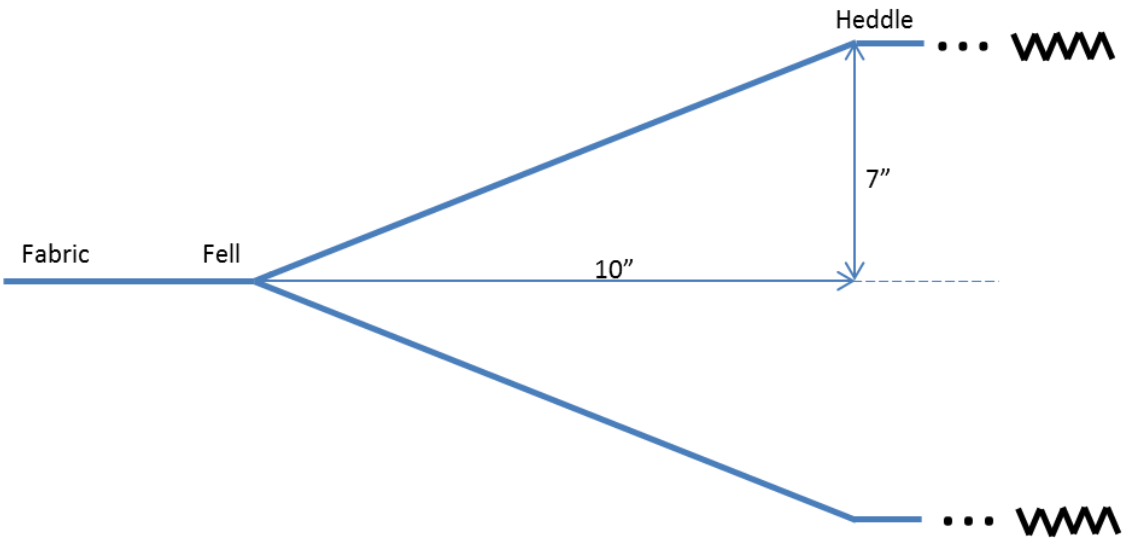

Figure 3-16. Machine heddle position

Heddle horizontal distance from fell is approximately 10 in. and vertical distance from fabric is 7 in. for a common weaving machine, as illustrated in Figure 3-16. In Dynamic Weaving Process Simulation, the size of contact search domain is determined by heddle position. Therefore, use of heddle position in simulation identical to a weaving machine creates a huge contact search domain. However, little warp and weft yarn interaction appears at the far end of domain. Contact searching, compression force calculation and friction calculation in the area have little effect on fabric micro-geometry constructed close to fell. Therefore nodal contact at the back is considered negligible.

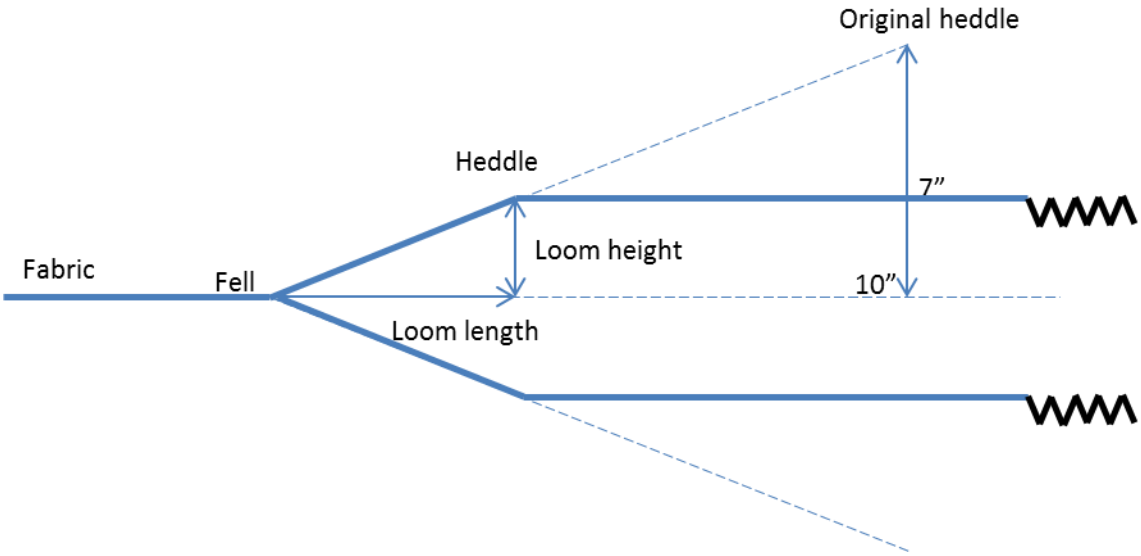

Figure 3-17. Heddle position approximation

Warp yarns pass through heddles and connect to tension devices in far area of a weaving machine. In simulation, warp yarn tension is applied through constant spring elements connected to warp yarn ends, and delivered through warp yarn nodal forces calculations as demonstrated in Section 3.4.2.1. The left yarn ends are assumed to be a fixed boundary. Heddle position has little effect on warp yarn tension during weaving process. Heddle position affects neither nodal contact nor yarn tension; therefore, the assumption is made that heddle position effect on fabric micro-geometry can be neglected.

Under such assumptions, heddle position approximation is implemented in Dynamic Weaving Process Simulation, as illustrated in Figure 3-17. Heddle position is defined by loom length and loom height, while maintaining identical ratio with machine dimension. Typically 1 in. to 3 in. loom length is adopted for most simulation according to fabric thickness. Using this approximation, contact search is performed in a much smaller domain, thereby saving computing time and resources.

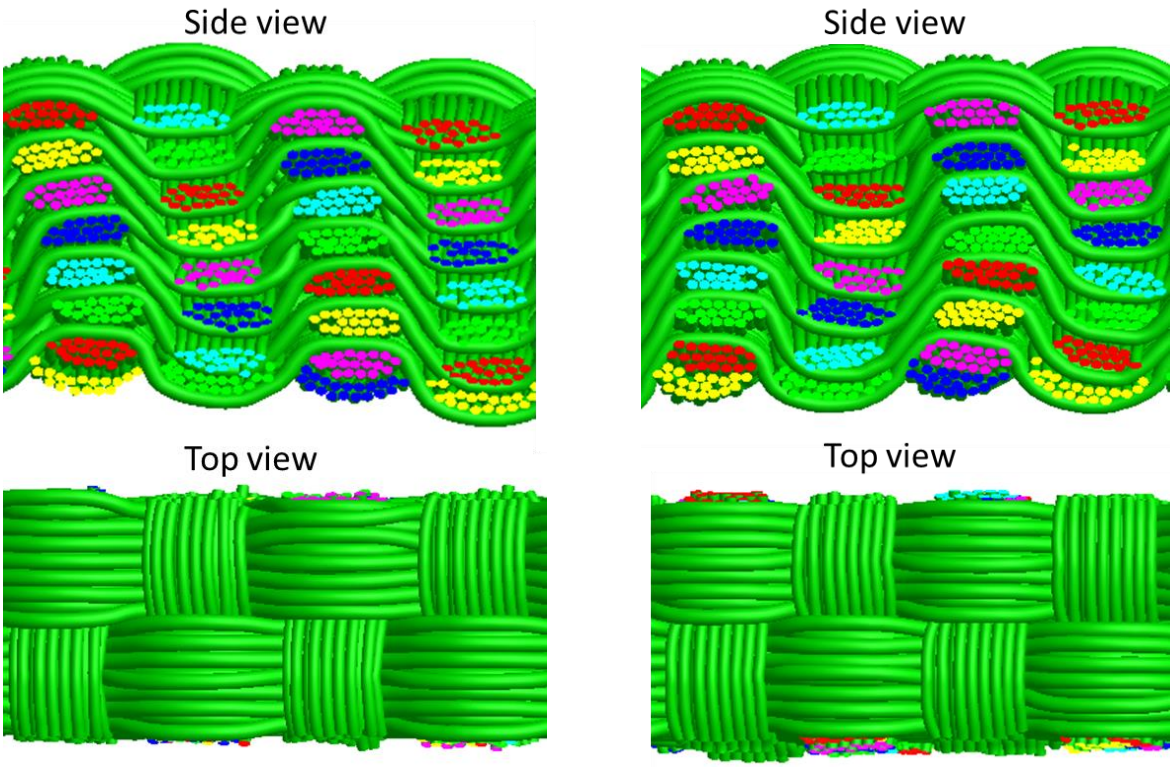

(a) 3” loom length (b) 1” loom length

Figure 3-18. Validate heddle position approximation

Two examples in Figure 3-18 validate the approximation using various loom length and loom height. Example (a) uses 3 in. loom length and example (b) uses 1 in. Both examples maintain 0.7 loom height to loom length ratio and use identical weaving process parameters. A comparison of simulated unit cells micro-geometries reveals that heddle position minimal affects fabric micro-geometry in Dynamic Weaving Process Simulation and can be neglected. However, overly small loom length and loom height is not feasible for simulation, and reasonable loom height should be set to approximately double of estimated fabric thickness.

3.4.3.3.2 Weaving process constrain

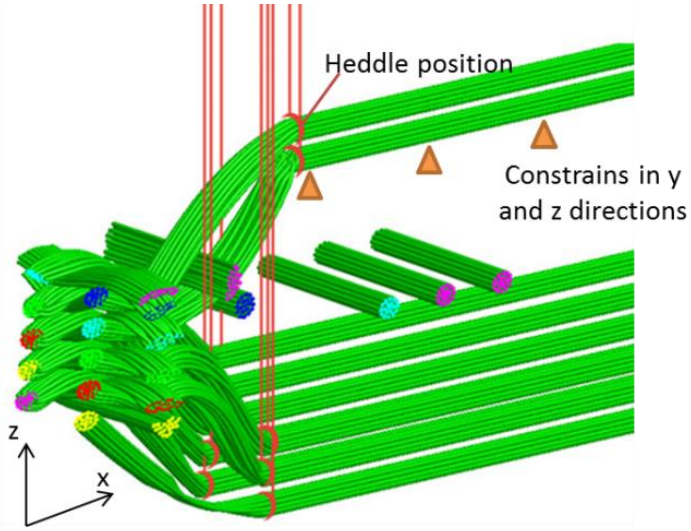

Figure 3-19. Weaving process

The weaving matrix introduced in Chapter 3 instructs warp yarns motions. In order to simulate machine weaving action, nodal movements of warp yarns outside the contact domain, behind the heddle position, are constrained in the z-direction based on the weaving matrix. When the weaving matrix indicates that a heddle is to move up or down, the corresponding warp yarn receives forced displacements in z direction. Displacements directions, including up or down, are determined by the weaving matrix and displacements are determined by weaving velocity. Warp weaving action is also simulated as constant acceleration motion. Warp yarns begins at zero velocity at original positions and perform instructed weaving action. Nodal velocity is set to zero after warp weaving action simulation is finished. Warp yarns within the contact search domain are subjected to no external constraints. A large amount of new contacts elements are established as warp yarns contact inserted weft yarns, fiber-to-fiber compression and friction forces are

determined as introduced in Chapter 3 and yarn deformation develops during simulated weaving action.

3.4.3.3.3 Warp yarn tension variation

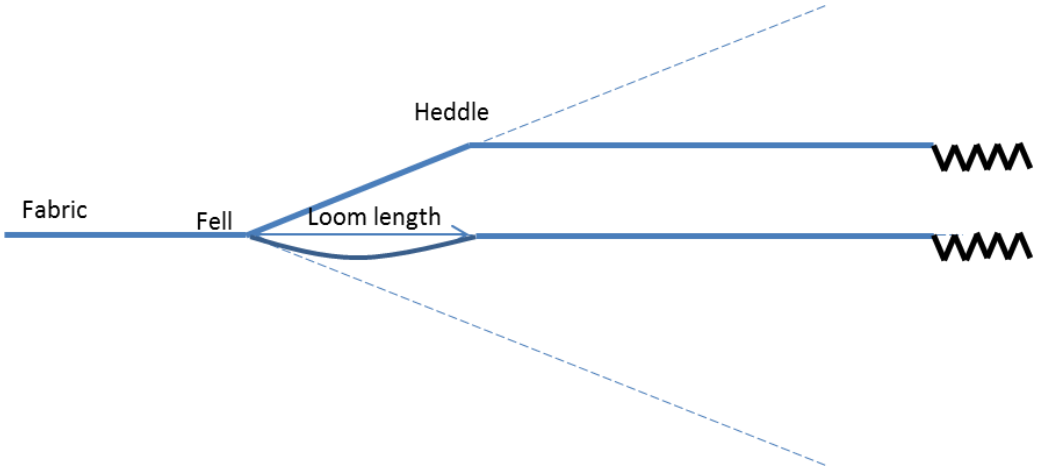

Figure 3-20. Warp yarn tension variation

Portion of warp yarns behind heddles are considered to be stored yarns used in subsequent weaving actions. Stored warp yarns gradually pass through heddles as weaving process simulation proceeds and lace newly inserted weft yarns in weaving actions. Constant tension is applied to warp yarns at far ends. The tension typically cannot pull back warp yarns that have already passed through the heddle. Process simulation detects that warp yarns are not constantly stretched straight due to differences in loom length and warp yarn length, as illustrated in Figure 3-20, thereby inducing warp tension variation during the weaving process. In one weaving action, when a warp yarn moves from its original position to the opposite position, it is gradually released as it approaches the middle position and then stretched as it reaches upper

or lower position. Therefore, in one weaving action, although applied with constant tension at the ends, warp yarns tension initially first decreases and then increases.

3.4.3.4 ***Taking-up***

Taking-up action, as demonstrated in Figure 3-21, collects woven fabric for continuous weaving. Fell position is fixed in simulation and displacement constrain is applied to portion of woven fabric in front of the fell. Taking-up action is determined by two process parameters: taking-up length and taking-up frequency. Taking-up length, defined by picks per inch (PPI), controls the fabric length collected at each taking-up action. Taking-up frequency is defined by the number of taking-up flags in one weft column. The example demonstrated in Figure 3-21 has eight layers of weft yarns and two taking-up flags are defined for one weft column. In this example taking-up frequency is one taking-up action for every 4 layers of weft yarns; therefore, the first taking-up is simulated when the fourth layer of weft yarn is inserted; the second taking-up action is simulated when the eighth layer of weft yarn is inserted. Taking-up length and taking-up frequency together determine the interval distance of two columns of weft yarns.

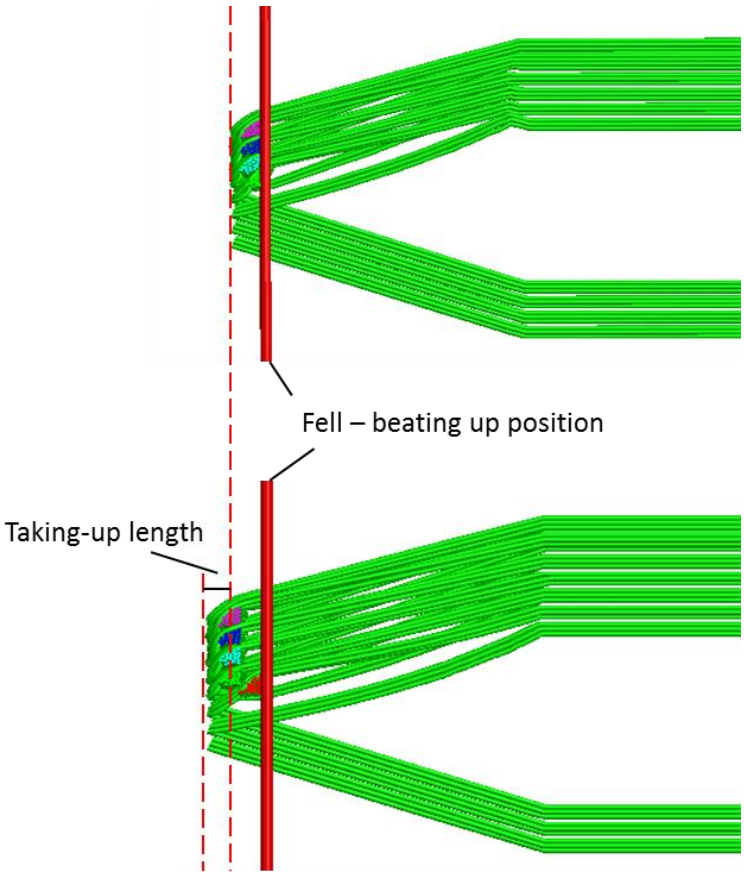

Figure 3-21. Taking-up

3.4.3.5 ***Re-mesh***

In weaving process, the fell is a fixed position; the harness cords only move up or down. The fabric is wrapped in a roll at user set velocity and frequency. Because fabric may continue to relax before it reaches a steady geometry in numerical simulation, micro-geometry deformation of the portion of collected fabric located to the left of fell should be calculated. The contact search domain must include collected fabric; therefore, the front plane of domain, originally set to be the x=0 plane, must moves left-ward, as illustrated in Figure 3-22. The movement is defined to start simultaneously with taking-up. Warp yarns are stretched and warp nodes

originally behind heddle position enter contact domain and participate in the following weaving process simulation.

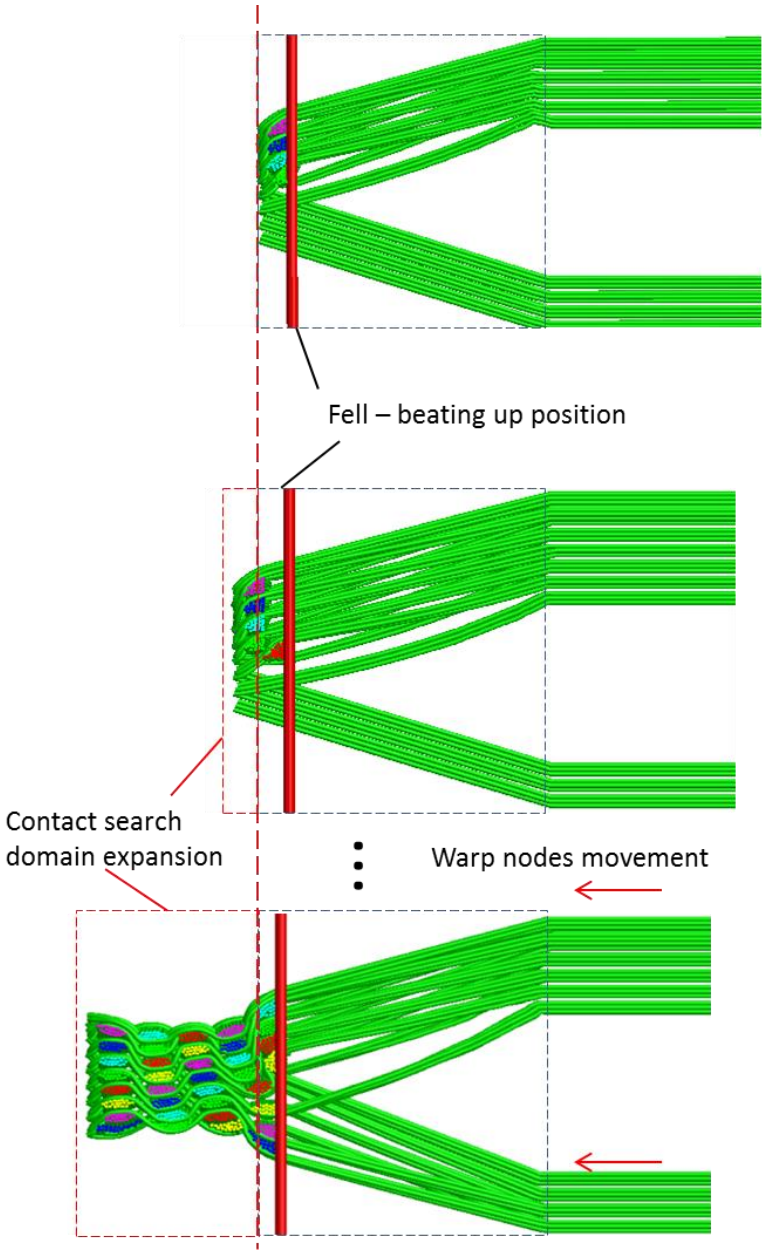

Figure 3-22. Contact search domain expansion

As the newly formed piece of fabric grows larger in simulation, the contact calculation requires additional computing resources and time, however, micro-geometry of the collected fabric becomes relatively steady. Weaving actions to form new fabric near fell has little effect on the geometry of the collected fabric in the front. Then the re-mesh function is performed. Nodal information of the front unit cell is removed from the geometry and new warp nodes are added at the back. The contact domain and amount of contact elements shrinks and the weaving process simulation continues until satisfaction.

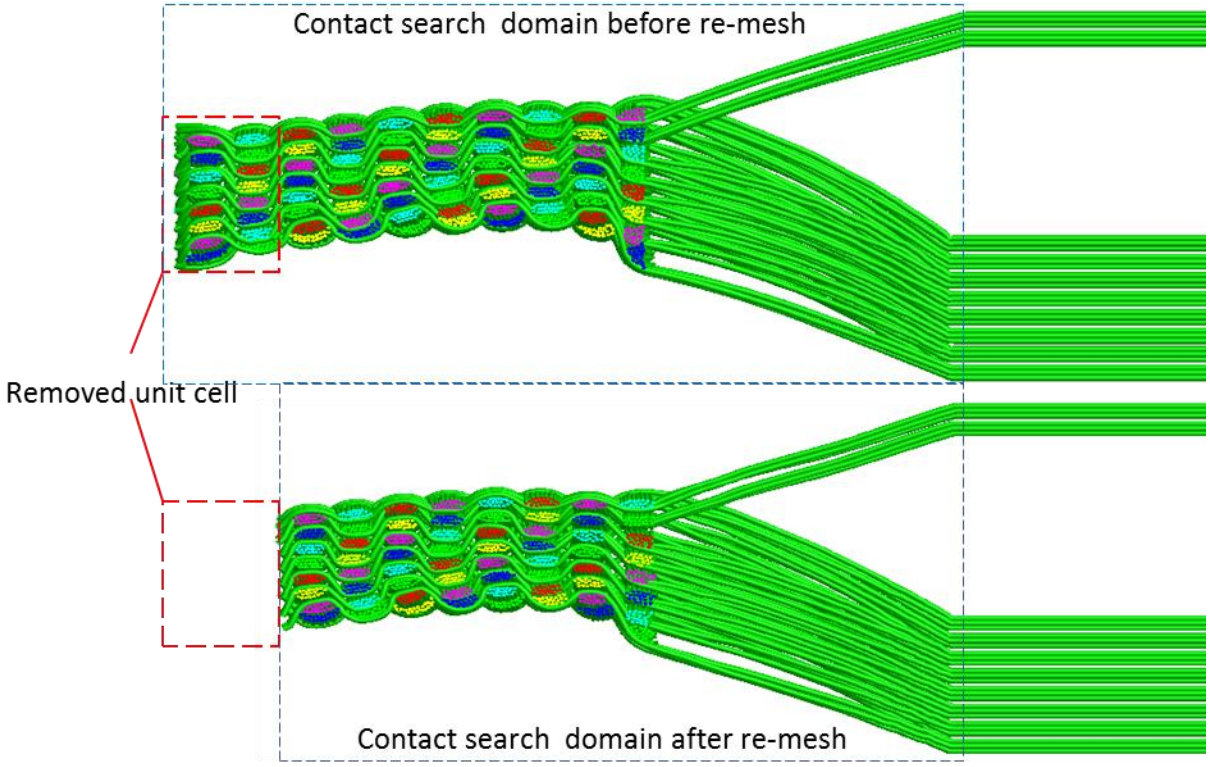

Figure 3-23. Re-mesh

3.4.4 *Contact search*

As introduced in Chapter 1, the Digital Element Approach calculates nodal compression forces when the distance between two nodes is smaller than fiber diameter. In order to effectively and efficiently determine all nodal contacting relations, a contact search algorithm was established. In the Dynamic Relaxation model, the contact search domain is defined as a cuboid containing the entire unit cell. Digital nodes and contact elements are evenly distributed in the cuboid without significant blank area. Then the cubic division method is implemented for the cuboid contact search domain. The domain is divided into small cubes, with cubic dimension typically defined as 1.4 times the fiber diameter. The cubes are identified by row, column and level IDs. Then all nodes are allocated to the cubes according to nodal coordinates.

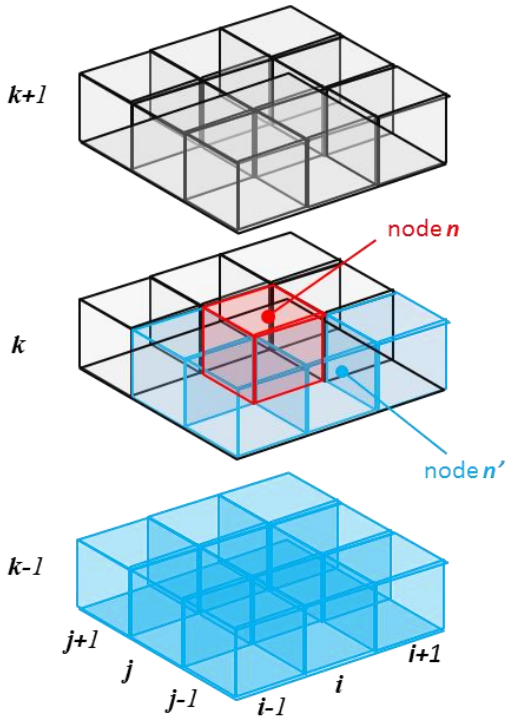

Figure 3-24. Contact search

Instead of calculating nodal distances between target node and all other nodes in a sub-domain, a forward search method is implemented to more effectively detect and record all contact elements within one sub-domain. As illustrated in Figure 3-24, node ***n*** is the target node searching for contacting nodes, instead of calculating nodal distances between node ***n*** and all other nodes in the domain, only nodes in neighboring 26 cubes must be checked in order to determine contacting nodes of a target node. The searching algorithm is demonstrated in Figure 3-24, node ***n*** is the target node located in the cube marked in red. The red cube is indexed by ***i***, ***j*** and ***k***, where ***i*** is the cube column number, ***j*** is the row number and ***k*** is the level number. The neighboring cubes include the 26 cubes on level ***k-1*** and ***k+1***, from column ***i-1*** to ***i+1***, row ***j-1*** to ***j+1***, as illustrated in Figure 3-24. Another complication is that searching nodes in all 26 neighboring cubes results in duplicated calculation. For example, node ***n'*** is in cube column ***i-1,*** row ***j+1***, level ***k,*** and the distance between node ***n*** and node ***n'*** is smaller than fiber diameter. During contact searching, node n determines node ***n'*** to be its contacting node and node ***n'*** determines node ***n*** to be its contacting node. Therefore, the contact forces on both nodes are calculated twice. To avoid duplication, 13 of the 26 neighboring cubes marked in blue are checked for contact, including all nine cubes at level ***k-1***, and four cubes on level ***k***. As Figure 3-24 illustrates, during contact searching, node ***n*** searches the cube in which node ***n'*** is located, and records node ***n'*** as its contacting node. However, while performing contact search for node ***n'***, the cube in which node ***n*** is located is not included in the 13 cubes selected for searching. This contact searching method, called the cubic forward searching method, detects all contacting nodes of node ***n*** in the 13 neighboring cubes and recorded them as a list. When nodal contact is established, nodal compressional and friction forces are calculated.

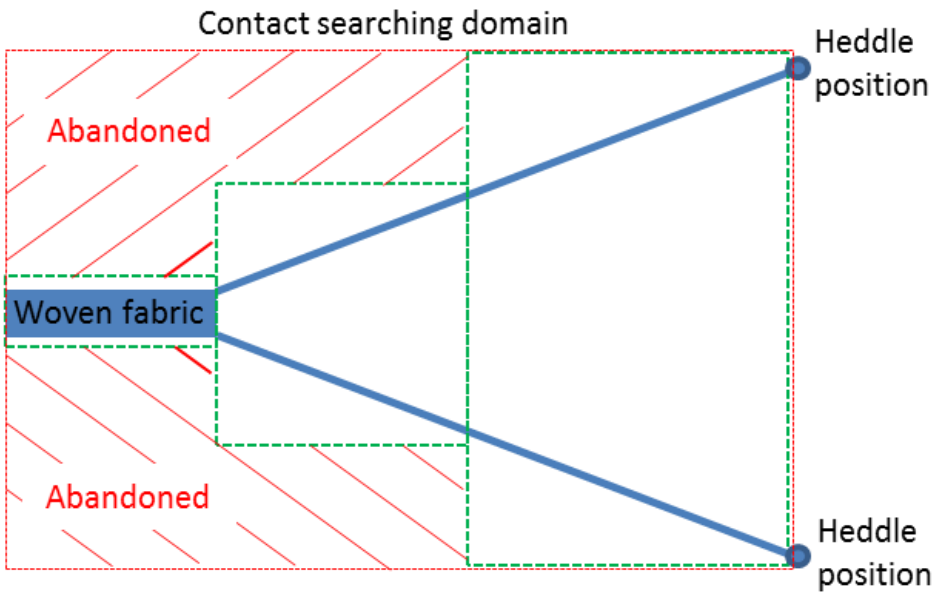

Figure 3-25. Contact search domain of Dynamic Weaving Process Simulation

As illustrated in Figure 3-25, the contact search domain in the Dynamic Weaving Process Simulation model was originally defined similar to the Dynamic Relaxation model using red dashes, with cuboid area defined by heddles vertical and horizontal positions relative to fell plane in order to detect all nodal contacting relationships. However, the contact search domain in Dynamic Weaving Process Simulation is much larger than the domain in Dynamic Relaxation, which simulates only one unit cell, and the domain does not present uniform distribution of nodes in the cuboid area defined by heddle positions. Contact searching is time-consuming and large contact search domain may inevitably lead to slower simulation. Because woven fabric thickness is less than the distance from heddle up position to heddle down position and woven fabric position remains steady after formation, large blank spaces exists in the front of the contact search domain, as illustrated in the red shadow in Figure 3-25. No digital nodes will enter the blank area in subsequent simulation, so the original contact search domain containing the

blank area is considered inefficiently use of computing time and resources. Therefore the contact search domain in Dynamic Weaving Process Simulation is subdivided into three sub-domains, as illustrated as green rectangles in Figure 3-25. The height of the first domain is estimated fabric thickness, the height of the third domain is heddle up-down distance and the height of the middle domain is the average of the two. In order to promote efficiency and maintain accuracy, the large blank space is not considered for contact search with this domain sub-division method.

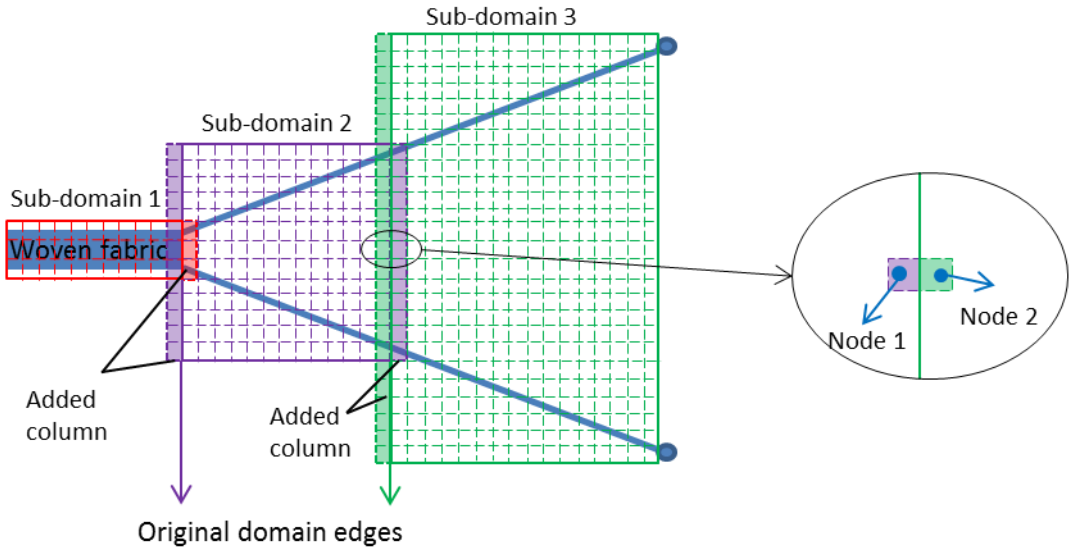

Figure 3-26. Contact search domain division

The cubic division method is implemented for each sub-domain and the three sub-domains are divided into small cubes as shown in Figure 3-26. Digital nodes within each sub-domain are allocated to cubes according to nodal coordinates. Because nodal contacts are searched within each sub-domain, the nodes near the sub-domain edges may miss contacting nodes. As demonstrated in Figure 3-26, assumes that node 1 is on the left side of domain edge, node 2 is on the right side of domain edge and the distance between node 1 and node 2 is smaller

than fiber diameter, so node 1 and node 2 should be a pair of contacting nodes, however, node 1 and node 2 belongs to sub-domain 2 and sub domain 3 respectively, if contact search can only detect contacting nodes within one sub-domain, edge nodes such as node 1 cannot find its contacting nodes in neighboring sub-domain such as node 2, thereby causing problems for compression and friction nodal force calculation. In order to solve the missing contact, every sub-domain is expanded by one cube length at each side, covering two extra columns of cubes in total, so the sub-domains contain overlapping areas as shown in Figure 3-26. Sub-domain expansion causes node 1 and node 2 to be in sub-domain 2, so node 1 can detect node 2 as one contacting node. Using the cubic forward searching algorithm, no duplications of contact element will be recorded. However, node 1 and node 2 are both in sub-domain 3 because of the extra column added to domain 3; therefore while performing contact search in domain 3, node 1 again adds node 2 to its contacting nodes list resulting in a duplication of node 2 in the list. In fact, duplications of all node 1's contacting nodes exist in the overlapping area of domain 2 and domain 3. Therefore, contact search in a domain is only implemented by nodes located within the original domain edges before adding the extra columns of cubes in order to avoid duplication. Contact search in performed by node 1 in sub-domain 2, because node 1 is within the un-expanded original edges of domain 2 and Node 1 can detect node 2 as its contacting node in sub-domain 2. Node 1 is outside of the original domain edges of domain 3, so contact search is not performed on node 1. As a result of this method, contact relationships on sub-domain edges can be accurately determined and recorded for nodal compression force calculation.

3.4.5 *Parallel computing*

The Dynamic Weaving Process Simulation approach models the loom kinetics and kinematics involved in the weaving process. However, the step-by-step simulation of the 3D weaving process requires additional calculation time and computer resource and only coarse digital element mesh can typically be used because of PC capacity limitations. In order to promote simulation efficiency, enable finer yarn discretization and improve fabric micro geometry accuracy, parallel computing was implemented for PC version of the simulator.

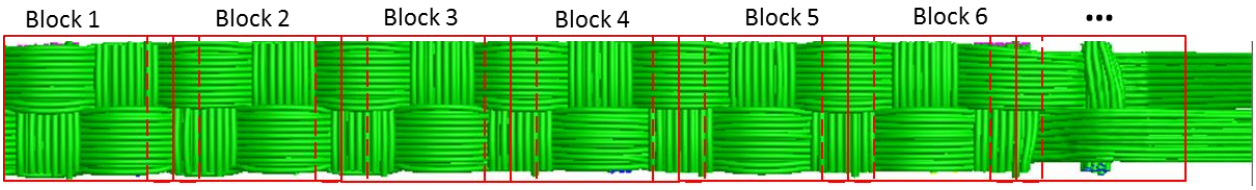

Figure 3-27. Parallel computing

Parallel programming uses OpenMP for PC code. Simple loop parallel coding is implemented for tension induced nodal forces and nodal displacement calculation. However, errors may occur in multi-threaded contact forces calculation while multiple threads attempts to access and edit one datum, resulting in random, highly error prone, and conflicted data editing. Therefore, nodal information of simulation model data is divided into several blocks and each block is sent to one thread, allowing multiple threads to work simultaneously for nodal forces calculation. The total number of blocks is determined by the number of threads used by simulation, as shown in Figure 3-27.

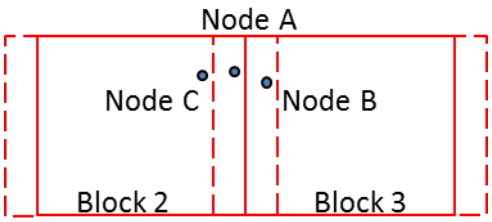

Figure 3-28. Thread conflict

An example of data editing conflict is illustrated in Figure 3-28. Node A and node C are located in block 2, while node B is located in block 3. While thread 2 is working on node A as target node and calculating compression force between node A and node C, thread 3 is simultaneously working on node B as target node. Thread 3 find node A to be its contacting node and it calculates compression force between node B and node A. Therefore, thread 2 and thread 3 attempts to access and edit the nodal force of node A. One of the two threads will certainly fail to correctly access node A, consequently resulting in an error. Such errors may accumulate during simulation and produce faulty simulation result. In order to solve the problem, one thread is only allowed to edit the nodal information of nodes within the current block. For example, while thread 2 and thread 3 simultaneously attempts to access node A, the request by node B in thread 3 is automatically rejected because node A is not in block 3. Another problem occurs when the data increment that thread 3 is trying to put on node A is lost. Therefore each block is expanded by two cubic lengths, containing an extra column of cube on each side, as illustrated by the dashed lines in Figure 3-28. Block 2 and block 3 then have overlapping area that contains two columns of cubic. Node A and node B are then both in block 2 and block 3. Therefore, thread 2 will work on node A and node B sequentially as target node, thereby avoiding the conflict of attempts to simultaneously edit node A or lose of the nodal force from node B.

A test was implemented to demonstrate the effectiveness of parallel computing. The test recorded the time required to calculate 100,000 time steps on a 4-core PC and an 8-core PC. The speed-up curve is shown in Figure 3-29. The test shows that the use of 4 threads saves approximately 50% of simulation time and the use of 8 threads saves approximately 70% of simulation time.

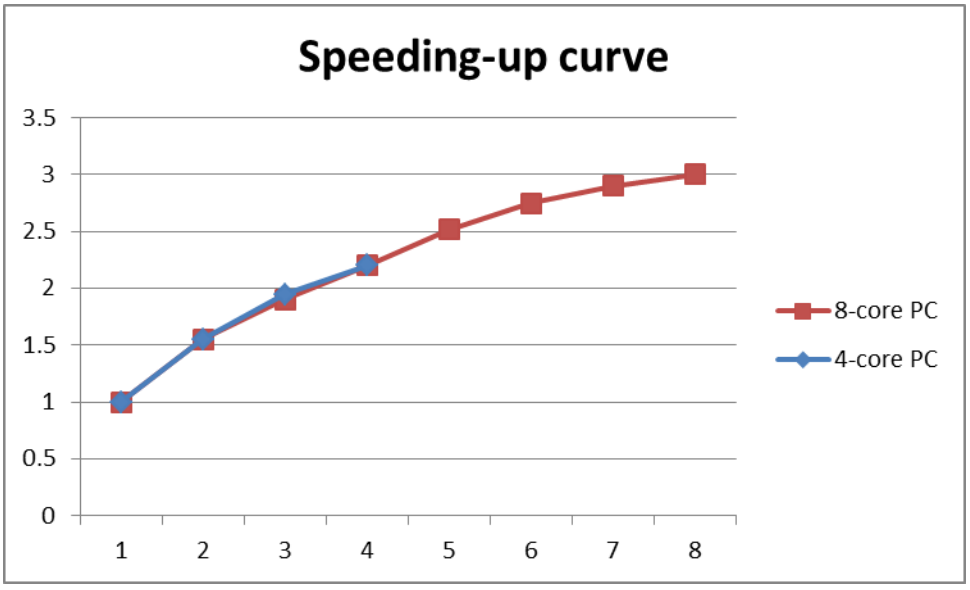

Figure 3-29. Speed up curve

3.5 Conclusions

Mechanical properties textile preforms for fiber-reinforced composites are determined by fabric internal structure. Because textile fabrics are produced by a variety of weaving processes, the processes kinematics and kinetics to manufacture 3D fabrics determine micro-structures and mechanical properties of fabrics. Therefore, a CAD/CAM Weaving Process Simulation model is established in order to study of textile fabric micro-geometry and manufacturing process. The

process simulation links manufacturing process with fabric micro-geometry, mechanical properties and weavability.

In order to establish an efficient simulation model, weaving machine components that are necessary and sufficient to perform all weaving functions must be identified. This chapter presents the key components of a weaving machine that are simulated in Dynamic Weaving Process Simulation. The weaving process of a Jacquard loom machine is explained in detail. A simulation model is established based on fabric pattern and weaving process dynamics. The weaving process simulation primarily consists of four steps following the underlying loom kinematics and kinetics: weft insertion, beating up, weaving and taking up. Weaving matrix is implemented in order to control weaving process.

Fiber level micro-geometry is simulated implementing the digital element approach. Tension-induced nodal force, nodal contact force and nodal friction are calculated. Contact search algorithm is improved and parallel computing is implemented in weaving process simulation to promote efficiency.

Chapter 4 - Dynamic Analysis of Weaving Process

4.1 Weaving Process and Reed Load

As high performance composite materials begin to gain applications in various industries, the need for 3D woven preforms with increasing thickness and complexity has grown significantly, consequently creating challenges for 3D weaving manufacturing capabilities. The weaving process kinetics and kinematics determine fabric micro-geometry and fabric properties. Weaving process parameters, including reed dent, warp movements, weaving velocity, impact velocity, taking-up velocity, yarn tension and fiber-to-fiber friction, also affect the design of weaving machine.

As introduced in Chapter 3, reed is a comb-like structure made from stainless steel located near fell. During weaving process, reed moves towards fell and push inserted weft yarn forward. It is a crucial component of a 3D loom because it lines up inserted weft yarns according to manufacturer designs and produces firm fabric structure. The reed is subjected to reaction force from fabric as it proceeds, such as weft yarns preventing reed from moving forward, and friction with warp yarns. Improper fabric design and weaving process may result in unendurable load on the reed and possible reed damage. Reed load estimation is implemented in Dynamic Weaving Process Simulation in order to predict maximum reed load for certain weave design and study the effects of weaving process parameters on reed load to avoid possible reed damage and determine weavability.

Example 1:

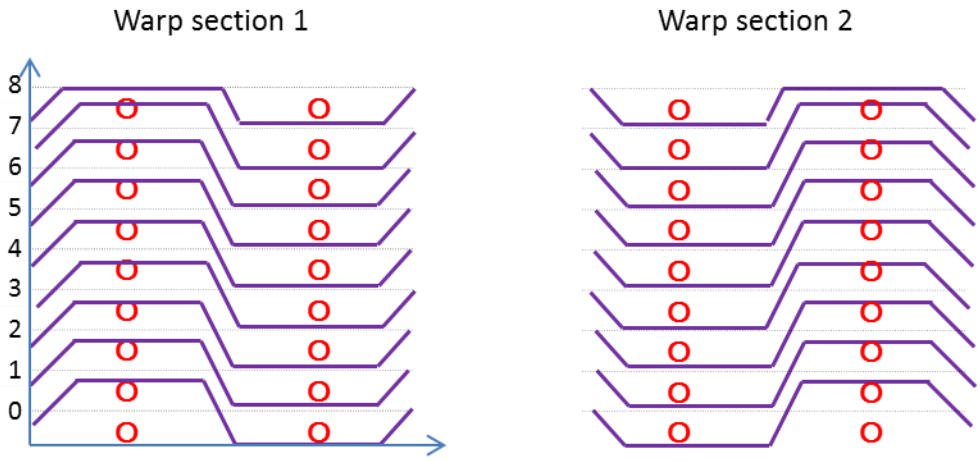

Figure 4-1. Unit cell topology

Example 1, a 3D woven fabric with eight layers and two columns of weft yarns and two warp sections in one unit cell, is used to investigate the effects of various weaving process parameters on reed load. Interlacing patterns of two warp sections are illustrated in Figure 4-1. The circles represent weft yarns and solid lines represent warp yarns. The fabric is woven from 125-yield S2 glass fiber with fiber density is 2460 kg/m^3. Yarn diameter calculated from yield number and density is 1.61e-4 m^2. Each warp section is arranged in one reed dent during manufacturing and reed dent dimension is 0.0039m.

4.1.1 *Mesh quality*

Fibering function is implemented in Dynamic Weaving Process simulation in order to refine mesh. As introduce in Chapter 3, 1 to 81 fibers-per-yarn meshes are available to perform process simulation. In reality, though, one yarn is composed of thousands of fibers, but simulation of every fiber is neither feasible nor necessary. Although finer mesh generates more precise results, finer mesh also consumes more computing resources and computing time. In

order to achieve simulation accuracy and efficiency, necessary, sufficient mesh quality to generate maximum reed load estimation must be determined.

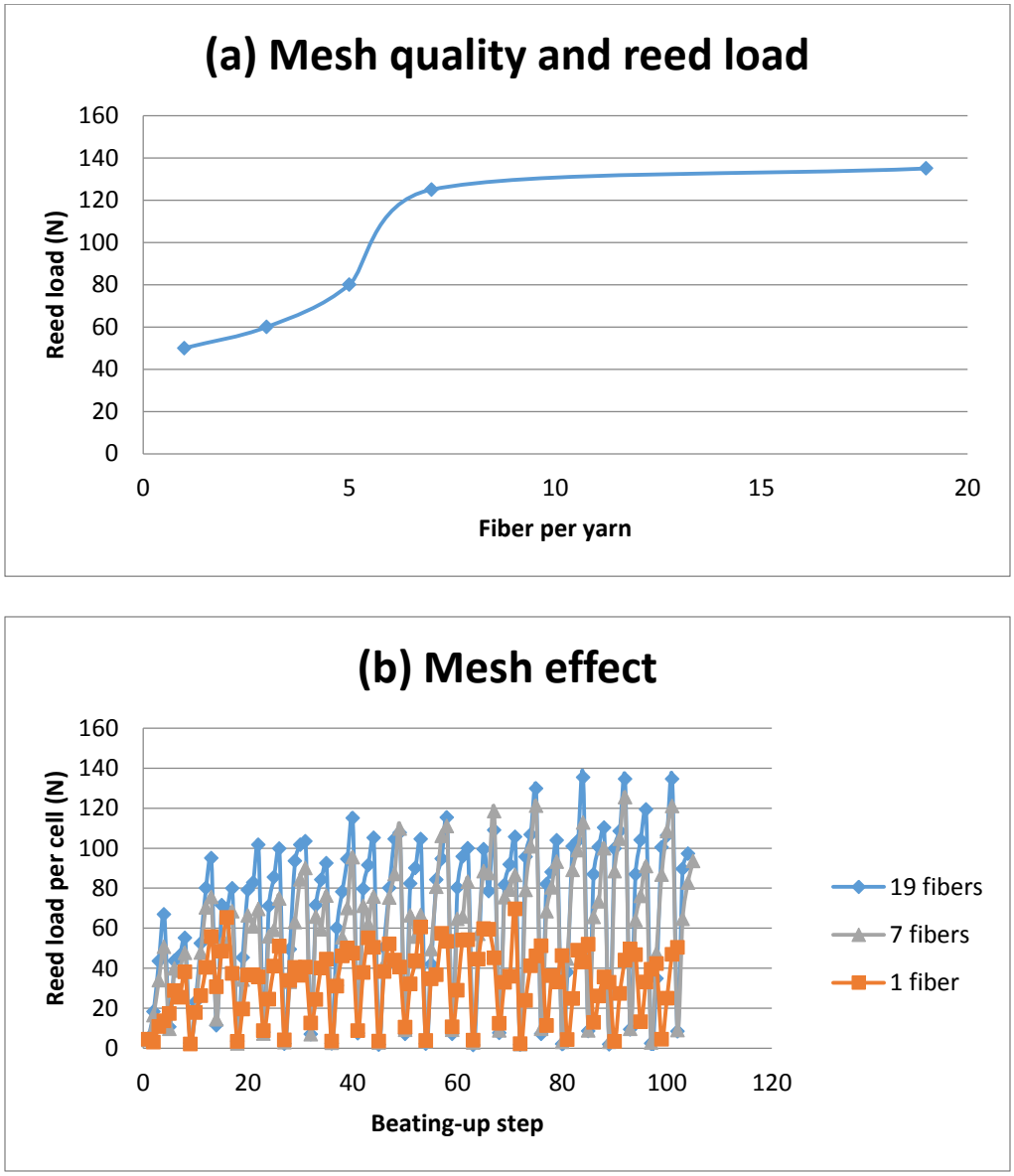

Figure 4-2. Mesh analysis

A test was conducted using 1, 3, 5, 7 and 19 fibers per yarn mesh as demonstrated in Figure 4-2 (a). The five examples used identical weaving parameters: friction coefficient μ=0.2, reed impact velocity=4.5m/s, applied tension at heddle position= 3N. Figure 4-2 (a) shows the

curve of reed load per unit cell calculated using various mesh quality. Maximum derived reed load was 50N using 1 fiber per yarn mesh, 60N using 3 fibers per yarn, 80N using 5 fiber per yarn, 125N using 7 fibers per yarn and 135N using 19 fibers per yarn. According to the curve, conclusion was made that calculated reed load increases significantly from 1 to 7 fibers-per-yarn mesh, becoming steady as continue to refine mesh to 19 fibers-per-yarn. Therefore, 7 to 19 fibers-per-yarn mesh were implemented for reed load estimation to provide efficiency and accuracy. Figure 4-2 (b) demonstrates reed load variation during the weaving process for 1, 7 and 19 fibers per yarn mesh. One point in the curve indicates the calculated maximum reed load at one beat-up step. Reed load initially increased as weaving began and stabilized to certain value for all selected mesh qualities. The curves with 7 fibers per yarn and 19 fibers per yarn stabilized at close value so conclusion was made that further mesh refinement has little effect on reed load estimation. Typically 7 to 19 fibers per yarn mesh provide accurate estimation.

4.1.2 *Taking-up action and reed load*

Taking-up action collects woven fabric for continuous weaving. As discussed in Section 3.4.3.4, taking-up action is defined by PPI and taking-up flags. PPI determines taking-up length, which controls collected fabric length in each taking-up action. Taking-up flags determines taking-up frequency, which controls the number of taking-up actions per weft column. Taking-up length and taking-up frequency determine the interval distance of two columns of weft yarns. Longer taking-up length and more frequent taking-up actions generate higher taking-up speed, typically indicating denser arrangements of weft yarns and tighter structure. Three examples with (a) 0.508 cm, (b) 0.339 cm and (c) 0.276 cm taking-up length were simulated using Dynamic Weaving Process Simulation, as shown in Figure 4-3. The taking-up frequency for all three examples were two per weft column. Other parameters included: friction coefficient μ=0.2, reed

impact velocity=4.5m/s, and applied tension at heddle position= 3N. A comparison revealed that shorter taking-up length used in example (c) produced tighter unit cell structure, including smaller unit cell length and larger fabric thickness and volume fraction.

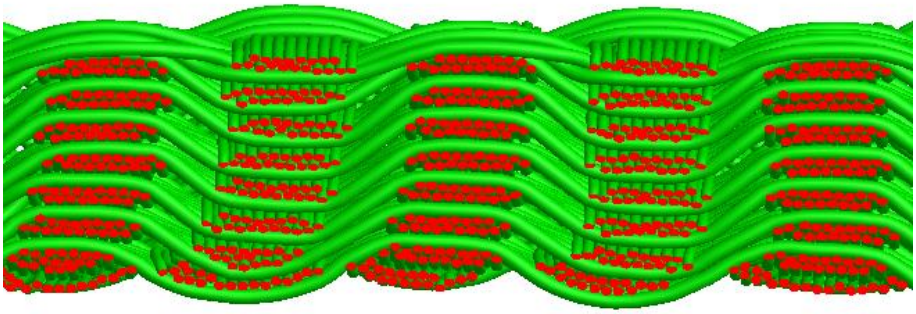

(a) 0.508 cm taking-up length (5 PPI)

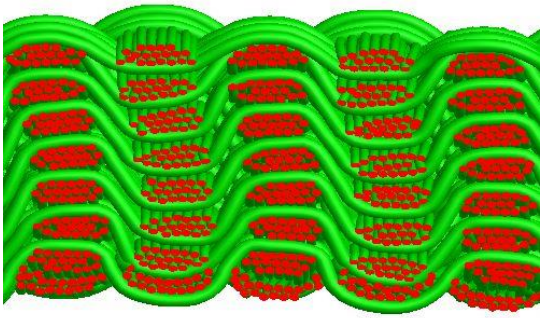

(b) 0.339 cm taking-up length(7.5 PPI)

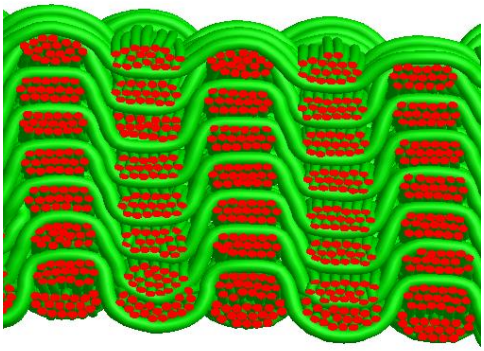

(c) 0.276 cm taking-up length(9.2 PPI)

Figure 4-3. Taking –up length

4.1.2.1 *Taking-up length and reed load*

Figure 4-4 shows the reed load during weaving process simulation of fabric example (a), (b) and (c) in Figure 4-3. One point on the line represents the maximum reed load in a specific beating-up action. Other parameters included: friction coefficient μ=0.2, reed impact

velocity=4.5m/s, applied tension at heddle position= 3N. As shown in Figure 4-4, maximum reed load varied at different beating-up steps. Maximum reed loads during the entire weaving processes for the three examples were (a) 44 N/cell, (b) 56 N/cell and (c) 76 N/cell. Conclusion was made that smaller taking-up length generates denser fiber distribution, so the fabric demonstrated greater preventing force for the reed to push inserted weft yarn into geometry, thereby producing greater maximum reed load.

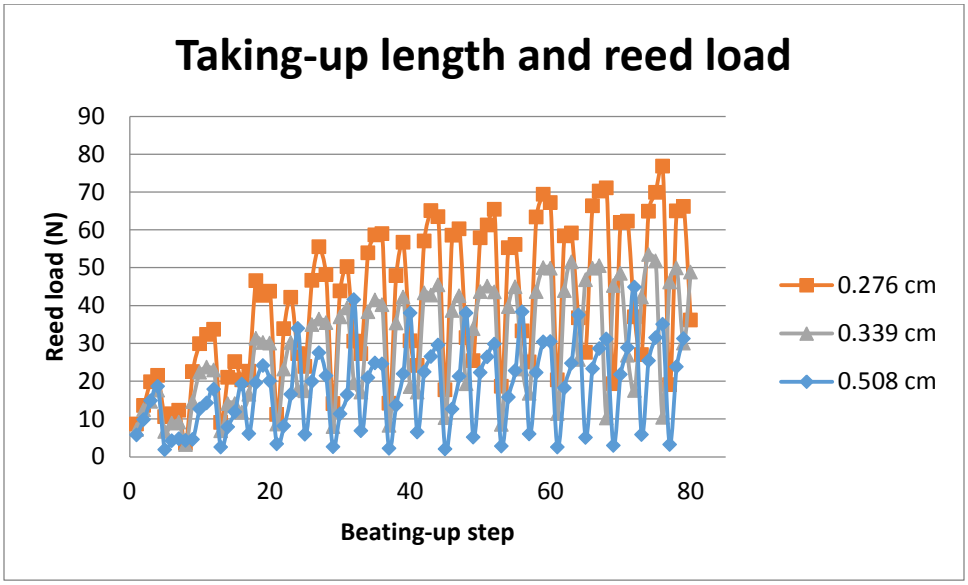

Figure 4-4. Taking-up length and reed load

4.1.2.2 ***Take-up frequency and reed load***

Taking-up frequency is defined for each weft column. As illustrated in Figure 4-5 (a), two taking-up actions per column was defined, so taking-up actions were simulated when the fourth and eighth weft yarn were inserted and woven. Taking-up frequency determines the number of weft yarns in a column contacting the reed, thereby affecting impact load on reed. Figure 4-5 (b) shows reed load of eight beating-up actions for the process of weaving one

column of weft yarns. Reed load increased as four weft yarns were inserted and then after the taking-up action was simulated as weft No.4 was inserted and woven, reed load decreased.

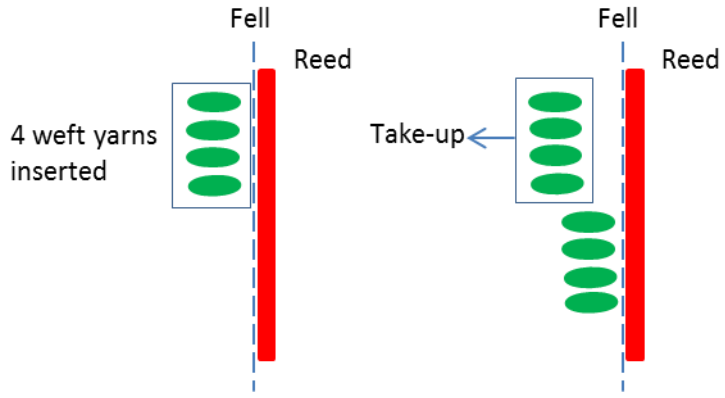

(a)

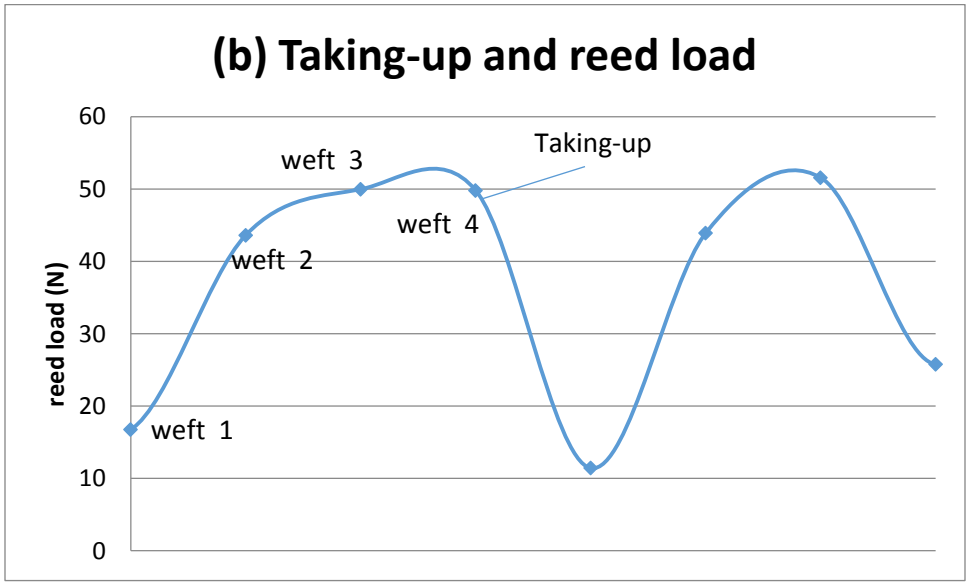

Figure 4-5. Taking-up frequency

The effect of taking up frequency on reed load is demonstrated in Figure 4-6. Three fabric examples, shown Figure 4-3 (b), were simulated using one, two and eight taking-up action per column. Other parameters included: friction coefficient μ=0.2, reed impact velocity=4.5m/s, applied tension at heddle position= 3N, taking-up length=0.339cm. As demonstrated by the three

curves in Figure 4-6, more frequent taking-up actions released reed load quickly, consequently generating lower reed load.

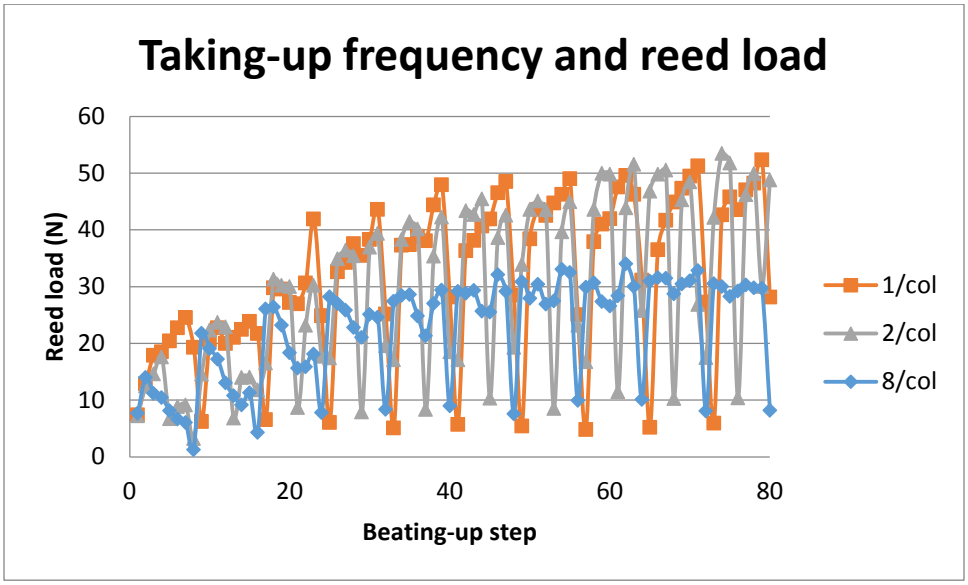

Figure 4-6. Taking-up frequency effect on reed load

4.1.3 *Heddle position and reed load*

As introduced in 3.4.3.3.1, heddle position approximation is implemented in Dynamic Weaving Process Simulation in order to promote efficiency and the effect of heddle position on fabric micro-geometry has been proven to be minimal. The effect of heddle position on reed load was also analyzed in order to provide accurate reed load estimation. Two examples are presented in Figure 4-7 using 1 in. and 3 in. loom length. Other parameters included: friction coefficient μ=0.2, reed impact velocity=4.5m/s, applied tension at heddle position= 3N, taking-up length=0.276cm and taking-up frequency=2/column. The two curves showed minimal deviation so the conclusion was made that heddle position effect on reed load can also be neglected. Therefore, 1 inch loom length is adopted in process simulation for efficiency.

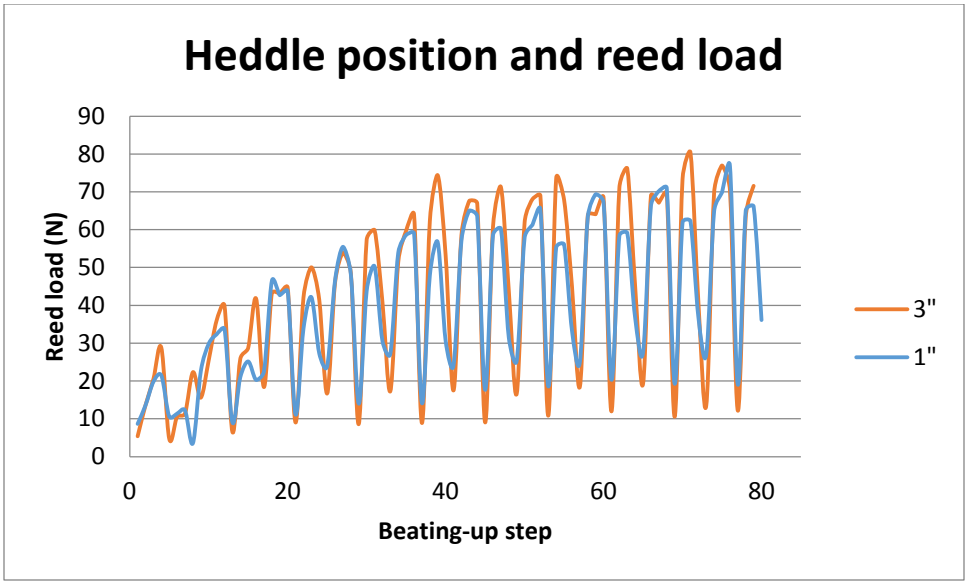

Figure 4-7. Heddle position and reed load

4.1.4 *Impact velocity and reed load*

Reed motion is simulated as constant acceleration movement in beating-up action. Reed starts at zero velocity from its original user defined position, pushes inserted weft yarn towards woven fabric and stops at fell. Impact velocity is maximum reed velocity as reaches fell. The maximum velocity is determined by reed travel distance s_r and travel time T defined by user:

$$v_{max} = \frac{2 \times s_r}{T} \tag{11}$$

Reed travel distance is typically 0.7 times loom length, so 0.7 inch is used in simulation. Multiple examples were simulated using various travel time as shown in Figure 4-8. The maximum reed velocities for the three examples were: 3m/s, 4.5m/s and 6m/s. Other parameters included: friction coefficient μ=0.2, applied tension at heddle position= 3N, taking-up length=0.276cm and taking-up frequency=2/column. Short travel time is preferred for improved manufacturing efficiency, but it also produces higher reed impact velocity. As shown in Figure

4-8, impact velocity significantly affected reed load. In addition, high velocity may cause unbearable reed load and damage reed during manufacturing.

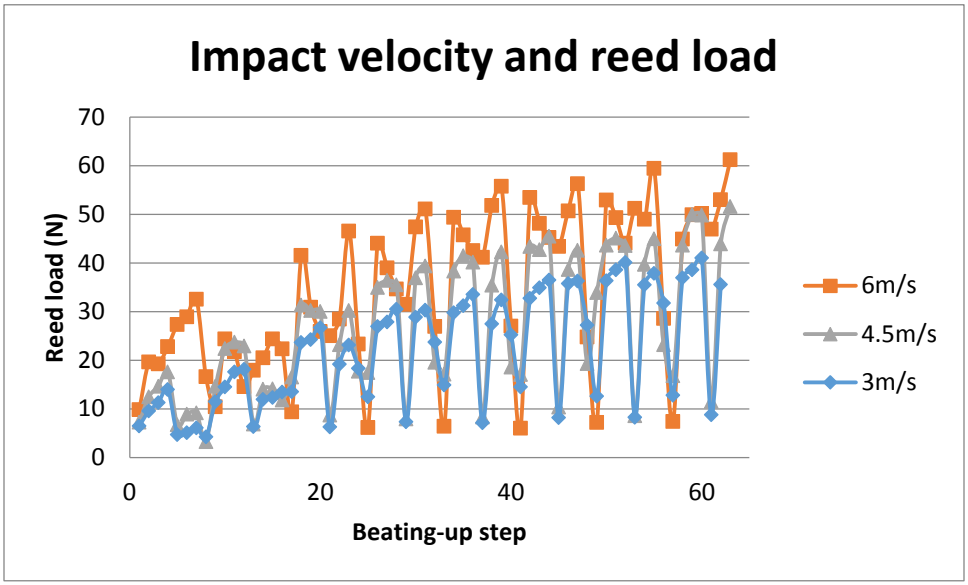

Figure 4-8. Impact velocity and reed load

4.1.5 *Boundary effect*

As introduced in Section 4.1, periodical boundary is implemented in weft direction and reed load is calculated without considering boundary effect. However, experimental results detected boundary effect, as demonstrated in Figure 4-9. The reed load-fabric width curve did not pass the origin point. Approximately eight inches of boundary exists.

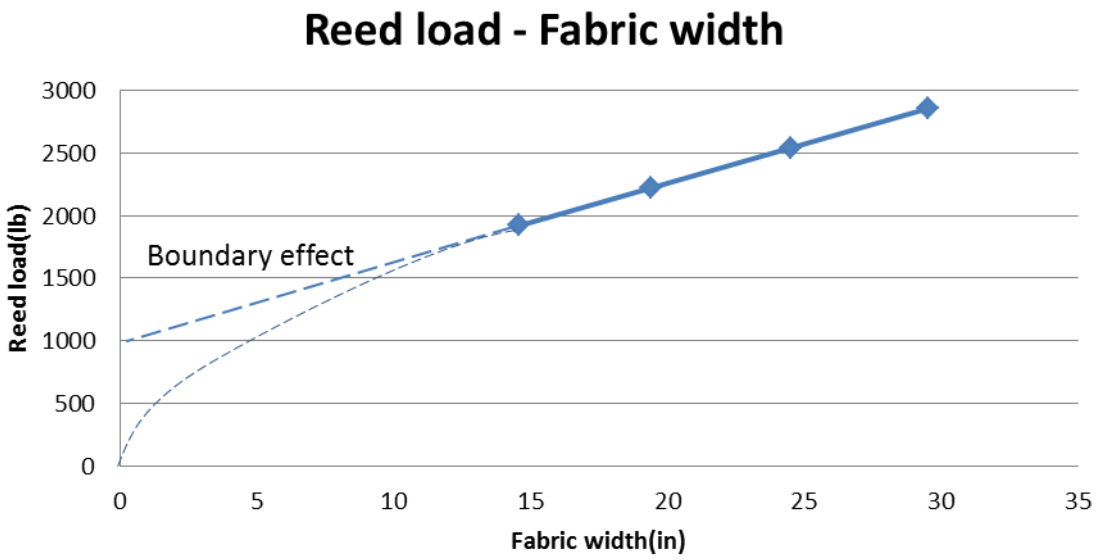

Figure 4-9. Reed load and fabric width

4.1.6 *Conclusion*

Parametric analysis was implemented using Dynamic Weaving Process Simulation and the effect of weaving process parameters on reed load is investigated. Weaving process parameters such as taking-up length, taking-up velocity and impact speed have major effect on reed load, thereby determining weavability. Other parameters including applied tension, heddle position and fiber-to fiber friction moderately affect reed load.

4.2 Weaving Process and Fabric Micro-Geometry

As introduced in Chapter 3, weaving process kinematics determines fabric topology and weaving process kinetics determines fabric detailed micro-geometry. Parameters analysis was implemented using Dynamic Weaving Process Simulation in order to study the effects of weaving process parameters on fabric micro-geometry.

4.2.1 *Applied tension effect on fabric micro-geometry*

Example 2:

Example 2 is used to investigate the effects of various weaving process parameters on fabric micro-geometry. It is 3D woven fabric with six layers and four columns of weft yarns and four warp sections in one unit cell, including two weaver sections and two warp stuffer sections. Reed was defined as 8.5 dent per inch, with one weaver and one warp stuffer section arranged in each dent. Unit cell length was 0.01354m and unit cell topology is shown in Figure 4-11 (a). The fabric was woven from 1250-yield and 250-yield and S2 glass fiber, and the fiber density was 2460 kg/m^3. The yarn diameter calculated from yield number and density was 8.05e-7 m^2 for weavers and 1.61e-4 m^2 for warp and weft yarns.

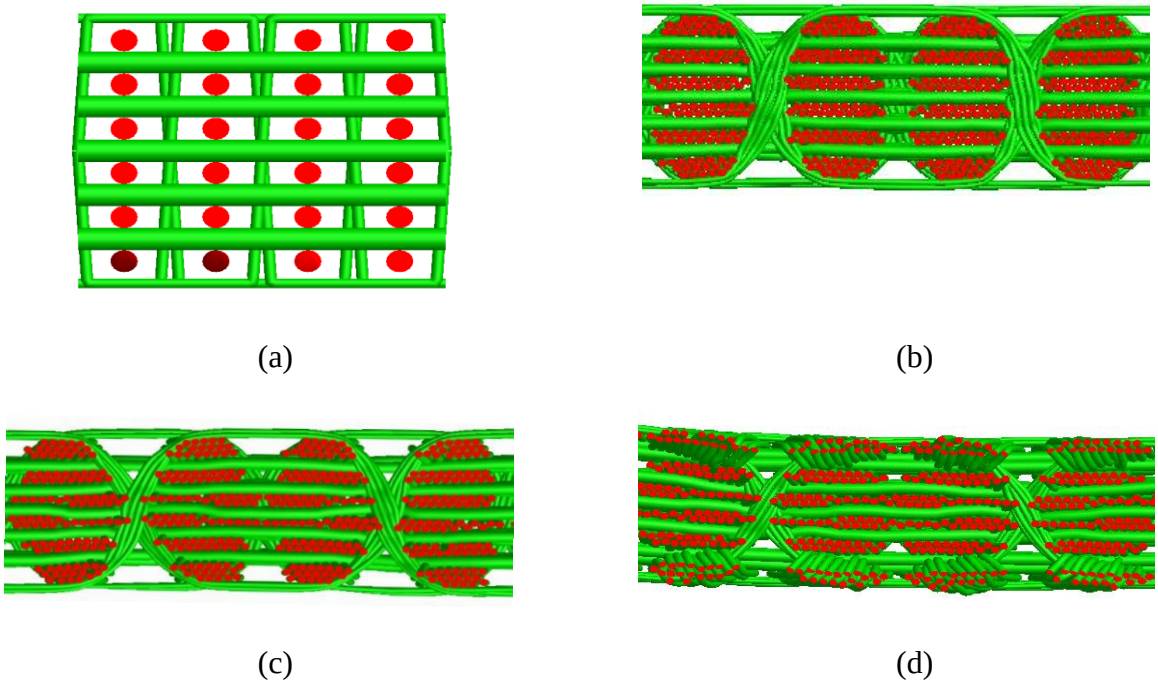

(a) (b)

(c) (d)

Figure 4-10. Yarn cross-section and weaving parameters relationship

Warp yarn tension depends on constant tension applied to warp ends. Fabric unit cell topology is shown in Figure 4-10 (a). The fabric unit cell has six layers of weft yarns and six warp sections located in two reed dents. Process simulation is implemented for the topology using friction coefficient μ=0.3, reed impact velocity=3m/s, applied tension at heddle position= 1N for example (b), 2N and 3N for example (c) and (d) respectively. Figure 4-10 demonstrates side views of three fabric examples. The fabric thicknesses for the three examples are: (a) 6.051mm; (b) 5.804 mm; (c) 5.472 mm. Fiber distribution in weft yarns are affected by applied tension so yarn cross-section shape varies for example (a) (b) and (c) as demonstrated in Figure 4-10. Through comparing the three examples, it can be concluded that applied tension play important role in determining fabric thickness and fiber distribution.

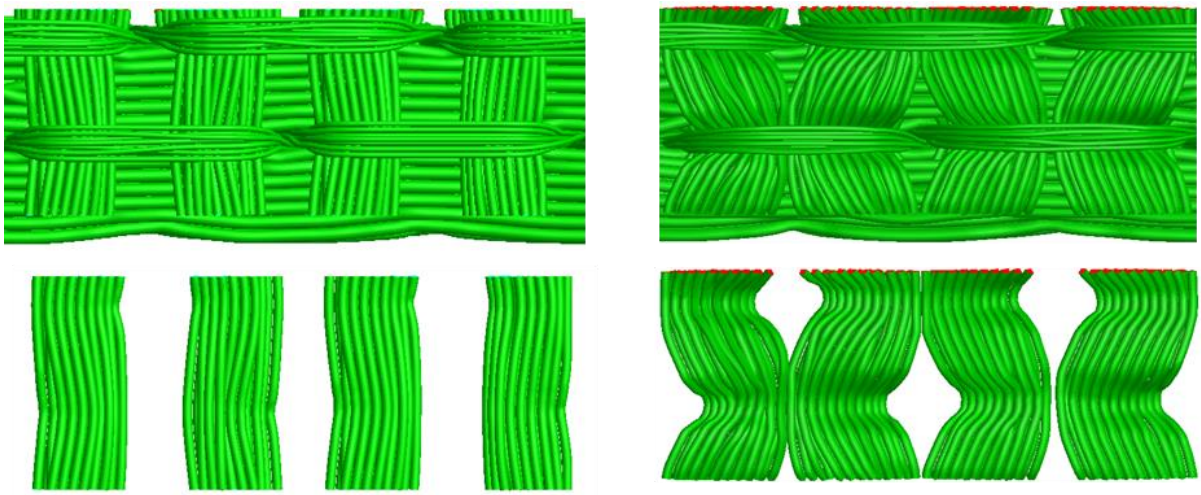

(a) (b)

Figure 4-11. Weft yarn path and yarn tension

Figure 4-11 shows the top view of example (b) and (d). Applied tension does not only affect weft yarn cross-sectional shape, but also weft yarn path. The first layers of weft yarns are

selected and the different weft yarn paths using various weaving tensions are shown. The curvature of weft yarn increases because of larger warp yarn tension. The parametric analysis of weaving process demonstrates that the effect of applied tension on fabric micro-geometry is significant. Fiber distribution and yarn path are very sensitive to change to applied tension.

4.2.2 *Friction effect on fabric micro-geometry*

Figure 4-12 shows the side views of two fabric examples simulated with different fiber-to-fiber friction coefficient. Minimal difference in fabric micro-geometry can be observed from example (a) and (b) using fiber-to-fiber friction coefficient 0.2 and 0.4 respectively, but through comparison with microscopic picture, one can tell that warp yarn path changes slightly. The effect of friction on fabric thickness is calculated to be 1-2%. From Dynamic Weaving Process Simulation, it is concluded that friction coefficient effect on fabric micro-geometry is not significant.

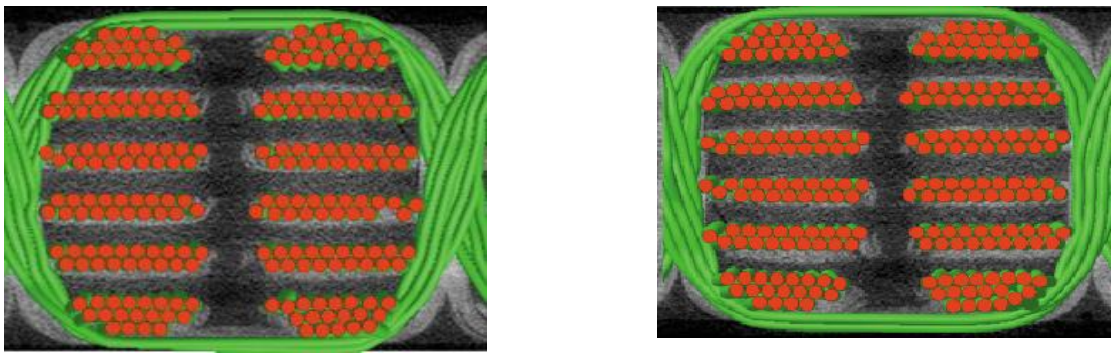

(a) μ=0.2 (b) μ=0.4

Figure 4-12. Fabric micro geometry and friction

4.2.3 *Beating-up effect on fabric micro-geometry*

Reed separates warp yarns and pushes inserted weft yarns towards fell in beating-up. Two examples are simulated in order to study the effect of beating-up action on fabric micro-geometry. As seen in Figure 4-13, example (a) is simulated without beating- up action, weft yarns are simply inserted near fell and a weaving action follows to interlace the inserted weft yarn. Example (b) is simulated with beating- up action, reed impact the inserted weft yarn a push it into the geometry. As Figure 4-13 shows, there tends to be more voids in fabric without beating-up action and the weft fibers can form a tighter structure and more evenly distributed with beating-up action.

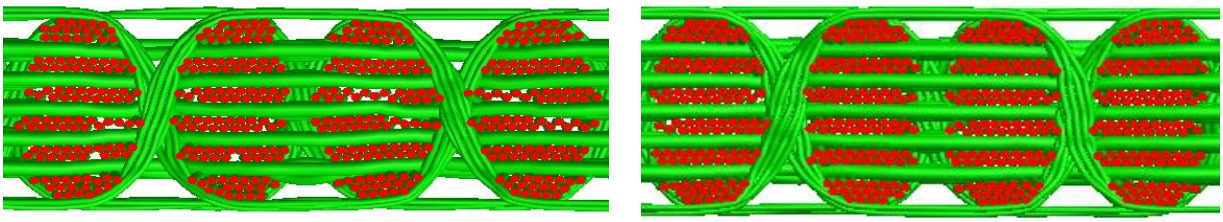

(a) No beating-up action (b) With beating-up action

Figure 4-13. Fabric micro geometry and beating-up action

4.3 Dynamic Relaxation and Dynamic Simulation

Dynamic relaxation with periodic boundary conditions is the most efficient existing approach to determine the micro-geometry of textile fabric using the digital element approach. Using periodic boundary conditions, the material domain in the numerical model only contains one unit cell and a periodic boundary zone. As such, required computer resource is not a concern. This method has been used to derive the micro-geometry of complex 3-D fabrics with

up to 30 layers of wefts. A fine digital element mesh can be adopted in the simulation and a high quality yarn geometry envelope can be generated.

In the dynamic relaxation approach, however, the micro-geometry of a unit cell is determined by minimizing potential energy. It is possible that the numerical simulation would yield different micro-geometries if different relaxation paths were adopted. Each unit cell might have multiple minimum energy state micro-geometries. The micro-geometries in the different minimum energy states could be significantly different. It is difficult to ascertain which minimum state micro-geometry is close to the actual fabric.

The step-by-step dynamic simulation approach, in contrast, models the loom kinetics involved in the weaving process. The step-by-step simulation of the 3-D weaving process thus takes much more computer resource. Usually only coarse digital element mesh can be used because of the limitation of PC capacity. However, the simulation results even from the coarser mesh can provide insight into the minimum potential energy state of the micro-geometry. The micro-geometry is not only uniquely determined by the unit cell topology. The weaving kinetics, modeled by the step-by-step dynamic simulation, plays an important role in determining which minimum potential energy state micro-geometry is formed during the weaving process. In order to elaborate this point, three examples are presented here as following.

4.3.1 *Determine fabric micro-geometry*

Refer to Figure 4-14. Figure 4-14 (a) displays the topology of the first example unit cell. Two micro-geometries of multiple minimum potential energy states are derived for the unit cell topology using different relaxation paths. They are shown in Figure 4-14 (b) and Figure 4-14 (c). In this example, the potential energy of state 2 shown in Figure 4-14-c is lower than that of state 1 shown in Figure 4-14 (b). However, it is difficult to deform the micro-geometry of state 1 to

the micro-geometry of state 2 because of the energy barrier between the two states. It is difficult to make a judgment to ascertain which state is the one closer to the actual unit cell geometry.

In the micro-geometry presented in Figure 4-14 (b) and (c), each yarn is discretized into more than 100 digital fibers. It is almost impossible to use such a fine mesh in the step-by-step dynamic simulation of the weaving process. Therefore, a coarser mesh, in which a yarn is discretized into 19 fibers, is used for a step-by-step simulation. The micro-geometry generated by the dynamic simulation is shown in Figure 4-14 (d). Although the potential energy of the state 2 micro-geometry is lower than that of the state 1 micro-geometry, the unit cell geometry derived from the 3-D step-by-step dynamic simulation is closer to the micro-geometry of state 1, which happens to be the one with the higher potential energy between the two. The state 1 micro-geometry should be selected as the one which can be further used for composite stress analysis.

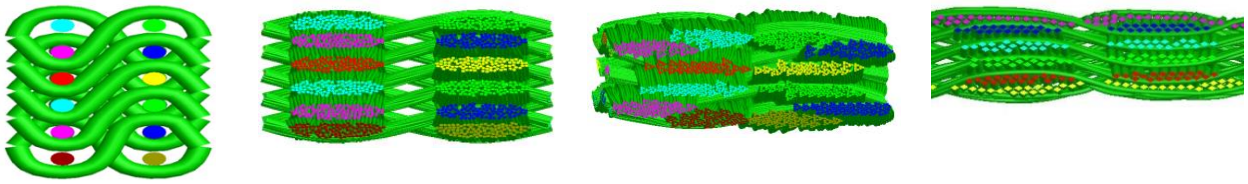

(a). Topology (b). Relax State 1 (c). Relax State 2 (d). Dynamic Simulation

Figure 4-14 Micro-geometry Comparison: Fabric 1

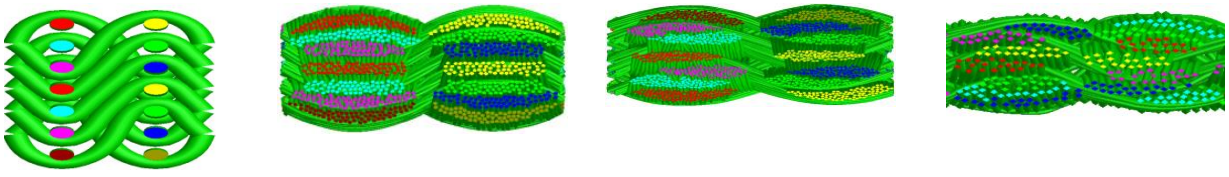

(a). Topology (b). Relax State 1 (c). Relax State 2 (d). Dynamic Simulation

Figure 4-15 Micro-geometry Comparison: Fabric 2

Similarly, the topology of the unit cell of the second example can yield two micro-geometries in two different minimum potential energy states. They are shown as state 1 and state 2 in Figure 4-15 (b) and (c). They are compared to the results derived from the step-by-step dynamic simulation of the 3-D weaving process which is shown in Figure 4-15 (d). One finds that the state 2 micro-geometry is closer to the one generated by 3D weaving process, which happens to be the micro-geometry with the lower potential energy between the two. Therefore, the state 2 micro-geometry should be selected.

The topologies of the unit cell of another example are shown in Figure 4-16. The Dynamic relaxation can yield two micro-geometries at two different minimum potential energy states for each fabric topology. They are shown as state 1 and state 2 in Figure 4-16 (b) and (c). They are compared to the results derived from the step-by-step dynamic simulation of the 3D weaving process which is shown in Figure 4-16 (d). One finds that the state 2 micro-geometry is closer to the one generated by 3-D weaving process, which happens to be the micro-geometry with the lower potential energy between the two. Therefore, the state 2 micro-geometries should be selected.

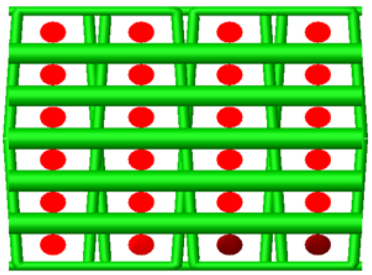

a. Unit cell topology

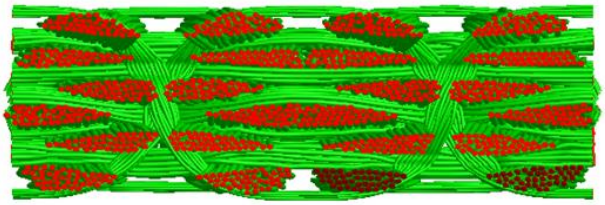

c. Dynamic Relax State 2

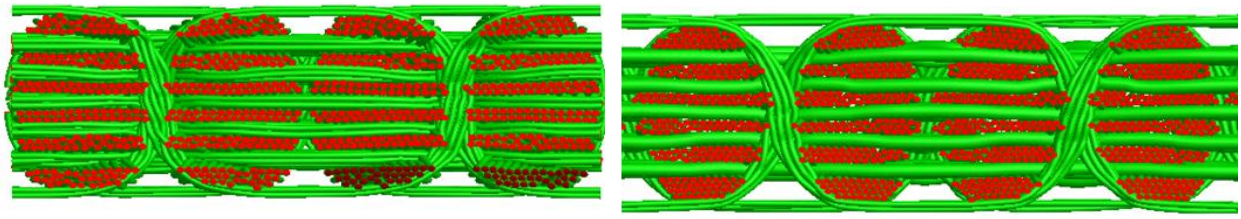

b. Dynamic Relax State 1 d. Dynamic Simulation

Figure 4-16. Fabric example 3

4.3.2 *Determine fabric thickness*

The dynamic relaxation method determines the micro-geometry of a unit cell based on minimum potential energy principle. With different relaxation paths, multiple fabric micro geometries and thickness at various minimum potential energy states may be reached with identical relaxation parameters. It is difficult to ascertain which thickness is closer to the real fabric. Another problem user will encounter using the dynamic relaxation method is to decide whether the fabric relaxation has reached its final result, because user can always continue the relaxation calculation and the fabric thickness will continue changing. As Figure 4-17 shows, as user continues to refine fibers and do relaxation calculation, the fabric pattern/micro geometry remains the same but the calculated fabrics thickness continues to drop from 6.85 to 5.46mm. During the entire relaxation process, the user has to rely on his estimation and experience to decide whether to continue or stop relaxation of a unit cell at certain fabric thickness. The cause for different fabric thicknesses with the same set of calculation parameters remains unclear. Compared with measurement of fabric samples, which determines the fabric thickness to be 6.045mm, the final result the user gets has 8% deviation.

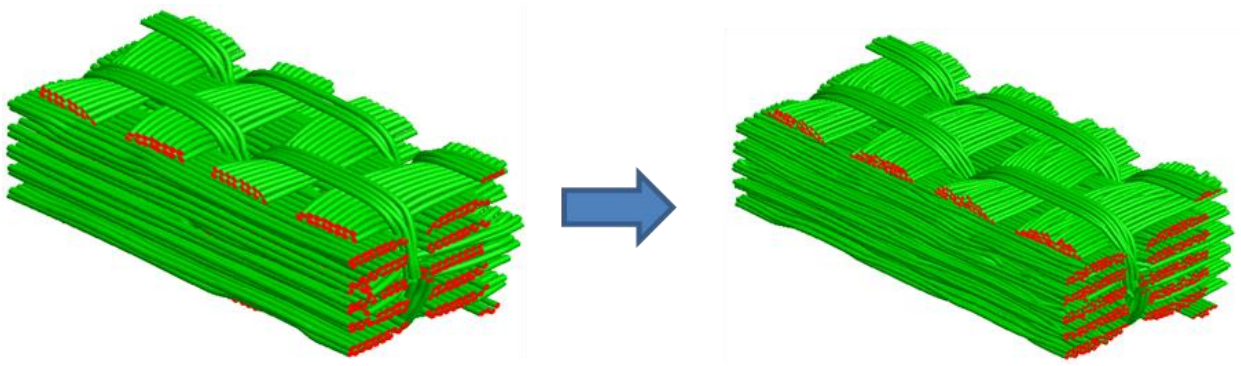

Figure 4-17. Dynamic relaxation process

The Dynamic simulation, on the other hand, determines fabric micro geometries and thickness using weaving process parameters. The fabric micro-geometry and thickness relates only to the weaving process parameters from input while the user's experiences and manipulation of the software have no effect on the final result. As Figure4-22-a shows, fabric thickness through Dynamic Simulation determines the fabric thickness is 6.051mm. Figure 4-10 shows fabric micro-geometries produced using various yarn tensions. Through comparison with microscopic picture Figure 4-10 (a) provides the closest match, which determines the fabric thickness is 6.051mm. The Dynamic Process Simulation generates more precise result compared with Dynamic Relaxation, and the thickness derived from Dynamic Simulation can act as guidance for relaxation calculation.

4.4 Weaving Process and Fabric Stress

Fabric properties are highly dependent on the fabric manufacturing process. The effect of textile manufacturing process on fabric stress and fabric damage must be researched in order to optimize the manufacturing process and fabric properties. Research reveals that warp yarns were a minimum of 20% weaker than unwoven yarns, and weft yarns were 3%-8% weaker.

Reductions in fiber strength could be caused by weaving processes. Therefore, stress analysis function is implemented in Dynamic Weaving Process Simulation in order to study stress distribution and variation during textile manufacturing process.

Example 3:

Example 3 is 2D plain woven fabric using 125-yield Kevlar fiber. Unit cell dimension is 0.0015m.

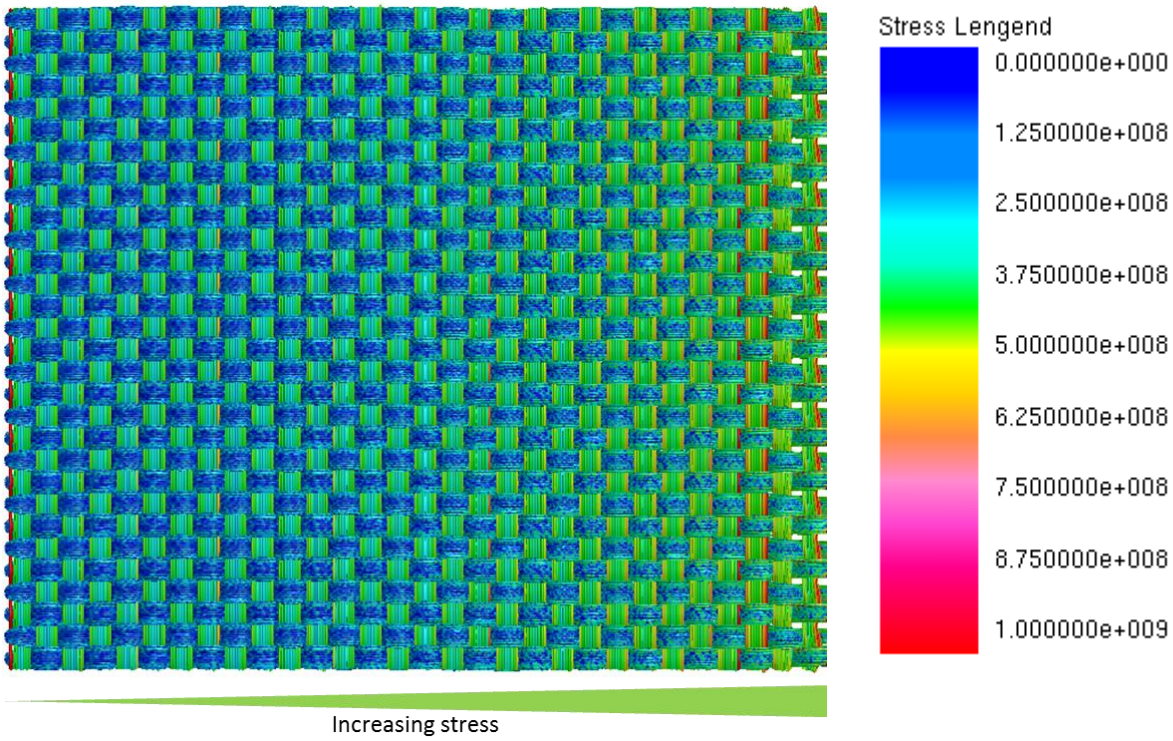

(b) 3N applied tension (c) Stress Legend

Figure 4-18. Yarn stress

Figure 4-18 (a) demonstrates the stress contour of a 2D woven fabric and (b) is the color-stress legend. The weaving process parameters used are: impact velocity=4.5m/s, friction coefficient μ=0.2, warp tension=3N. As Figure 4-18 (a) shows, yarn stress are gradually released

as weaving proceeds, so the front portion of fabric demonstrates smaller stress than the portion of fabric that are newly manufactured.

4.4.1 *Applied tension effect on fabric stress*

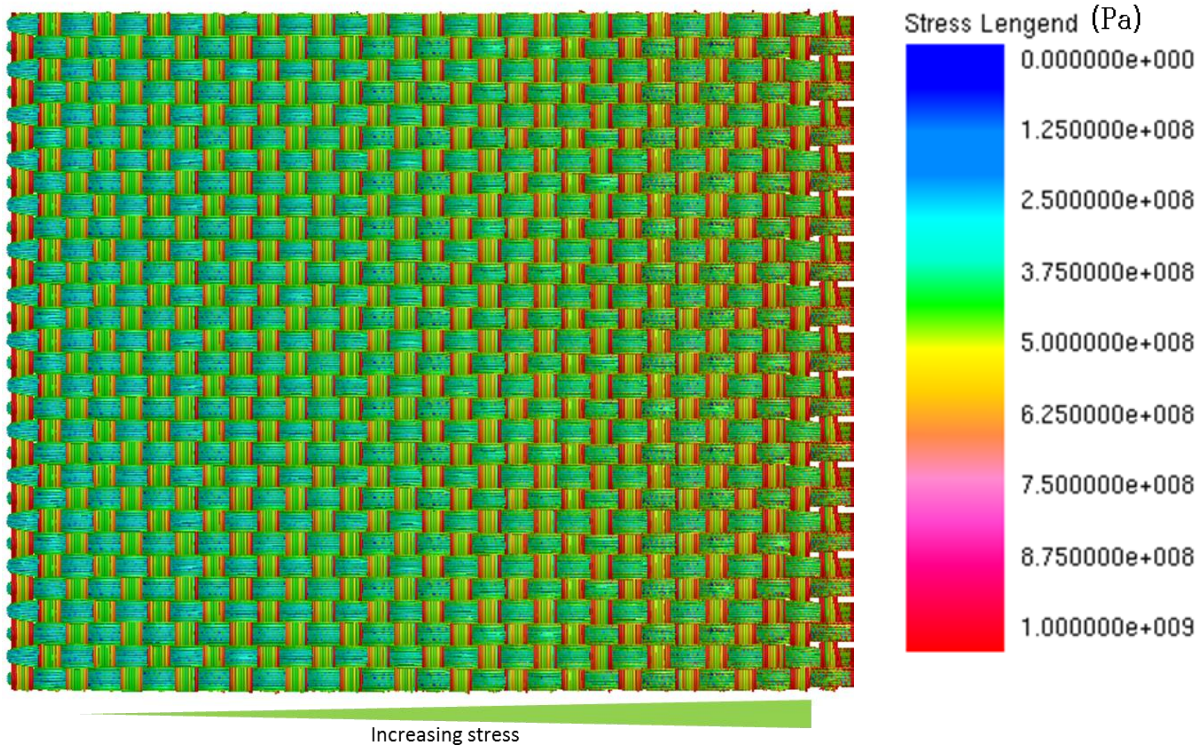

(a) 10N applied tension (b) Stress Legend

(c) Side View

Figure 4-19. Yarn stress

Constant tension is applied to warp yarns and the effect of warp yarn tension on fabric stress is researched using Dynamic Weaving Process Simulation. An identical 2D woven example as the fabric in Figure 4-19 (a) is simulated in comparison with stress contour

demonstrated in Figure 4-18 (a). The only weaving process parameter changed is applied constant tension to warp yarn, which uses 10N in example demonstrated in Figure 4-19 (a). Through comparing the two examples, yarn stress during manufacturing on both warp yarns and weft yarns increase significantly as applied warp yarn tension increases. The applied tension does not only affect warp yarn stress, but also weft yarn. Figure 4-19 (c) shows the side view of the stress contour of the 2D woven fabric. The stress in one weft yarn is not uniform. The fibers show larger stress on the edge than in the middle fibers.

4.4.2 *Friction effect on fabric stress*

Fiber-to fiber friction coefficient is defined by user. The method to determine friction force is introduced in 3.4.2.3. Friction effect on fabric stress during manufacturing is researched using Dynamic Manufacturing Process Simulation. Figure 4-20(a) demonstrates the stress analysis of a 2D woven fabric and (b) is the color-stress legend. The weaving process parameters used are: impact velocity=4.5m/s, friction coefficient μ=0.3, warp tension=3N. Comparing Figure 4-20 (a) and Figure 4-18 (a), one can tell that no significant effect on fabric stress is observed from friction variation.

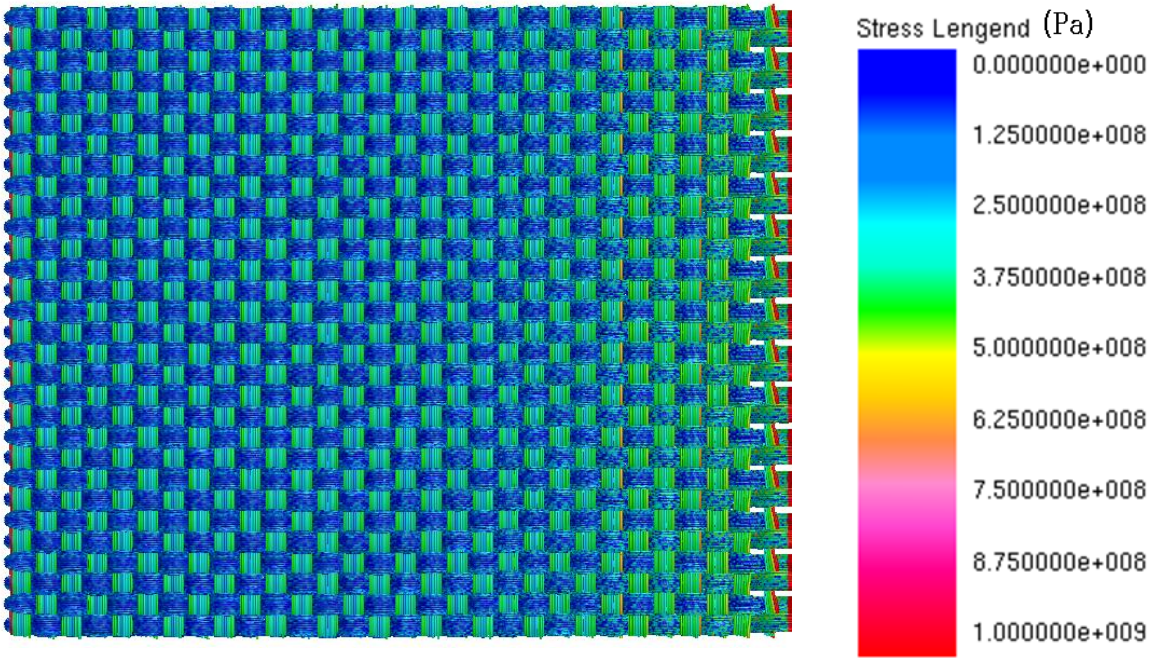

(a) 0.3 friction (b) Stress Legend

Figure 4-20. Friction and stress

4.4.3 *Weaving speed effect on residual stress*

The effect of weaving velocity and reed impact velocity is defined by heddle and reed travel distance and time. Improving manufacturing efficiency typically reduces action time and impact velocity increases. An example demonstrated in Figure 4-21 is simulated using half simulation time of example demonstrated in Figure 4-18 (a). The effect of impact velocity on fabric stress is very significant according to the comparison. Yarn stress is gradually released as weaving proceeds, but the yarn stress during manufacturing affects yarn tension, fabric micro-geometry and therefore, fabric mechanical properties may be greatly affected.

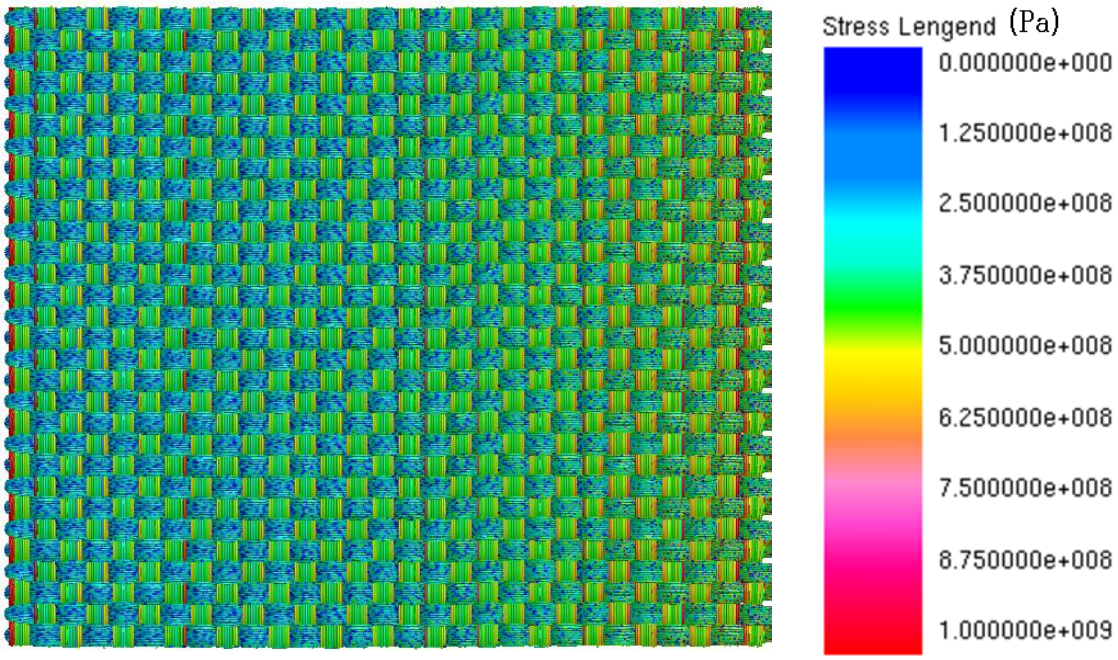

(a) 9m/s impact velocity (b) Stress legend

Figure 4-21. Impact velocity and stress

4.4.4 *Conclusions*

Fabric stress is determined by manufacturing process. Weaving process parameters such as applied tension, friction and reed impact velocity all play important roles in fabric stress and fabric damage during manufacturing process, and thus affects fabric mechanical properties.

4.5 Conclusions

The Dynamic Weaving Process Simulator implements the Digital Element Approach, strictly follows the physics of manufacturing process, and simulates all weaving actions and process dynamics. The relationship between design and manufacturing process parameters, such

as yarn tension, weaving velocity, reed spacing, beating-up velocity, and friction coefficient, and fabric micro-geometries are studied. The effect of manufacturing process and machine behavior are investigated.

The dynamic relaxation approach derives fabric micro-geometry based on fabric topology and minimum potential energy theory. However multiple fabric micro-geometries may be derived at various minimum potential energy states. Although it takes much more computer resource to determine the fabric micro-geometry using the step-by-step dynamic simulation of 3D weaving process than that using the dynamic relaxation approach, the numerical results derived from even a coarse digital element mesh provides insight into the unit cell micro-geometry. This, in turn, provides guidance for a dynamic relaxation approach, in which a finer digital element mesh can be used and a higher quality cross section shape for each yarn can be derived correctly.

Chapter 5 - Conclusions

Traditional textile techniques implemented natural materials to produce simple consumer products such as clothing and blankets. The creation of synthetic fibers and high-performance fibers enabled application of textile materials in high performance products. Textile fabrics including woven, braided, knitted and stitched fabrics reinforced composites have gained application in military and commercial aircrafts frames, airplane engine blades, ballistic panels, helmets, aerospace components and net-shape joints.

Fabric mechanical properties are determined by micro-structure, including placement or lacing pattern of yarns and fiber distributions; fabric micro-geometries are determined by the manufacturing process. Proper fabric design requires investigation of fabric mechanical properties and fabric micro-geometries. Therefore, the study of textile fabrics, fabrics design and textile manufacturing require a reliable and efficient CAD/CAM tool that simulates fabric manufacturing process, models fabric micro-geometry and links manufacturing process with fabric micro-geometry, mechanical properties and weavability.

A numerical model for step-by-step dynamic simulation of 3D weaving processes was developed and a dynamic weaving process simulator was developed based on this numerical model. Digital element approach was implemented to simulate loom kinematics and kinetics in order to determine fabric micro-geometry, mechanical properties and process weavability.

The dynamic weaving process simulator followed the physics of the actual 3-D weaving process. Weaving kinematics was defined by weaving matrices, thereby determining fabric unit cell topology. Yarn discretization was implemented for fiber level simulation, and a dynamic explicit solver was employed to calculate detailed fabric geometry deformation during weaving process. Weaving process simulation primarily consisted of four steps: one weft yarn was

inserted to fell position, then a beating-up action pushed inserted weft yarn against woven fabric; in the third step, warp yarns changed up and down positions according to weaving matrix, and taking-up action collected woven fabric for continuous weaving. Jacquard Loom was used in the weaving simulation model, so the position of each warp was controlled independently. Therefore, 3D fabrics with complex weaving patterns can be produced.

Weaving process kinetics considered in this model included weaving velocity, reed number, reed dent, beating-up speed, fiber-to-fiber friction, yarn tension and fiber strength. An explicit algorithm was employed to simulate the weaving process and derive fabric micro-geometry. Tension-induced nodal force, nodal contact force and nodal friction were considered in this model. Nodal acceleration and nodal displacement at each time step were calculated, and fabric deformation during weaving process was determined. Parallel computing was implemented in order to promote simulation efficiency, enable finer yarn discretization and improve fabric micro geometry accuracy. In addition, a re-mesh function was developed to improve the efficiency of the computer simulation.

Effects of manufacturing process parameters, such as applied tension, friction and reed impact velocity, on fabric stress distribution and variation were studied using the weaving process simulation. The research concluded that weaving process parameters play important roles in determining fabric stress and fabric damage, and consequently affecting fabric mechanical properties.

The relationship between weaving process parameters and reed load was also investigated in this research. Reed has a comb-like structure that performs beating-up action during manufacturing. Thick complex fabric design can generate large load on reed and induce reed damage during manufacturing. Therefore, parametric analysis was implemented using

weaving process simulator to estimate maximum reed load and study the effects of fabric pattern and process parameters on reed load. The research concluded that weaving process parameters such as taking-up length, taking-up velocity and impact speed have major effect on reed load and determines weavability. Other parameters including applied tension, heddle position and fiber-to fiber friction have moderate effect on reed load.

This research also compared process simulation and dynamic relaxation model. The dynamic relaxation approach derives fabric micro-geometry from fabric topology. Fabrics relax to minimum potential energy state and multiple fabric micro-geometries can be generated at various minimum potential energy states in dynamic relaxation calculation. The dynamic simulation of 3D weaving process determines fabric micro-geometry based on weaving process parameters. The step-by-step simulation cost additional computing time but numerical results provide guidance for a dynamic relaxation approach. Effects of weaving process parameters on fabric micro-geometry can by studied using the process simulation model.

References

[1] Miao, Yuyang, Eric Zhou, Youqi Wang, and Bryan Cheeseman. Mechanics of textile composites: micro-geometry. Composites Sciense and Technology 68, no. 7-8 (2008): 1671-1678.

[2] Miao, Yuyang, Lejian Huang, Youqi Wang, Daniel Swenson, Chian-Fong Yen, and Bryan Cheeseman. Explicit digital element approach with periodic boundary in determining textile micro-geometry. ASC 24 Technical Conference. Newark, Delaware, 2009.

[3] Wang, Y., & Sun, X. (2001). Digital element simulation of textile process. Composites Science and Technology, 64, 311-319.

[4] Zhou, C., Sun, X., & Wang, Y. (2003). Multi-chain digital analysis in textile mechanics. Composites Science and Technology, 64, 239-244.

[5] Website, https://en.wikipedia.org/wiki/Hand_spinning#cite_note-1.

[6] Website, http://inventors.about.com/od/bstartinventions/a/Body_Armor.htm. Mary Bellis.

[7] Website, http://en.wikipedia.org/wiki/Boeing_787_Dreamliner#cite_note- Toray_2005_0412-202

[8] Frances Romeo. A Brief History of Body Armor. Time. April 07, 2009.

[9] Ravi B. Deo. James H. Starnes, Jr. Richard C. Holzwarth. Low-Cost Composite Materials and Structures for Aircraft Applications.

[10] Brian S. Hayes, Luther M Gammon . Optical Microscopy of Fiber-Reinforced Composites, chapter 1. ASM International, 2010

[11] J.C. Halpin, The Role of the Polymeric Matrix in the Processing and Structural Properties of Composite Materials,L. Nicolais and J.C. Seferis, Ed., Plenum Press, New York, 1983

[12] Brian N. Cox, Gerry Flanagan. Handbook of Analytical Methods for Textile Composites. National Aeronautics and Space Administration, 1997

[13] Kamiya, Ryuta, Cheeseman, Bryan A, Popper, Peter, Chou, Tsu-Wei. Some recent advances in the fabrication and design of three-dimensional textile preforms: A review. Composites Science and Technology, v 60, n 1, p 33-47, Jan 2000

[14] Huang, L.J., Wang, Y.Q., Miao, Y.Y., Swenson, D., Ma, Y., & Yen, C.F. (2013). Dynamic relaxation approach with periodic boundary conditions in determining the 3-D woven textile micro-geometry. Composite Structures, 106, 417-425.

[15] Collier, J. R., Collier, B.J., O'Toole, G., Sargan, S.M.. Drape prediction by means of finite-element analysis. Journal of the Textile Institute, 1991, 82(1): 96-107. [145]

[16] Pierce, F.T.. The geometry of cloth structure. Journal of the textile institute, 1937, 28(3):T45-T96. [500]

[17] Kemp, A.. An extension of Peirce's cloth geometry to the treatment of nonlinear threads. Journal of Textile Institute, 1958, 49:T44–T48.

[18] Hearle, J.W.S., Shanahan, W.J.. An energy method for calculations in fabric mechanics. Part I: Principles of the method. Journal of Textile Institute, 1978a, 69: 81–110.

[19] Shanahan, W.J., Hearle, J.W.S.. An energy method for calculations in fabric mechanics. Part II: Examples of the application of the method to woven fabrics. Journal of Textile Institute, 1978b, 69: 92–100.

[20] Hearle, J.W.S., Potluri, P., Thammandra, V.S.. Modelling fabric mechanics. Journal of Textile Institute, 2001, 92(3): 53-69.

[21] Sabit Adanur and Tianyi Liao. 3D modeling of textile composite preforms. Composites Part B: Engineering, v 29, n 6, p 787-793, 1998

[22] Sabit Adanur and Tianyi Liao. Predicting the mechanical properties of nonwoven geotextiles with the finite element method. Textile Research Journal, v 67, n 10, p 753-760, Oct 1997

[23] Kuhn, J., Charalambides, P.. Modeling of plain weave fabric composite geometry, Journal of Composite Material, 1999, 33(3): 188–220. [40]

[24] Rao, M.P, Pantiuk, M, Charalambides P.G. Modeling the Geometry of Satin Weave Fabric Composites. Journal of Composite Materials, v 43, n 1, p 19-56, January 2009

[25] Hivet G, Boisse P. Consistent mesoscopic mechanical behavior model for woven composite reinforcements in biaxial tension. Composites Part B: Engineering, v 39, n 2, 345-61, March 2008

[26] Charmetant A, Wendling A, Hivet G, Vidal-Sallé E,Maire E, Boisse P. Simulation and tomography analysis of textile composite reinforcement deformation at the mesoscopic scale. Proceedings of the 10th International Conference on Textile Composites - TEXCOMP 10: Recent Advances in Textile Composites, p 135-142, 2010, Proceedings of the 10th International Conference on Textile Composites - TEXCOMP 10: Recent Advances in Textile Composites

[27] Hua Lin, Brown L.P, Long, A.C. Modelling and simulating textile structures using TexGen. Advanced Materials Research, v 331, 44-7, 2011

[28] Lin Hua, Zeng, Xiesheng, Sherburn Martin, Long Andrew C, Clifford Mike J. Automated geometric modelling of textile structures. Textile Research Journal, v 82, n 16, p 1689-1702, October 2012

[29] Lin H, Long A.C, Sherburn M, Clifford M.J. Modelling of mechanical behaviour for woven fabrics under combined loading. International Journal of Material Forming, v 1, n SUPPL. 1, p 899-902, July 2008

[30] Lomov SV, Gusakov AV. Computation of the porosity of one and multi-layered woven synthetic fabrics. Chimicheskie Volokna 1998:52–5.

[31] Lomov SV, Gusakov AV. Mathematical modelling of 3D and conventional woven fabrics. International Journal of Clothing Science and Technology. 1998, 10(6):90–1

[32] Lomov SV, Huysmans G, Luo Y, Parnas R, Prodromou A, Verpoest I, et al. Textile composites models: integrating strategies. Compos Part A 2001;32(10):1379–94.

[33] Lomov SV, Gusakov AV, Huysmans G, Prodromou A, Verpoest. I. Textile geometry preprocessor for meso-mechanical models of woven composites. Composites Science and Technology. 2000;60:2083–95.

[34] Lomov SV, Huysmans G, Verpoest I. Hierarchy of textile structures and architecture of fabric geometric models. Textile Research Journal. 2001;71(6):534–43.

[35] Lomov SV, Truong Chi T, Verpoest I, Peeters T, Roose V, Boisse P. Mathematical modelling of internal geometry and deformability of woven preforms. International Journal of Material Forming 2003; 6(3–4):413–42.

[36] Durville, D.. Finite element simulation of textile materials at the fiber scale. SAMPE 2009, Baltimore, United States.

[37] Durville, D.. Simulation of the mechanical behavior of woven fabrics at the scale of fibers, International Journal Material Forming, 2010, 3(2): 1241–1251.

[38] Durville, D.. Microscopic approaches for understanding the mechanical behavior of reinforcement in composites. Composite reinforcements for optimum performance, 2011, 461-485.

[39] Porat I, Greenwood K, Li Z. CAD/CAM of three-dimensional woven structures (preforms) for fibre-reinforced composites. Composites Part A (Applied Science and Manufacturing), v 27A, n 2, 111-17, 1996

[40] Tacibaht Turel, Sayavur Bakhtiyarov and Sabit Adanur. Effects of Air and Yarn Characteristics in Air-Jet Filling Insertion Part I: Air Velocity and Air Pressure Measurements. Textile Research Journal, v 74, n 8, p 657-661, August 2004

[41] Website, https://sites.google.com/site/arttextilesfbec/production-methods/weaving